

AFCRL-65-290

AD620034

ABSORPTION OF SOLAR RADIATION BY ATMOSPHERIC CO₂

Thomas G. Kyle, David G. Murcraay,
Frank H. Murcraay and W. J. Williams

Department of Physics
University of Denver

Contract AF 19(604)7429

Project No. 8662

Task No. 866201

SCIENTIFIC REPORT NO. 5

April 1965

DDC
SEP 8 1965
TISIA E

This research was supported in part by the Advanced Research Projects Agency under ARPA Order Number 363-62 and was monitored by AFCRL.

Prepared for
Air Force Cambridge Research Laboratories
Office of Aerospace Research
United States Air Force
Bedford, Mass.

CLEARINGHOUSE FOR FEDERAL SCIENTIFIC AND TECHNICAL INFORMATION		
Hand copy	Microfilm	
3.00	0.75	55
ARCHIVE COPY		

**BEST
AVAILABLE COPY**

Requests for additional copies by agencies of the Department of Defense, their contractors, or other government agencies should be directed to

Defense Documentation Center (DDC)
Cameron Station
Alexandria, Virginia 22314

Department of Defense contractor must be established for DDC services or have their "need-to-know" certified by the cognizant military agency of their project or contract.

All other persons and organizations should apply to the

Clearinghouse for Federal Scientific
and Technical Information (CFSTI)
Sills Building
Port Royal Road
S. Field, Virginia 22151

AFCRL-65-290

ABSORPTION OF SOLAR RADIATION BY ATMOSPHERIC CO₂

Thomas G. Kyle, David G. Murcray,
Frank H. Murcray and W. J. Williams

Department of Physics
University of Denver

Contract AF 19(604)7429

Project No. 8662

Task No. 866201

SCIENTIFIC REPORT NO. 5

April 1965

This research was supported in part by the Advanced Research Projects Agency under ARPA Order Number 363-62 and was monitored by AFCRL.

Prepared for
Air Force Cambridge Research Laboratories
Office of Aerospace Research
United States Air Force
Bedford, Mass.

TABLE OF CONTENTS

	<u>Page</u>
ABSTRACT	vi
INTRODUCTION	1
THE 4.3 μ BAND OF CARBON DIOXIDE	2
SLANT PATH ABSORPTION	4
EXPERIMENTAL DATA	6
Instrumentation	6
Data Reduction	6
THEORETICAL CALCULATIONS	7
DISCUSSION	11
FOOTNOTES	14

LIST OF TABLES

<u>Table No.</u>		<u>Page</u>
I.	Vibrational Constants	12
II.	CO ₂ Bands in Calculation	12
III.	Parameters Associated with Spectra	13

LIST OF FIGURES

FIGURE		<u>Page</u>
1	Comparison of Theoretical and Experimental Transmittance at 10.7 km	15
2	Comparison of Theoretical and Experimental Transmittance at 12.4 km	16
3	Comparison of Theoretical and Experimental Transmittance at 14.1 km	17
4	Comparison of Theoretical and Experimental Transmittance at 15.2 km	18
5	Comparison of Theoretical and Experimental Transmittance at 15.8 km	19
6	Comparison of Theoretical and Experimental Transmittance at 18.3 km	20
7	Comparison of Theoretical and Experimental Transmittance at 18.8 km	21
8	Comparison of Theoretical and Experimental Transmittance at 19.7 km	22
9	Comparison of Theoretical and Experimental Transmittance at 21.6 km	23
10	Comparison of Theoretical and Experimental Transmittance at 22.0 km	24
11	Comparison of Theoretical and Experimental Transmittance at 23.0 km	25
12	Comparison of Theoretical and Experimental Transmittance at 23.4 km	26
13	Comparison of Theoretical and Experimental Transmittance at 23.8 km	27
14	Comparison of Theoretical and Experimental Transmittance at 24.3 km	28
15	Comparison of Theoretical and Experimental Transmittance at 25.6 km	29
16	Comparison of Theoretical and Experimental Transmittance at 26.1 km	30

LIST OF FIGURES (Cont.)

FIGURE		<u>Page</u>
17	Comparison of Theoretical and Experimental Transmittance at 26.6 km	31
18	Comparison of Theoretical and Experimental Transmittance at 27.0 km	32
19	Comparison of Theoretical and Experimental Transmittance at 27.4 km	33
20	Comparison of Theoretical and Experimental Transmittance at 27.9 km	34
21	Comparison of Theoretical and Experimental Transmittance at 28.8 km	35
22	Comparison of Theoretical and Experimental Transmittance at 29.2 km	36
23	Comparison of Theoretical and Experimental Transmittance at 29.6 km	37
24	Comparison of Theoretical and Experimental Transmittance at 30.0 km	38
25	Comparison of Theoretical and Experimental Transmittance at 30.4 km	39
26	Comparison of Theoretical and Experimental Transmittance at 30.8 km	40
27	Comparison of Theoretical and Experimental Transmittance at 31.4 km	41
28	Comparison of Theoretical and Experimental Transmittance at 31.7 km	42
29	Comparison of Theoretical and Experimental Transmittance at 32.0 km	43
30	Comparison of Theoretical and Experimental Transmittance at 32.3 km	44
31	Comparison of Theoretical and Experimental Transmittance at 32.5 km	45

ABSTRACT

The absorption spectra of the 4.3 micron band was measured at altitudes from ten to thirty kilometers along slant paths in the atmosphere using the sun as a radiation source. These spectra were obtained by the use of a balloon-borne grating spectrometer having a resolution of 0.5 cm^{-1} . This resolution is high enough to require a line by line calculation to interpret the spectra. By making two assumptions it has been possible to calculate spectra using a small computer that agree quite well with the observed spectra. The primary approximations used were the assumption of like rotational structure for all isotopes and excited states, and the assumption of constant displacement between the various states of C^{12} and C^{13} . At the higher altitudes the Lorentz broadening theory resulted in a satisfactory agreement between the calculations and the experimental results, but at the lower altitudes use of the empirical modification proposed by Benedict was necessary to obtain agreement in the region of the high frequency end of the band. The calculations cover the frequencies from 2235 cm^{-1} to 2415 cm^{-1} .

INTRODUCTION

In a previous paper¹ it was shown that the observed high altitude slant path transmittance in the vicinity of the 4.3μ CO₂ band agreed very well with that predicted by Plass.² The results given by Plass were adequate for a resolution of about 5 cm^{-1} which was about the resolution of the experimental data presented in that paper. Plass' results are not adequate for comparison with spectra with a resolution higher than this and his method of calculation cannot be extended to compare with higher resolution data since he did not attempt to calculate the absorptions on a line by line basis but rather used a model to represent the band.

During a balloon flight made by our group on May 14, 1964, numerous solar spectra were obtained covering this wavelength region with a resolution of between 0.5 cm^{-1} and 0.7 cm^{-1} . In order to compare the results observed during this flight with the results one would predict on a theoretical basis, it has been necessary to arrive at a method of calculating the transmission to be expected along such slant paths. This was done by calculating the transmission one would expect with infinite resolution and then degrading the results until a resolution comparable with that achieved during the flight was obtained. Plass pointed out that because of the number of individual lines present in this region it is difficult to perform a line by line analysis even with a large computer. By carefully considering the physics of the absorption, we have arrived at a method of calculating the transmittance so that individual spectra can be calculated in a short time on a Burroughs Datatron 205 computer which is a relatively small, slow machine. The method of performing the calculations and a comparison of the observed and theoretical transmittance curves are discussed in this report.

THE 4.3 μ BAND OF CARBON DIOXIDE

The strong atmospheric absorption at 4.3 μ is due to carbon dioxide. Since carbon dioxide is one of the most thoroughly investigated of all molecules and all available evidence indicates that it is uniformly distributed in the earth's atmosphere, this band is an excellent band for comparison of theoretical and experimental slant path transmittances. The theory of the CO₂ absorption is discussed in detail by Plass.³ In order to calculate the transmittance expected at various wavelengths on a line by line basis, it is necessary that the line positions, line strengths, half widths, line shapes and the various factors that affect these parameters along the absorbing path be known. The line positions for the 4.3 μ band have been studied by a number of investigators,⁴ the most comprehensive treatment previous to that of Plass³ being that given by Courtoy.⁵ The strength of the individual lines in the band have not been measured but they can be determined by using well known equations and a knowledge of the total band strength.⁶ Unfortunately the band strengths for the excited states involved in conjunction with the fundamental band are not known. The population of these states is low for the temperatures likely to be encountered in the atmosphere. These states account for only a small fraction of the absorption by the fundamental band, so a fairly inaccurate estimate of the strengths of the lines of the excited states will not produce a large error in the computed spectra.

When the collision frequency of an absorbing gas is high enough, the line width is primarily determined by pressure broadening. Plass has shown that for CO₂ in the atmosphere, pressure broadening will predominate over all other broadening up to altitudes in the vicinity of 50 kms. Thus for this study pressure broadening should predominate and the line shape function should be that given by Lorentz,⁷ i. e.

$$k(\nu) = \frac{c/\pi}{(\nu-\nu_1)^2 + a^2} \quad (1)$$

In this expression a is the collision frequency of the absorbing molecules.

The carbon dioxide 4.3 μ band provides an advantageous situation for investigation of the frequency dependency of the line shape. The band reaches a head at 2397 cm⁻¹. This makes it possible to measure the transmittance in the wing above the band head without interference from locally occurring lines. It has been found that in this region the Lorentz line shape has to be modified. Winters, Silverman and Benedict,⁸

suggested that the Lorentz line shape be modified as follows: the Lorentz line shape is assumed to hold for a frequency difference from the line center less than a certain amount $\Delta\nu_0$. The value of $\Delta\nu_0$ is not critical, but can be considered to be less than 3 cm^{-1} . For a frequency such that the difference from the line center is greater than $\Delta\nu_0$ the Lorentz shape is multiplied by an exponential factor: i. e. :

$$k(\nu) = \frac{a/\pi}{(\nu-\nu_i)^2 + a^2} \quad \nu, \quad |\nu-\nu_i| < \Delta\nu_0 \quad (2)$$

$$k(\nu) = \frac{a/\pi}{(\nu-\nu_i)^2 + a^2} e^{-a(|\nu-\nu_i| - \Delta\nu_0)^b}, \quad |\nu-\nu_i| > \Delta\nu_0. \quad (3)$$

Laboratory investigations have shown that the empirical constants a and b depend on the broadening gas used for pressurizing. The values used in this paper are $a = b = 0.46$.

Since the half width a for a Lorentz line is given by the collision frequency, it is possible to show that the half width satisfies the following relation.

$$a = a_0 \frac{P}{P_0} \left(\frac{T_0}{T} \right)^{1/2} \quad (4)$$

where a_0 is the half width at temperature T_0 and pressure P_0 and a is the half width at pressure P and temperature T . For this study all lines were assumed to have a half width under standard conditions ($T_0 = 273^\circ\text{k}$, $P_0 = 1 \text{ atm}$) of $.07 \text{ cm}^{-1}$.

SLANT PATH ABSORPTION

When the path traversed by the radiation is a slant path in the atmosphere, the pressure and temperature environment of the absorbing gas varies along the path and, therefore, the half width varies along the path. In addition, the line strength depends on temperature, thus predicting transmittance on such a path becomes a more complex problem than the problem of predicting the transmittance along a laboratory path in which the half width and line strength are constant. In this study we are interested in comparing theoretical transmittances with those observed using the sun as a source. In this case the pressure along the absorption path varies from the atmospheric pressure present at the altitude which the spectrum was obtained to that at which the CO_2 dissociates photochemically. In this case it was found that the pressure dependence overshadows the temperature dependence and it was possible to ignore the variation of temperature along the path. In this study all calculations were performed using a temperature of 45°C for the absorbing CO_2 .

Both theory and experiment indicate that to a very good approximation the density of the atmosphere decreases exponentially with increasing altitude. If the effects of temperature are neglected the absorption by a group of lines may be expressed as follows

$$T = \exp - \int_{X_1}^{X_2} \sum_i \frac{S_i \rho' a_0}{\pi k} \frac{d(a_0 e^{-kx})}{(\nu - \nu_i)^2 + a_0^2 e^{-2kx}} \quad (5)$$

where it is assumed that the atmospheric density fits a relation of the type $\rho = \rho_0 e^{-kx}$. ρ' in these expressions is the density of the absorber, not atmospheric density and hence may be distributed in some manner other than exponentially.

Not many possible forms for the density as a function of altitude can be readily integrated. One which can be integrated is the case of uniform mixing which is applicable for CO_2 . Let the fractional concentration of the absorber be c . The equation for the transmittance can then be integrated with the following result.

$$T = \exp - \sum_i \frac{S_i c \rho_0}{2k\pi a_0} \left\{ \ln \frac{(\nu - \nu_i)^2 + a_0^2 e^{-2kx_1}}{(\nu - \nu_i)^2 + a_0^2 e^{-2kx_2}} \right\} \quad (6)$$

Re-express this in terms of the half width by observing $a = a_0 e^{-kx}$ and

$$T = \prod_i \left\{ 1 - \frac{a_1^2 - a_2^2}{(\nu - \nu_i)^2 + a_1^2} \right\}^{\frac{S_i c \rho_0}{2\pi k a_0}} \quad (7)$$

This result was first derived by Strong and Plass.⁹ This can be transformed into a convenient approximation by taking the natural logarithm of both sides and expanding the right hand part in a power series and discarding all but the first term. When the exponential is taken on both sides, the result becomes

$$T = \exp - \left[\sum_i \frac{S_i c \rho_0}{2\pi k a_0} \frac{a_1^2 - a_2^2}{(\nu - \nu_i)^2 + a_1^2} \right] \quad (8)$$

Near the line center the two results disagree by a considerable amount. The amount of disagreement depends on the half width and on the line strength. It is possible to improve the approximation for absorption near the line center by using a smaller value of the half width in the denominator. This smaller value may be obtained by use of the Curtis-Godson approximation which uses the average half width.

EXPERIMENTAL DATA

Instrumentation

The experimental data with which the calculations are compared were obtained during a balloon flight made May 14, 1964, from Holloman AFB, New Mexico. On this flight a 1/2 meter double pass Czerny-Turner type grating spectrometer was flown in conjunction with a biaxial pointing control ("sun seeker") which oriented a plane mirror so that the solar radiation was reflected onto a 25 cm diameter 150 cm focal length mirror which focused the radiation on the spectrometer slit. The spectrometer was equipped with a Bausch and Lomb replica grating 102 mm square with 75 lines per mm and blazed at twelve microns in the first order. The third order was used on this flight. The orders were separated by a prism spectrometer predisperser. The radiation was interrupted at a 100 cps rate on the second pass through the instrument. The radiation intensity was measured by the use of a Schwarz thermocouple. The ac output of the thermocouple was amplified using a solid state pre-amplifier and amplifier. The amplified signal was recorded by means of an on-board tape recorder and was also telemetered to the ground.

A relatively large region was scanned on each side of the 4.3 μ band. Three minutes were required to obtain a spectral scan and the spectrometer scanned continuously. High cirrus clouds were present at launch and as a result the seeker did not acquire the sun until the balloon reached an altitude of 10.7 kms and no spectra were obtained below this altitude. Above this altitude the seeker functioned properly and data were obtained almost continuously until the equipment was cut down.

Data Reduction

At the highest altitude reached by the balloon the absorption was weak enough to permit drawing a vacuum envelope which should be fairly accurate in view of the slow variation of the envelope outside of the band. A template was made of the envelope obtained in this manner and the template was used to draw the same envelope on the other records. The percent transmittance was determined at selected wavenumber points across the band and from these points the percent transmittance versus wavenumber plots were constructed.

THEORETICAL CALCULATIONS

The range of wavenumbers for which the experimental and theoretical results can be compared is limited on the low frequency end by the occurrence of significant atmospheric absorption by nitrous oxide. The high wavenumber end was limited to the highest frequency for which appreciable absorption occurred in the experimental data. The wavenumber range was thus determined to be from 2235 cm^{-1} to 2415 cm^{-1} . The transmittance was calculated at 1800 points, after which a slit function appropriate to the spectrometer used was applied to degrade the actual transmittance calculated to the observed transmittance.

Comparison of the exact and approximate expressions indicate that for strong lines the two expressions are in fairly good agreement even when the transmittance is small (~ 0.2). Since the major absorption in the 4.3μ region is due to strong lines and using the approximate expression greatly reduced the amount of computation required, all calculations were performed using equation 8. Examination of equation 8 indicates that if α_1 , which varies with altitude is replaced in the denominator by a constant the quantities involved in the sum become independent of altitude. Thus, using the exponential approximation and a constant value for the half width in the denominator it is only necessary to perform the extensive summations once. The variation of transmittance with altitude was allowed for by changing the multiplicative variable in the numerator. For the particular intervals involved in the calculation the only points where the use of a constant half width made a noticeable difference was in the interval closest to the line center. The value of the half width which was used in the denominator was 0.003 cm^{-1} .

In order to calculate the strengths of the isotopic and excited states the assumption was made that the matrix of the transition is the same for all these cases. A large degree of simplification in the calculations was also obtained by the approximation that all the isotopes and excited states had the same rotational spacing. The values of J which are permitted depend on the state and isotope. The states and isotopes considered are given in Table I along with the constants involved. These do not happen to be the states with the highest occupational numbers. For example there is more $\text{C}^{12}\text{O}^{16}\text{O}^{17}$ than there is $\text{C}^{13}\text{O}^{16}\text{O}^{18}$, but the former is not considered. This was neglected on the basis of the importance of the relative strength of the state in relation to the other states surrounding it.

The frequencies and strengths were actually calculated for only the C^{12} isotopic species. The assumption of like rotational structure for all states and species permitted the frequencies and strengths of the C^{13} species to be generated from those of C^{12} by a displacement of 65.8 cm^{-1} downward in the frequency, and a reduction in the strength by a factor of 0.011. The line positions were only calculated to tenths of wavenumbers. In view of the assumption of like rotational structure, there can definitely be errors larger than this. The assumption of a constant displacement between the C^{12} and C^{13} species for all states results in some states being displaced from their actual position for the C^{13} species. These errors did not significantly affect the overall results, but probably affected the apparent strength of certain lines in the observed spectra. The strengths were calculated for a temperature of -45°C . The strength of lines with high J values increased rapidly with the temperature, but almost the only change in the lines of low J values was due to the change in the value of the partition function. Some of the early calculations were carried out with the strengths found at different temperatures. These results indicated that the effect of temperature was not as large as had been expected.

The value of the band strength was assumed to be $2800 \text{ cm}^{-2} \text{ atmos}^{-1}$. The range of J values to be used for each of the cases considered was determined by calculating the strengths for a wide range of J and then discarding all values less than $0.01 \text{ cm}^{-2} \text{ atmos}^{-1}$. It should be pointed out that the smallest value mentioned above was for a C^{12} species, so the smallest value actually used was a factor of about 100 less. The range of strengths used thus covered a range of values differing in magnitude by a factor of about one million. A total of 548 lines were considered. As mentioned above only half of these were actually calculated. The rest were generated from these. That is, their effect was generated by a procedure given below. Table II lists the states and J values which were used in the calculation.

In performing the sum of the strength over the frequency squared, the lines were divided into two groups. The group of the eighty strongest lines of the C^{12} species of molecules were considered to be the only lines of importance in the contribution to wing effects for frequencies greater than about one wavenumber from the line center. These eighty lines comprised 97.1 percent of the total strength. The contributions of each of these lines was considered at each point of the interval over which the transmittance was calculated. The remainder of the C^{12} lines were considered as giving a significant contribution over the range from their center to the next line of the group. This meant that at each point

of the region where the transmittance was calculated there were eighty-two lines from the C^{12} molecules contributing to the transmission. Eighty of these were strong lines, and the weak lines on the left and the right of the frequency under consideration were also included. This method of calculation was used for both the Lorentz line shape and the Benedict modification to the Lorentz line shape. In the case of the Benedict modification the weak group of lines were closely enough spaced that no modification was required.

After the calculation for the contributions of the strong lines at each point was completed the contributions of the weak lines were computed and the two sets of results were added together. This gave the effects of the molecules containing a C^{12} atom, but the assumption of like rotational structure and constant displacement meant that this is the same result, except for a factor of 0.011, as would be obtained for the C^{13} containing molecules. This was the method for generating the effects of the C^{13} molecules. The value at each point of the interval was multiplied by 0.011, and added to the value at the point 65.8 cm^{-1} lower in frequency. In the calculations for Figure 3 and Figure 6, one of the strong lines of the C^{13} species was inadvertently omitted. This line is located at about 2293 cm^{-1} . The effect of the omission is immediately evident.

In the calculation of the transmittance, the atmosphere was assumed to be composed of 0.033 percent carbon dioxide by volume at all altitudes. The coefficient of the altitude in the exponential form of the density dependence was taken as $1.56 \times 10^{-6} \text{ cm}^{-1}$. The half width at standard temperature and pressure in air was taken as 0.066 cm^{-1} . The half width should be proportional to the density and to the square root of the absolute temperature. The equations have been derived by assuming an isothermal atmosphere, but the half widths used were corrected for the temperature. The values of the half widths, altitudes, and sun angles used are shown in Table III.

After the calculation of the actual transmittance the spectral resolution was degraded until it approached the experimental by the application of a slit function. The form of the slit function for the present study was arrived at by starting with a gaussian function and modifying it numerically until an approximate agreement between the data and the theory was obtained in terms of the difference between peaks and valleys for lines of different spacing. The transmission was calculated at 0.1 wavenumber intervals, and the slit function was applied at 0.3 wavenumber intervals.

These calculations have been carried out for comparison with thirty-one experimental spectra. Figures 1 through 31 show this comparison for experimental spectra taken at 31 different altitudes.

In the figures the solid line represents the values calculated according to the Lorentz line shape. The dotted portions of the curves were calculated using the Benedict modification. These are included only where there was significant disagreement between the two. The experimental data are shown as a + for each datum read. A dashed line joins these points in most places in order to aid interpretation of the figures. In some places where data are missing the lines have still been dashed in for the sake of appearance.

DISCUSSION

The present calculations have been carried out on a relatively slow computer of rather limited memory. With a higher speed computer it would be practical to use a finer net of points and more accurately located lines. By the use of such computations it should be possible to refine the present knowledge of band strengths and half widths to some extent. These are the fundamental parameters of absorption spectra, and yet the present state of knowledge about them leaves a great deal to be desired.

At least one systematic deviation between the theory and the spectra should be mentioned. This is the high frequency side of the $C^{12}O_2^{16}$ band. The theory always seems to be below the experimental values here. This could be the result of several different factors. This is the region of high line density, so an error near the line centers, in the region of rapid variation of the shape factor, could be at fault. If this were the case the same sort of error, but of greater extent, should be present on the high frequency side of the $C^{13}O_2^{16}$, because the density of lines is even greater here. This does not appear to be the case.

It is possible that the envelope in the experimental spectra was drawn incorrectly in the region. The use of another envelope was considered, but not adopted because the new envelope did not appear as plausible as the one used. If the envelope is in error the disagreement between theory and experiment should decrease as the transmission decreases. Any decrease that does occur is not as large as would be expected on this basis. It might be mentioned that errors in the calculation near the line centers would also be expected to decrease with the transmittance since the absorption near the line center then contributes less relative to the overall absorption.

The assumption that the matrix of the transition for the excited states was the same as that of the ground state seems to have resulted in an overestimation of the effects of these states. This is the cause of the hump in the transmittance on the low frequency side of the $C^{12}O_2^{16}$ band center. The inclusion of more excited and isotopic states should tend to reduce this hump. This hump is an indication of the effect of the excited state. The lines of the excited state are too weak and too closely spaced to be resolved, but none occur in this region for a comparatively wide interval due to the requirement that J be greater than or equal to k . This results in only lines of the primary band being present. Even if some very weak lines were present the hump would be reduced by a greater extent than those regions on either side of it.

TABLE I
Vibrational Constants

Species Constant	$C^{12}O_2^{16}$	$C^{13}O_2^{16}$	$C^{12}O^{16}O^{18}$	$C^{13}O^{16}O^{18}$	$C^{12}O_2^{18}$
$V_1(\text{cm}^{-1})$	1354.91	1354.91	1316.08	1316.08	1277.25
V_2	673.00	653.83	667.83	648.53	662.66
V_3	2396.49	2328.22	2378.07	2309.34	2359.66
x_{11}	-3.75	-3.74	-3.54	-3.54	-3.33
x_{22}	-.63	-.64	-.62	-.63	-.61
x_{33}	-12.63	-11.85	-12.43	-11.66	-12.24
x_{12}	3.65	3.50	3.52	3.37	3.39
x_{13}	-19.37	-18.89	-18.67	-18.20	-17.98
x_{23}	-12.53	-11.75	-12.34	-11.56	-12.15

TABLE II
 CO_2 Bands Used in Calculation

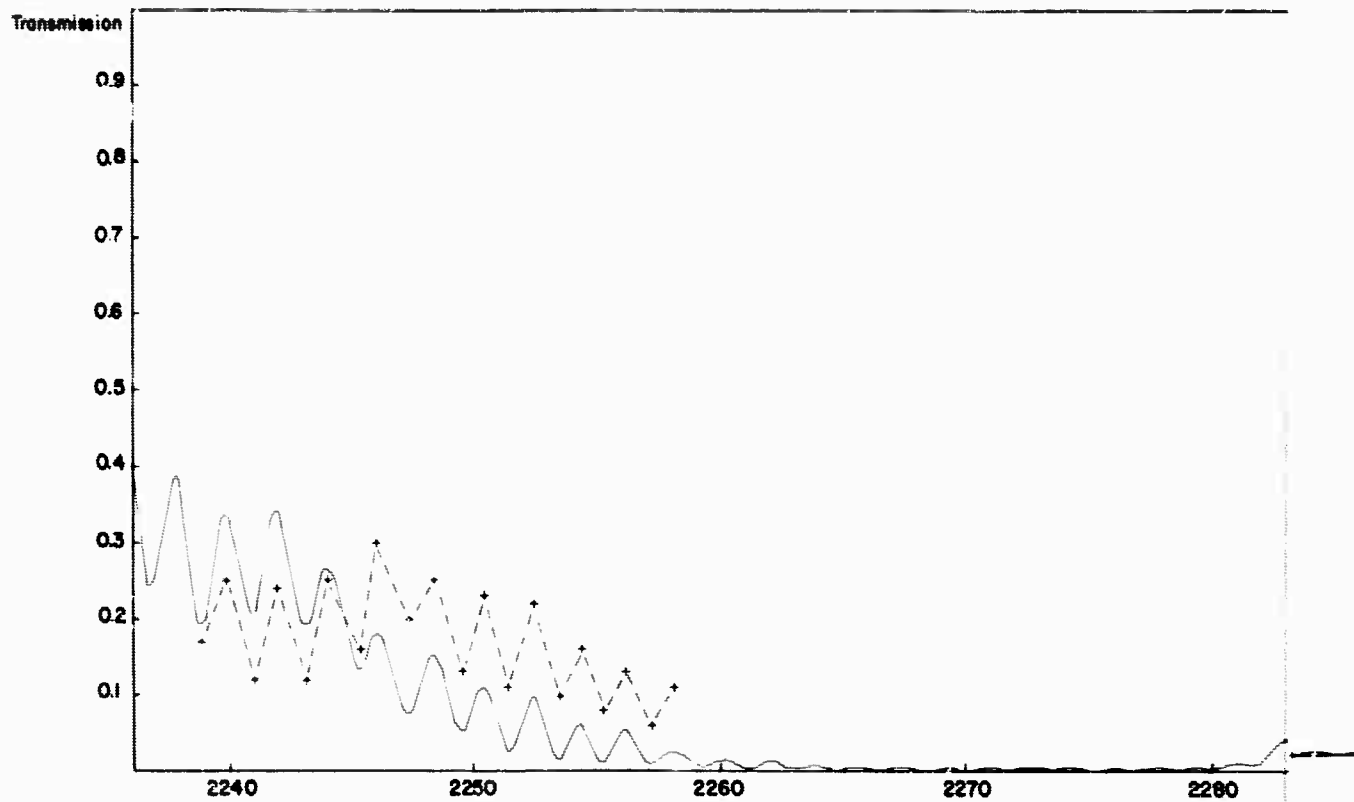
Isotope	State	Permitted J	Band Center Used	Highest J
$C^{12}O_2^{16}$	(0, 0 ⁰ , 0)	Even	2349.5	70
$C^{12}O_2^{16}$	(0, 1 ^{±1} , 0)	Even or Odd	2339.2	54
$C^{13}O_2^{16}$	(0, 0 ⁰ , 0)	Even	2283.7	70
$C^{13}O_2^{16}$	(0, 1 ^{±1} , 0)	Even or Odd	2273.4	54
$C^{12}O^{16}O^{18}$	(0, 0 ⁰ , 0)	Even or Odd	2331.8	48
$C^{13}O^{16}O^{18}$	(0, 0 ⁰ , 0)	Even or Odd	2266.0	48

TABLE III
Parameters Associated With Spectra

<u>Record</u>	<u>Time</u> <u>hr:min:sec</u>	<u>Altitude</u> <u>km</u>	<u>Sun Angle</u> <u>Degrees</u>	<u>Half Width</u> <u>cm⁻¹</u>
13	6:27 :15	10.7	14.65	1.84×10^{-2}
15	6:33 :20	12.4	15.88	1.47×10^{-2}
18	6:42 :33	14.1	17.74	1.08×10^{-2}
20	6:48 :28	15.2	18.97	9.26×10^{-3}
21	6:51 :30	15.8	19.59	8.30×10^{-3}
26	7:06 :40	18.3	22.71	5.60×10^{-3}
27	7:09 :42	18.8	23.33	5.14×10^{-3}
29	7:15 :46	19.7	24.58	4.36×10^{-3}
33	7:27 :52	21.6	27.09	3.19×10^{-3}
34	7:30 :55	22.0	27.72	2.97×10^{-3}
36	7:36 :59	23.0	28.97	2.59×10^{-3}
37	7:40 :00	23.4	29.60	2.42×10^{-3}
38	7:43 :01	23.8	30.23	2.25×10^{-3}
39	7:46 :02	24.3	30.86	2.10×10^{-3}
42	7:55 :05	25.6	32.75	1.72×10^{-3}
43	7:58 :07	26.1	33.38	1.58×10^{-3}
44	8:01 :08	26.6	34.01	1.48×10^{-3}
45	8:04 :09	27.0	34.64	1.35×10^{-3}
46	8:07 :09	27.4	35.27	1.29×10^{-3}
47	8:10 :10	27.9	35.90	1.20×10^{-3}
49	8:16 :10	28.8	37.16	1.03×10^{-3}
50	8:19 :10	29.2	37.80	9.82×10^{-4}
51	8:22 :11	29.6	38.43	9.29×10^{-4}
52	8:25 :11	30.0	39.06	8.66×10^{-4}
54	8:31 :11	30.4	40.32	8.26×10^{-4}
55	8:34 :11	30.8	40.95	7.78×10^{-4}
57	8:40 :11	31.4	42.21	7.03×10^{-4}
58	8:43 :11	31.7	42.83	6.75×10^{-4}
59	8:46 :11	32.0	43.46	6.50×10^{-4}
60	8:49 :11	32.3	44.09	6.21×10^{-4}
61	8:52 :10	32.5	44.72	5.84×10^{-4}

FOOTNOTES

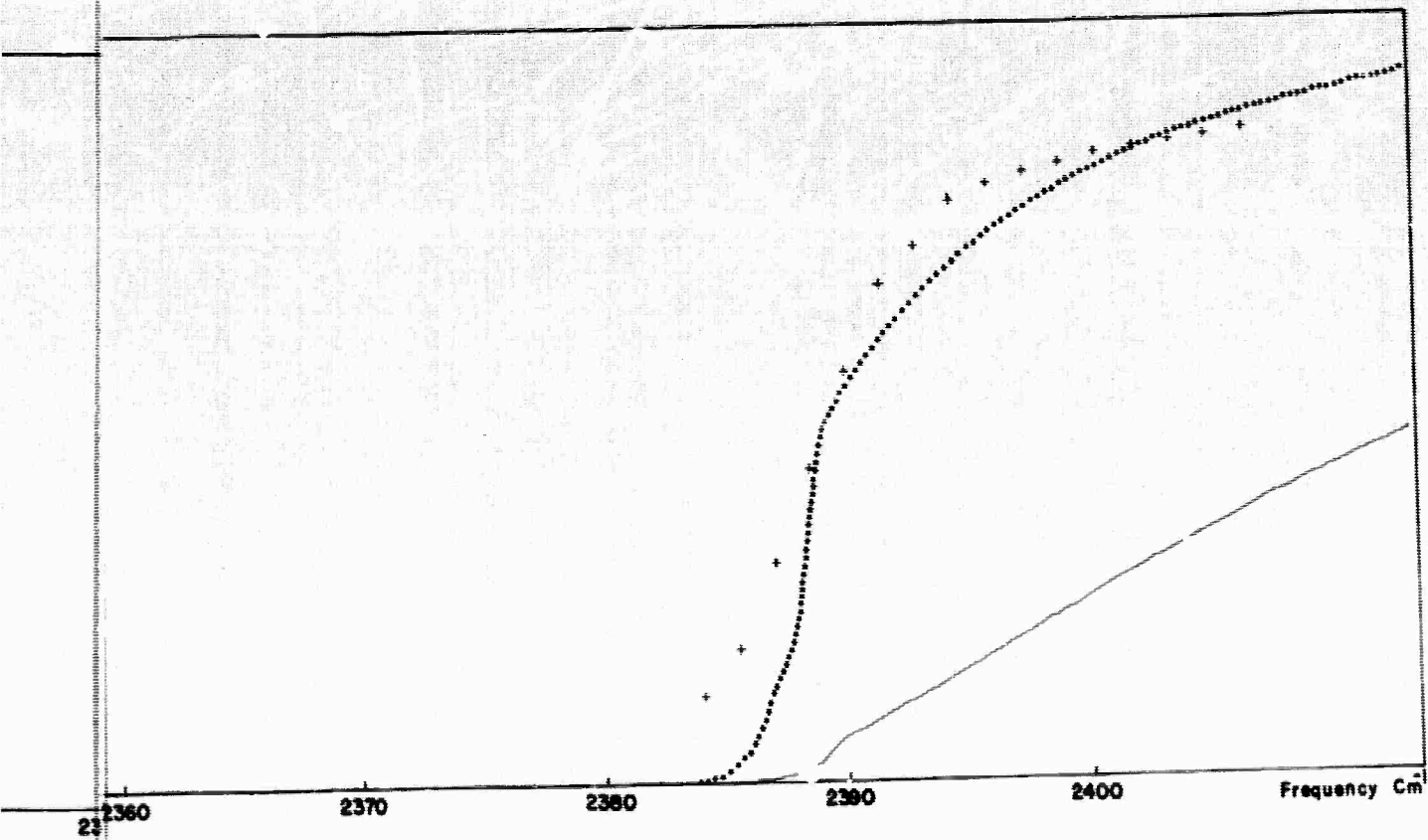
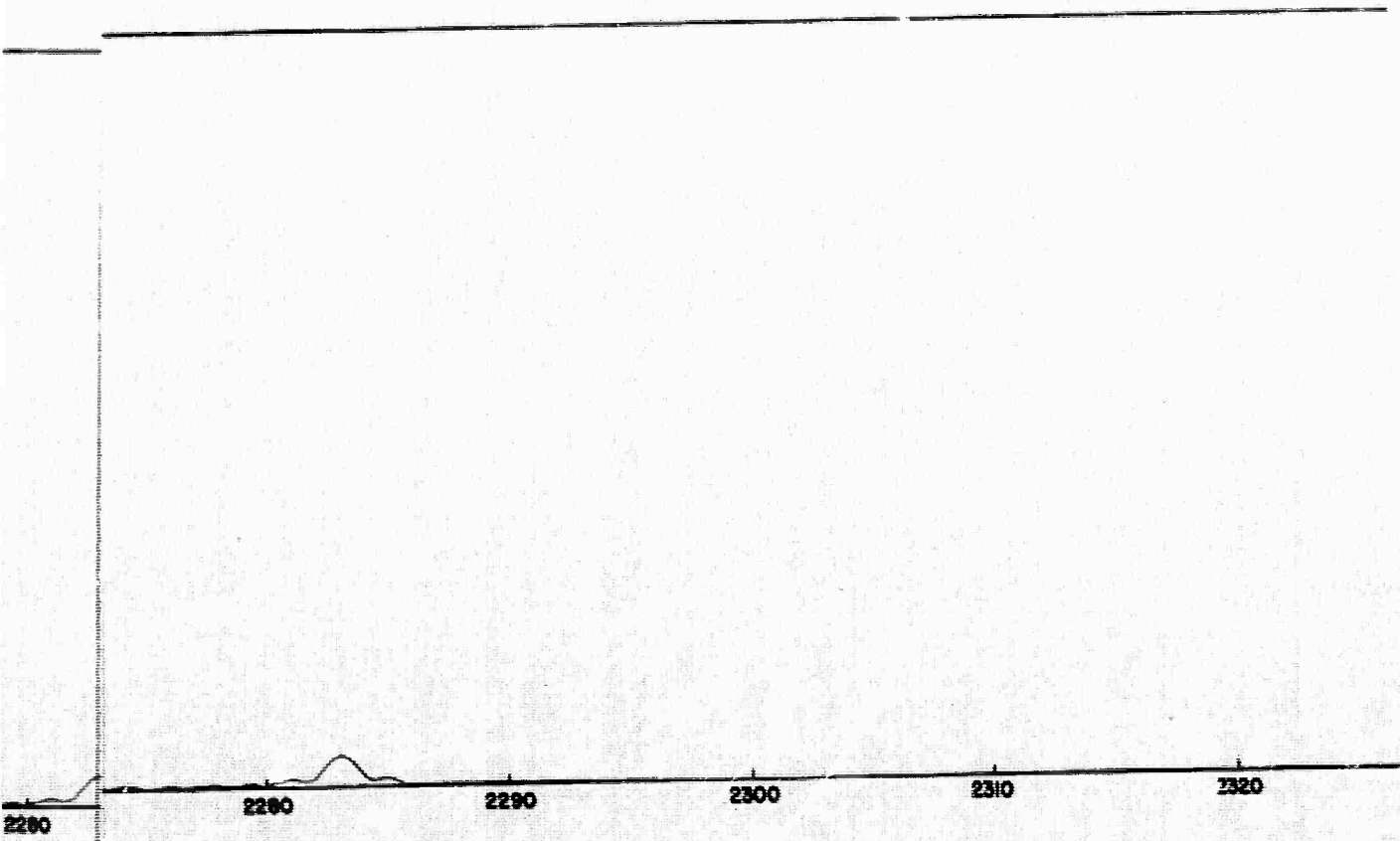
- ¹ D. G. Murcray, F. H. Murcray and W. J. Williams, *J. Opt. Soc. Amer.* 55, (1965).
- ² G. N. Plass, P. J. Wyatt, V. R. Stull, *Applied Optics* 3, 479(1964).
- ³ G. N. Plass, P. J. Wyatt, V. R. Stull, *Applied Optics* 3, 243(1964).
- ⁴ D. M. Dennison, *Rev. Mod. Phys.* 12, 175(1940).
- ⁵ C. P. Courtoy, *Can. J. of Phys.* 35, 608(1957).
- ⁶ D. M. Dennison, *Rev. Mod. Phys.* 3, 280(1931).
- ⁷ H. A. Lorentz, *Proc. Roy. Ac. (Amsterdam)*, 8, 591(1906).
- ⁸ B. H. Winters, S. Silverman, and W. S. Benedict, *J. Quant. Spec. Rad. Trans.* 4, 527(1964).
- ⁹ J. Strong and G. N. Plass, *Astrophys. J.* 112, 365(1950).



2320 2330 2340 2350 2360 2360

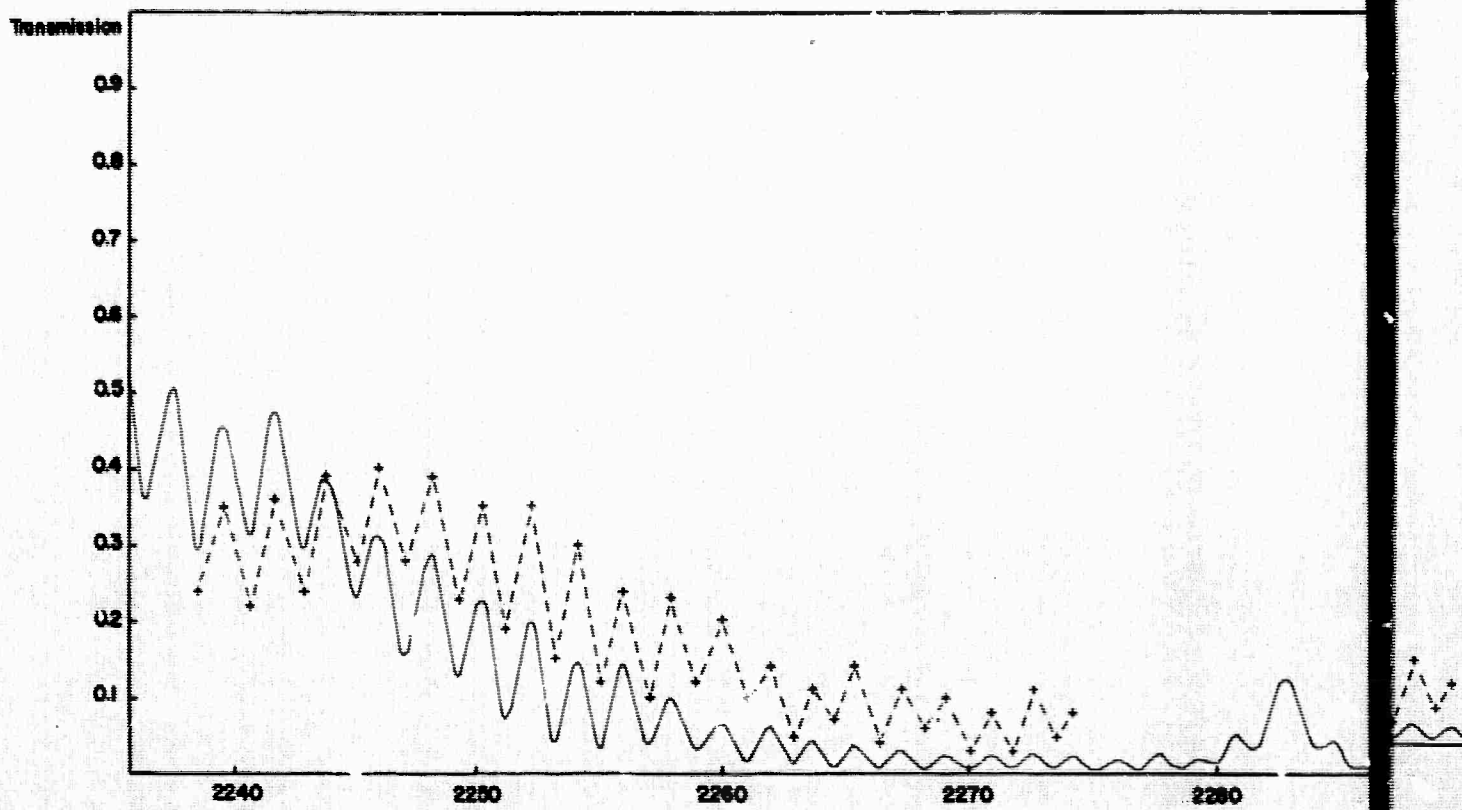
Figure 1. (Record 13) Comparison between Experimental and Calculated Transmission for the 4.3μ CO_2 Band at an Altitude of 10.7 km. (— calculated; +----+ experimental; Baseline)

A



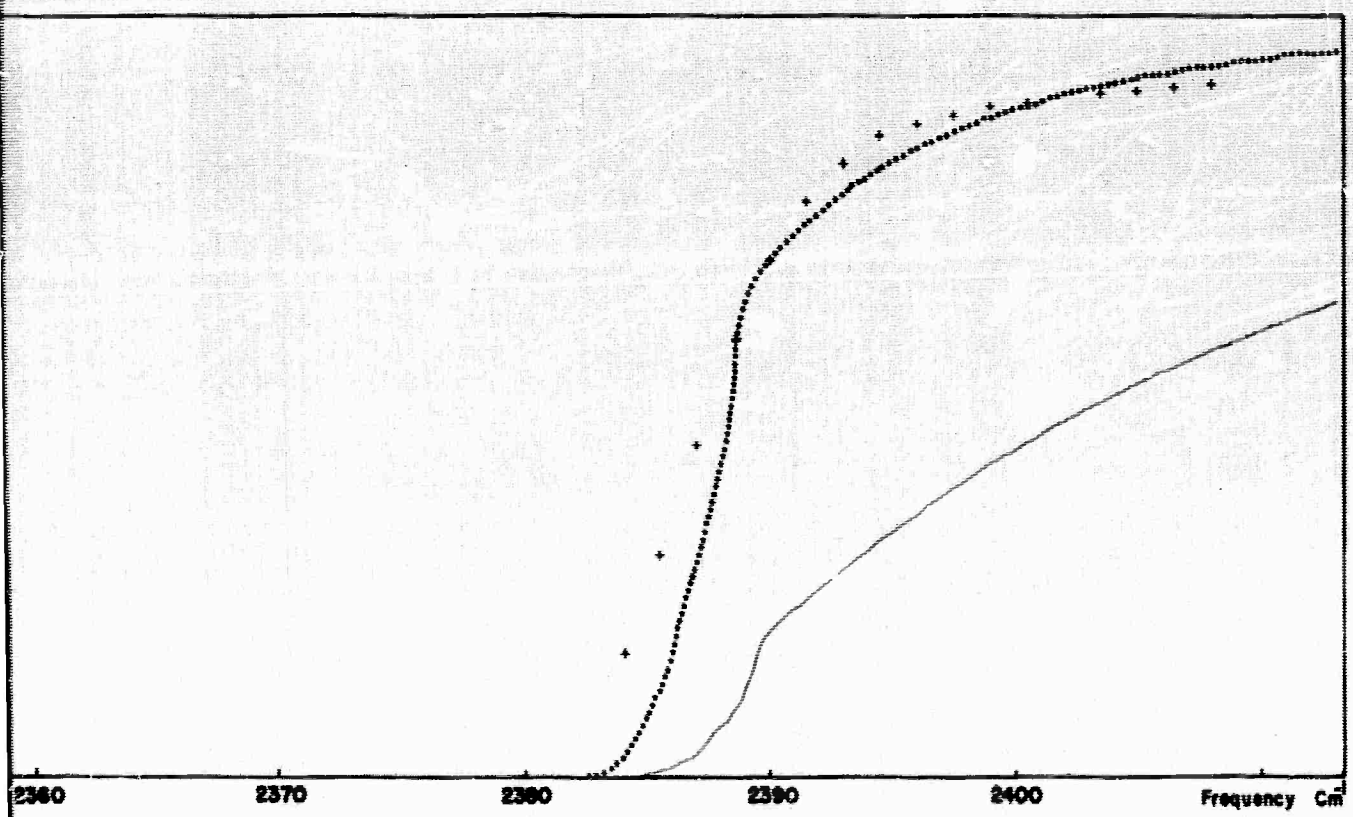
Comparison of Experimental and Theoretical Spectral Transmittance Data
at an Altitude of 10.7 km and a Solar Elevation of 14.65 Degrees.
(... Experimental; Benedict modification)

B



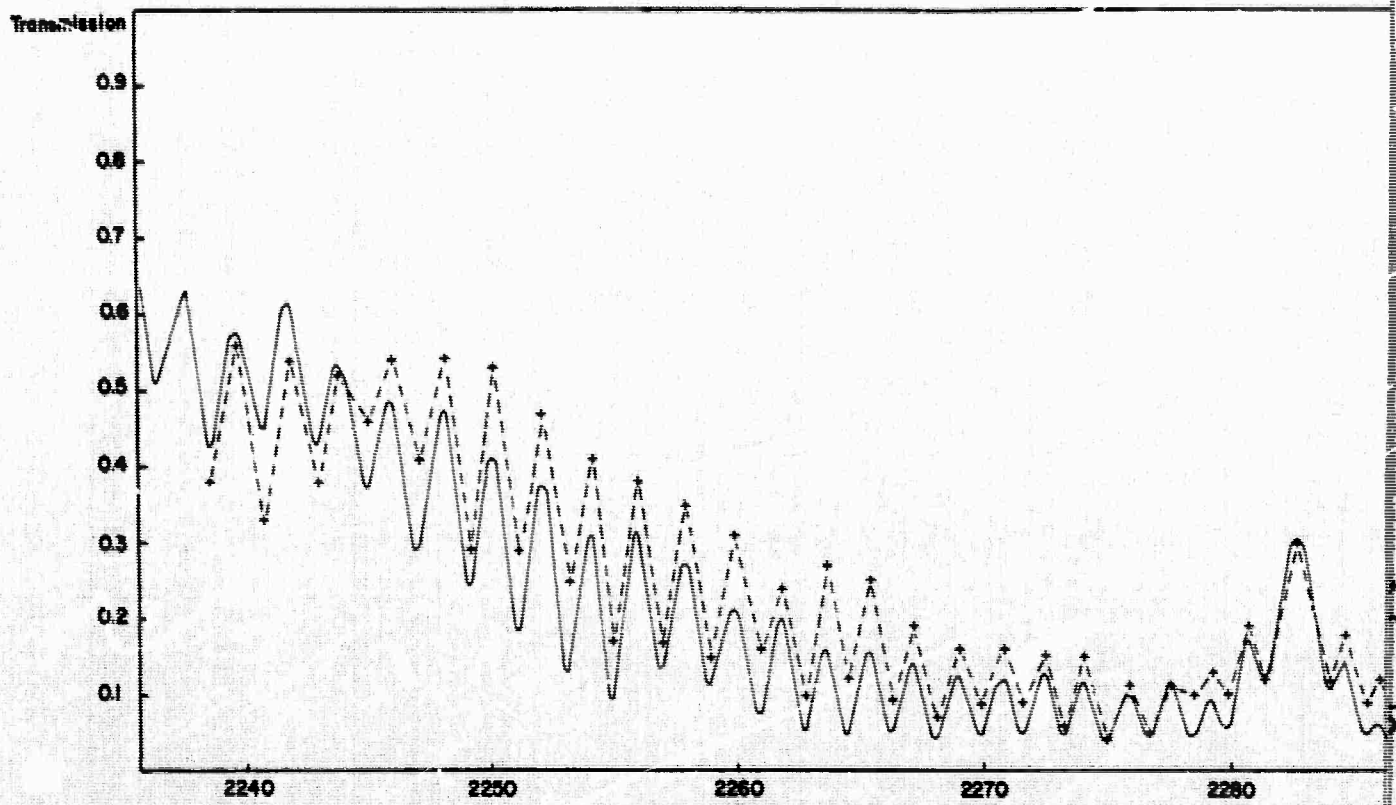
2320 2330 2340 2350 2360 2370 2380

Figure 2. (Record 15) Comparison between Experimental and Calculated Transmission for the 4.3μ CO_2 Band at an Altitude of 12.4 km and 1000 mb. (— calculated; +---+ experimental; Benedict)



Experimental and Theoretical Spectral Transmittance Data
at an Altitude of 12.4 km and a Solar Elevation of 15.88 Degrees.
(--- Experimental; Benedict modification)

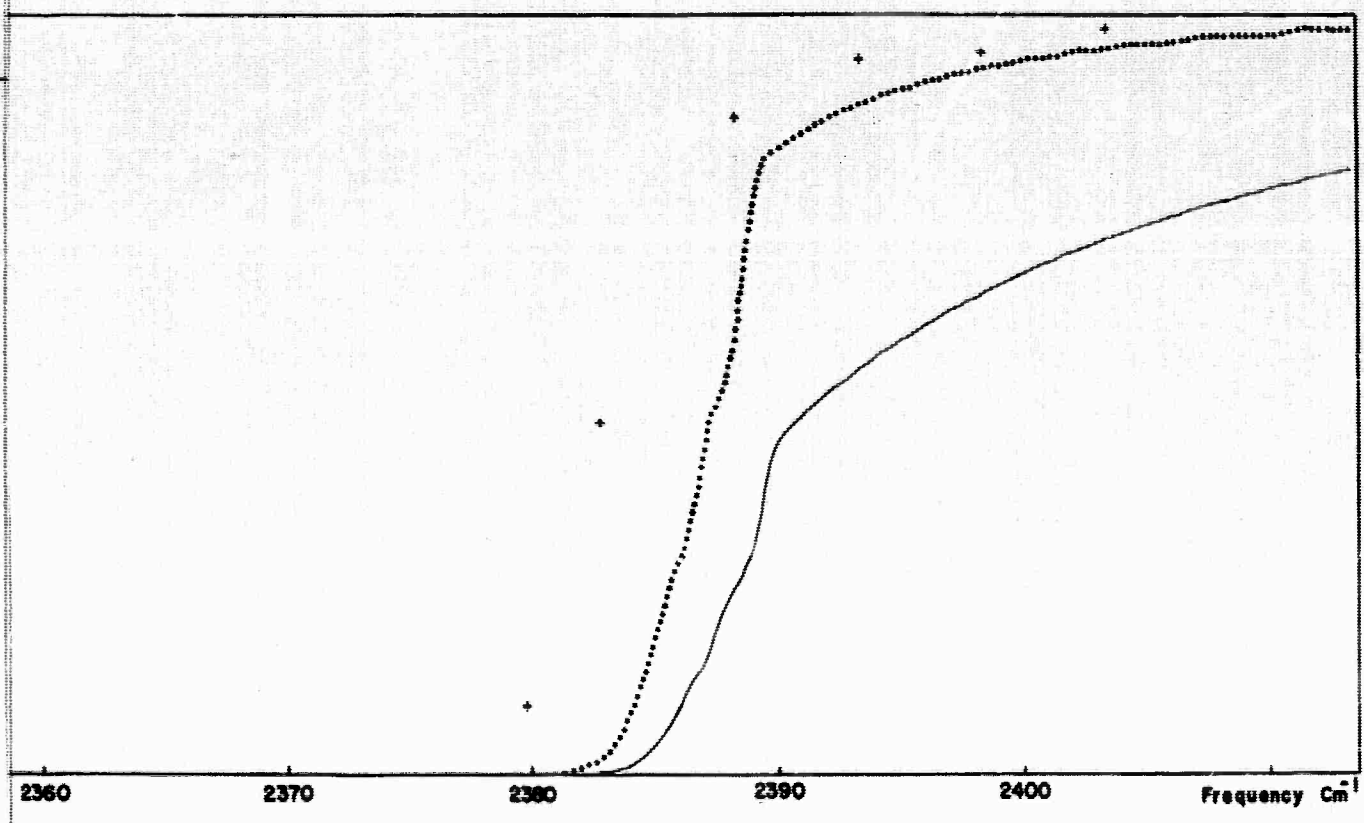
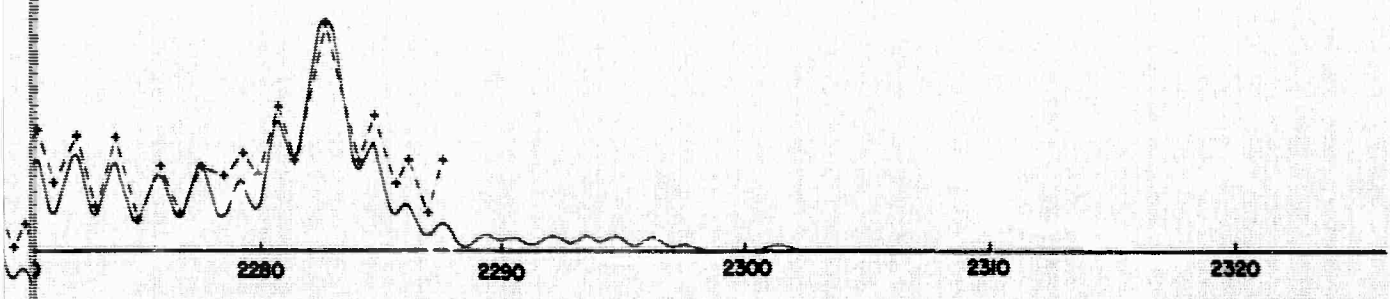
B



2320 2330 2340 2350 2360 2370

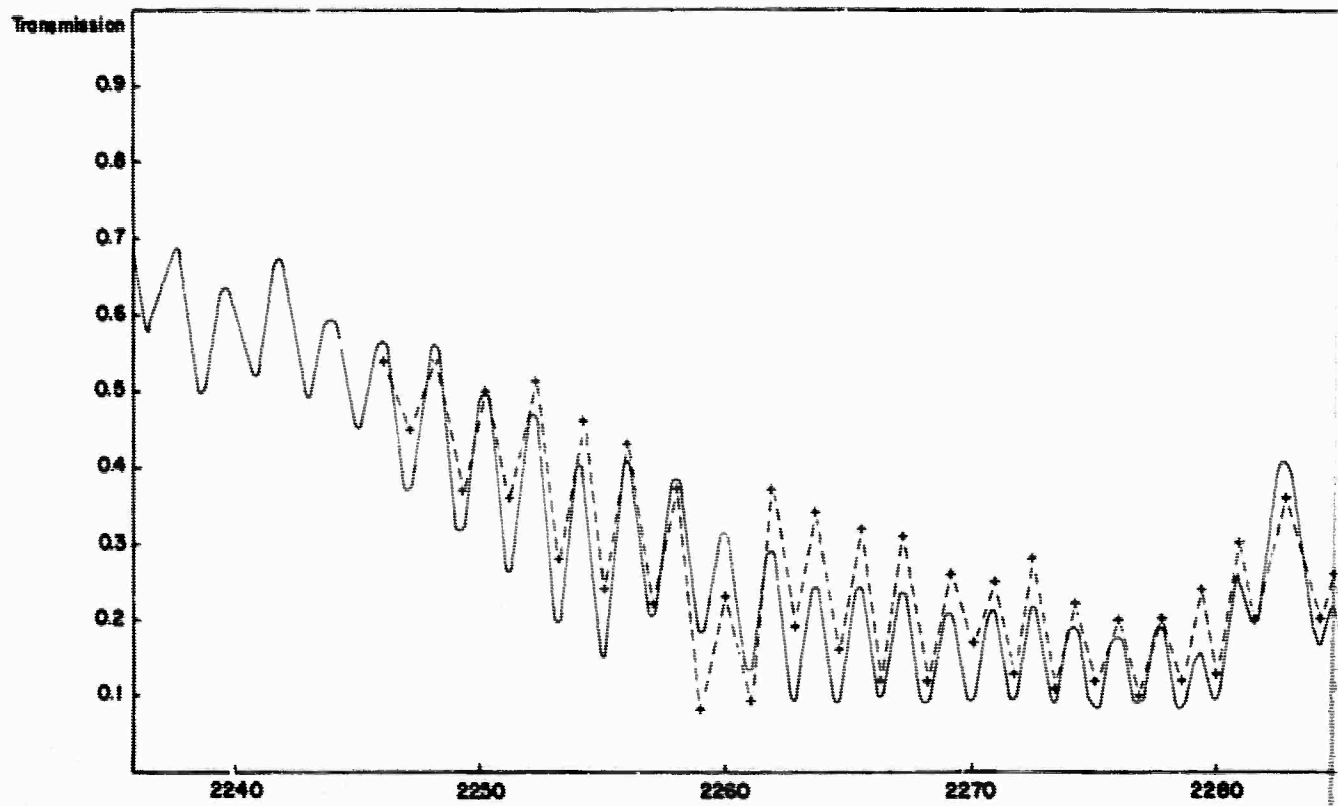
Figure 3. (Record 18) Comparison between Experimental and Calculated for the 4.3μ CO_2 Band at an Altitude of 14.1 km and Benedict's (— calculated; +---+ experimental; ··· Benedict's)

A



Comparison of Experimental and Theoretical Spectral Transmittance Data
at an Altitude of 14.1 km and a Solar Elevation of 17.74 Degrees.
(Experimental; Benedict modification)

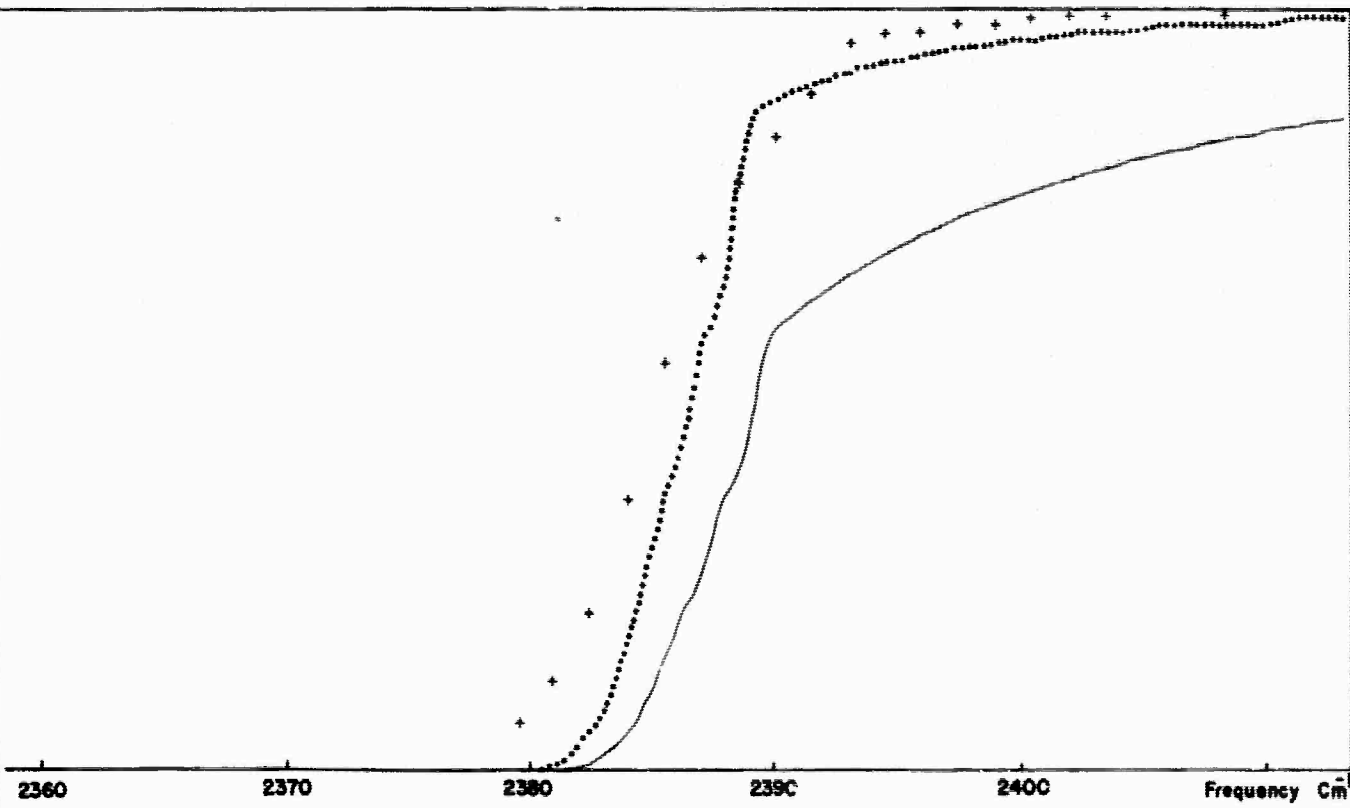
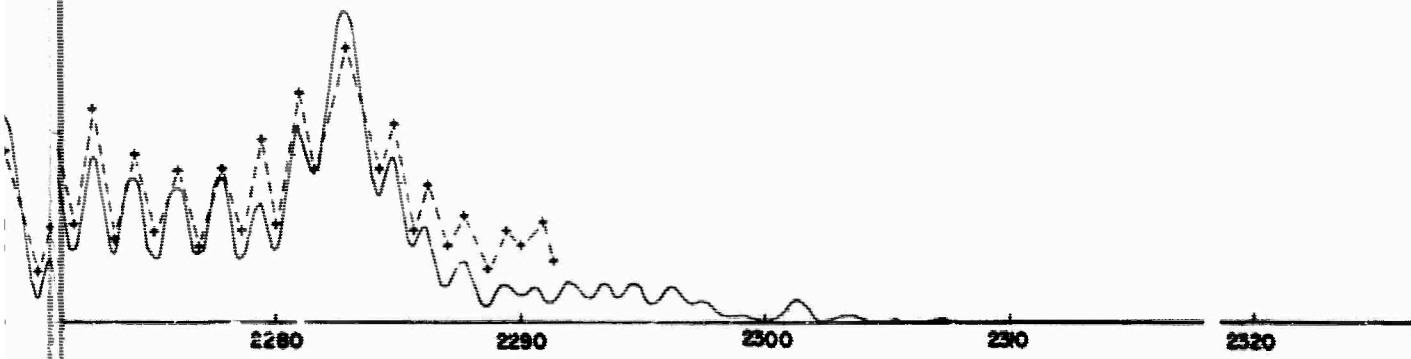
B



2320 2330 2340 2350 2360 2370

Figure 4. (Record 20) Comparison between Experimental and Calculated Transmission for the 4.3μ CO_2 Band at an Altitude of 15.2 km; (— calculated; +----+ experimental; ···· Benedict's)

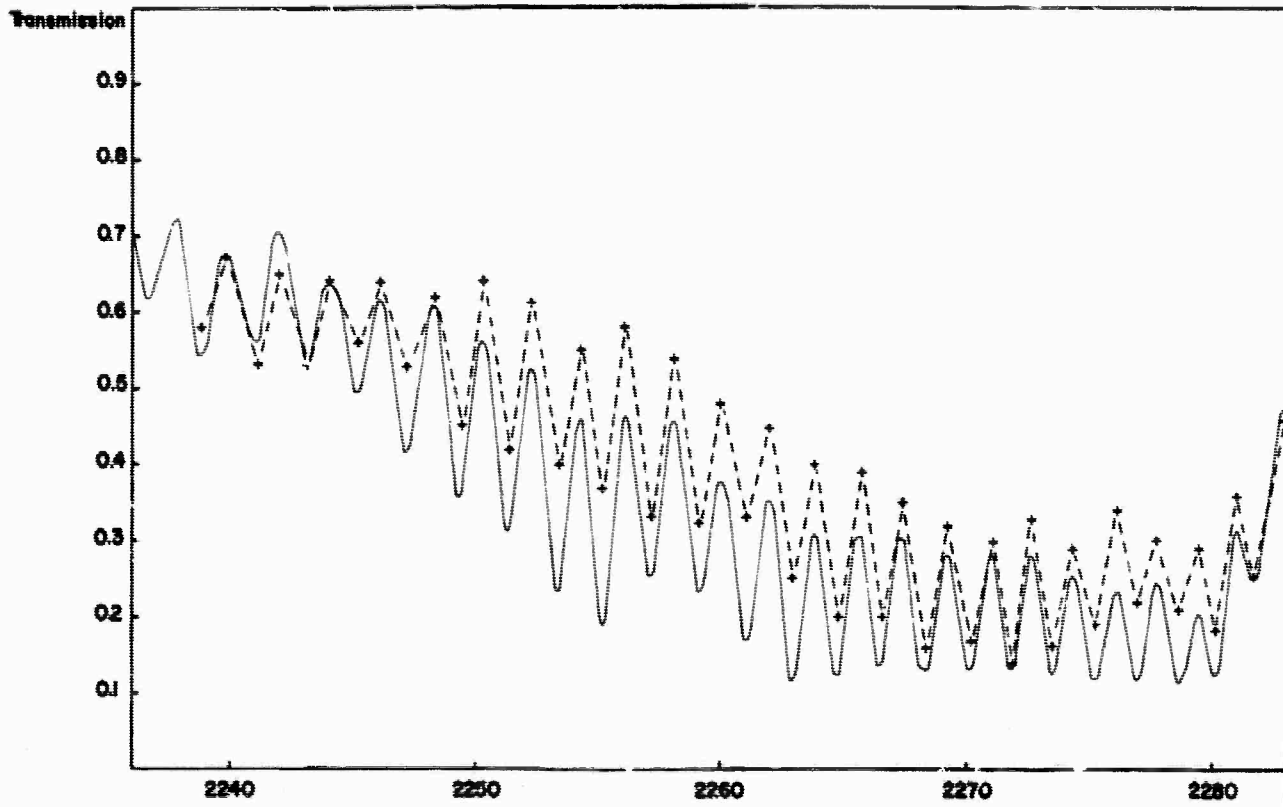
A



Comparison of Experimental and Theoretical Spectral Transmittance Data
at an altitude of 15.2 km and a Solar Elevation of 18.97 Degrees.
(Experimental; Benedict modification)

370
al a
m
ene

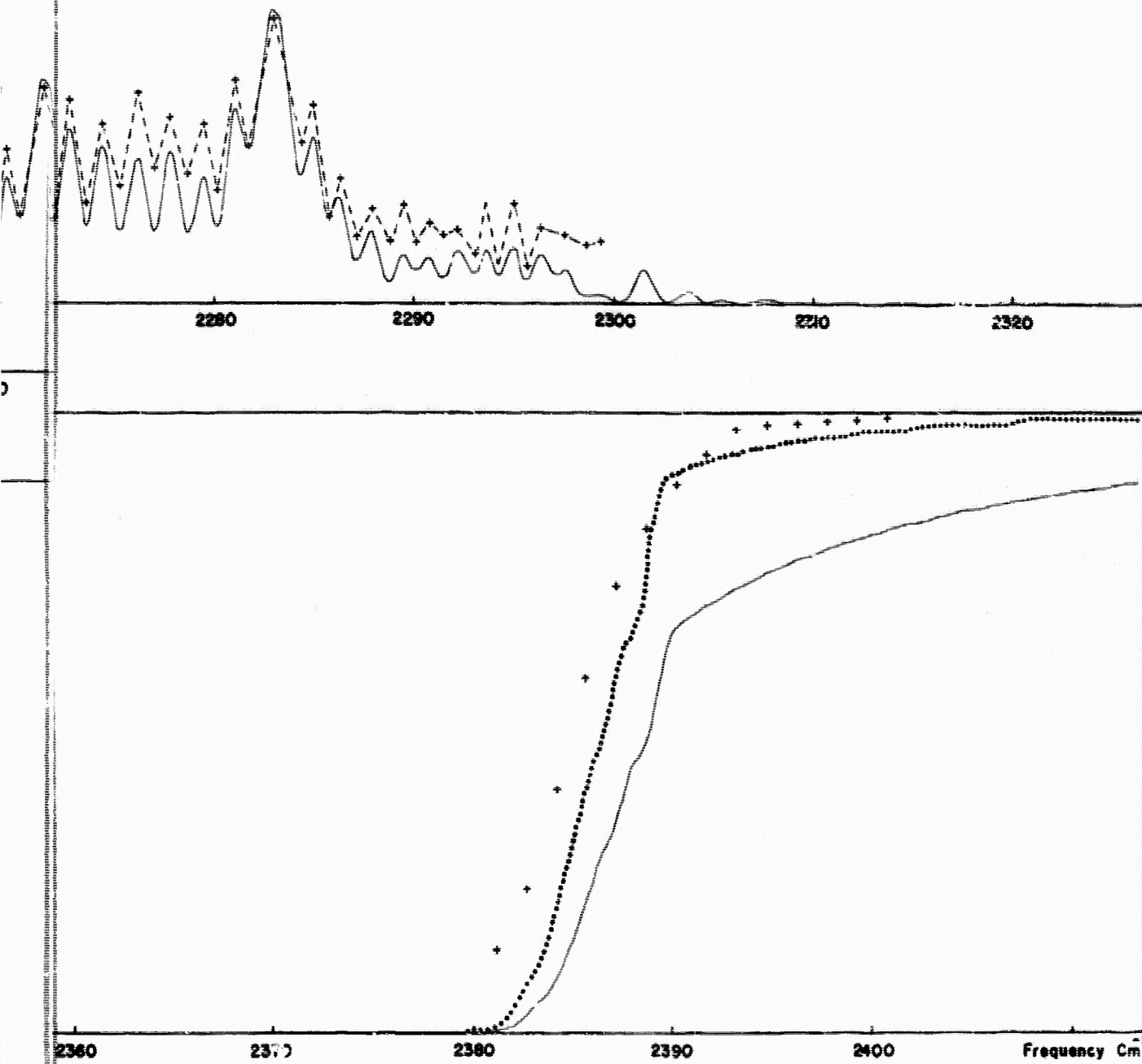




2320 2330 2340 2350 2360 2370

Figure 5. (Record 21) Comparison between Experimental and Calculated Transmission for the 4.3μ CO_2 Band at an Altitude of 15.8 km (— calculated; +---+ experimental; Be)

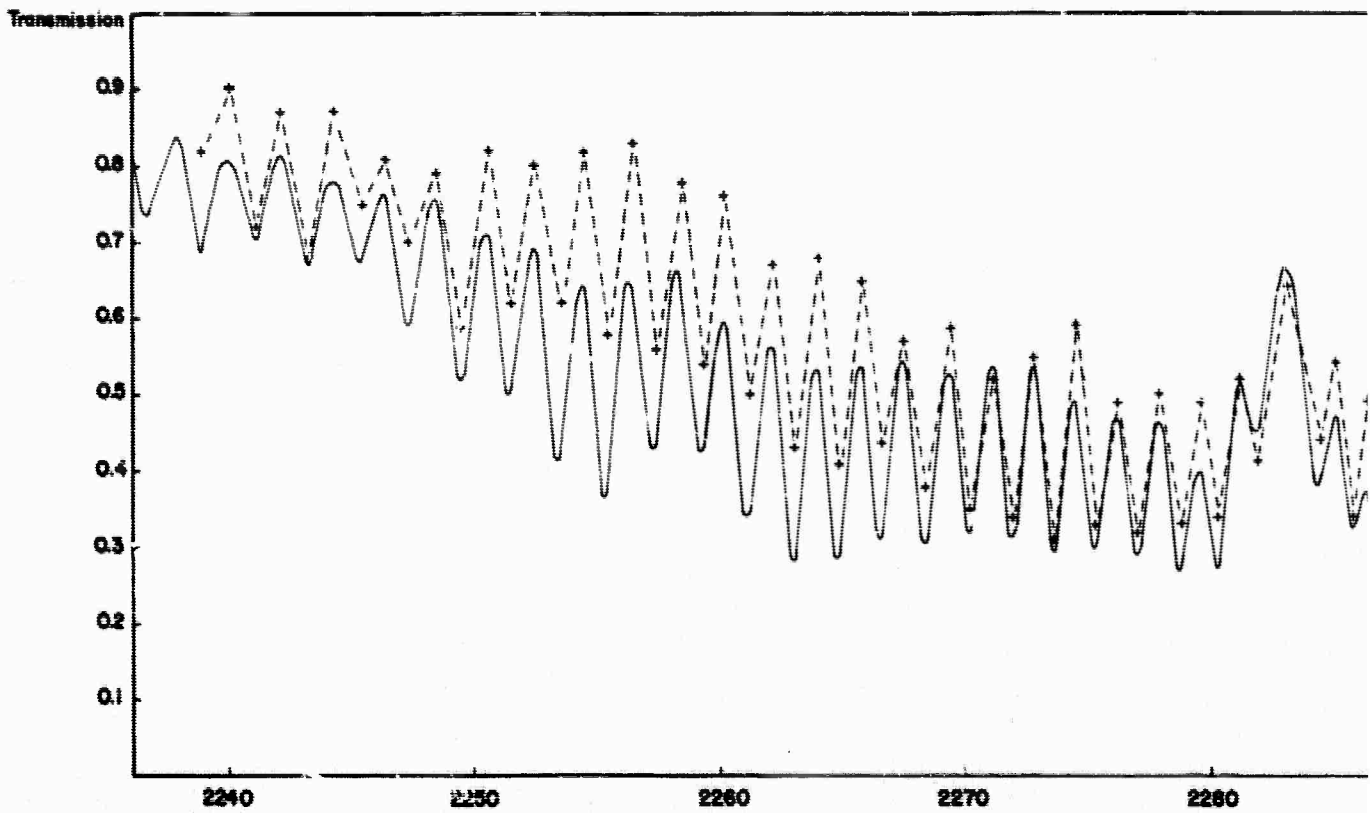




237
 Experimental and Theoretical Spectral Transmittance Data
 at an Altitude of 15.8 km and a Solar Elevation of 19.59 Degrees.
 (..... Benedict modification)

8 km
 Be

8



2320

2330

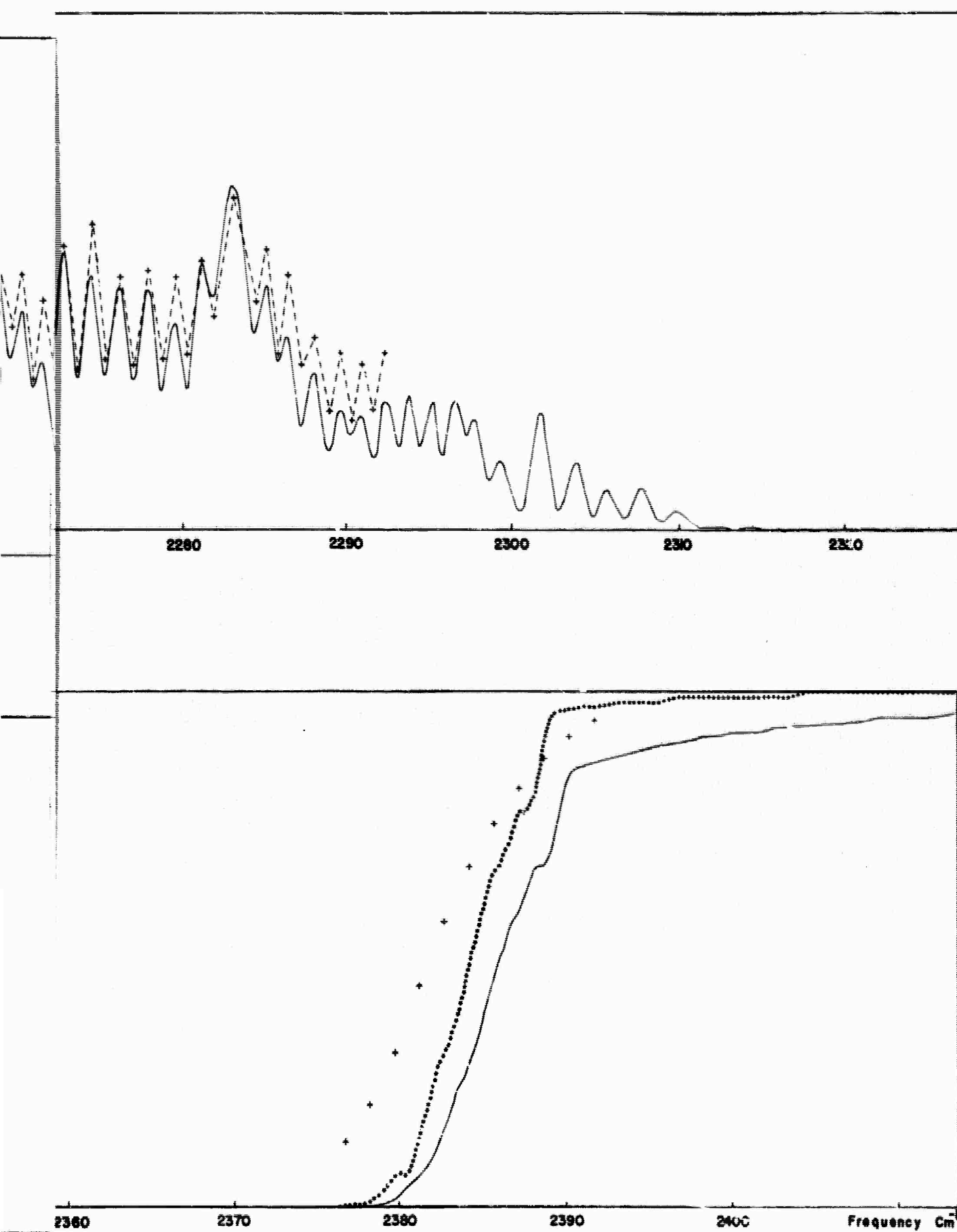
2340

2350

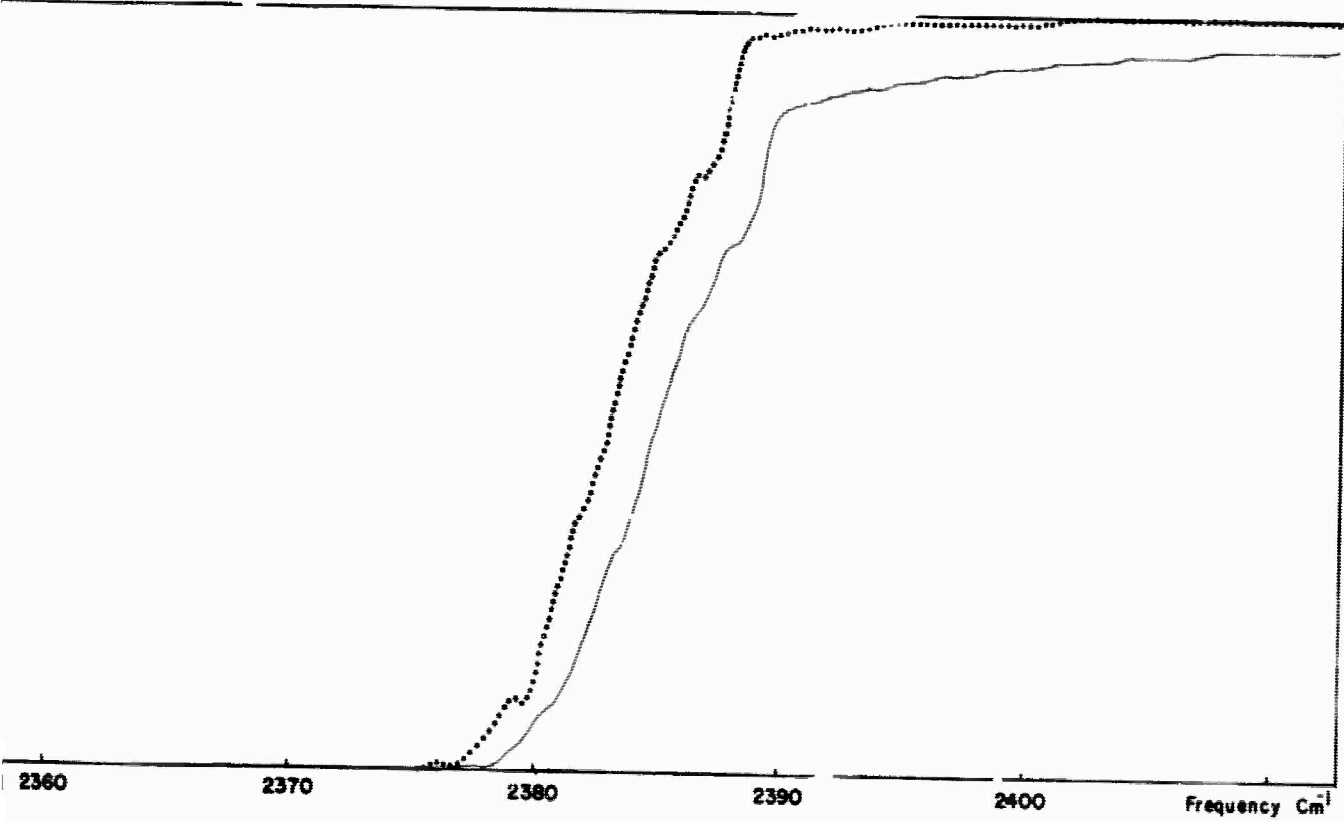
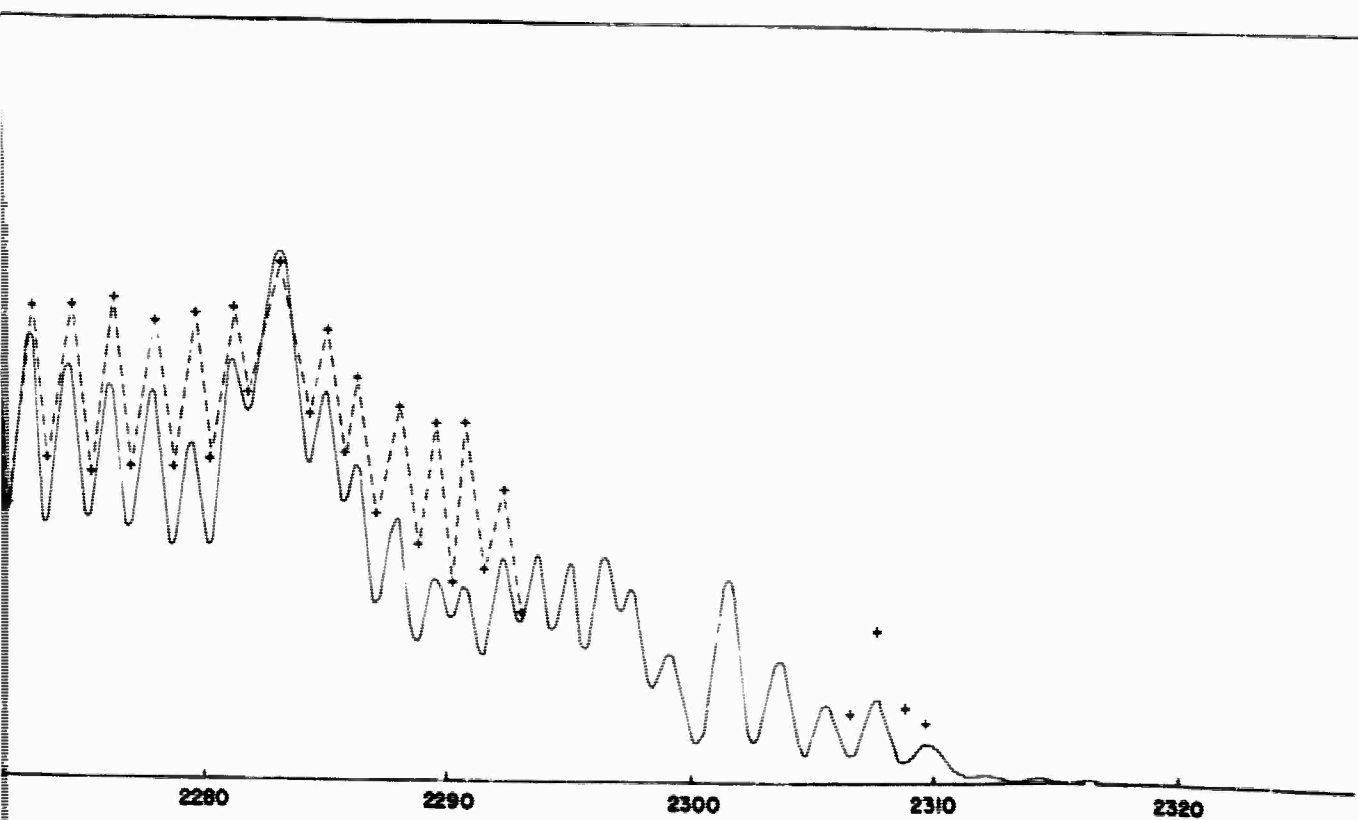
2360

2370

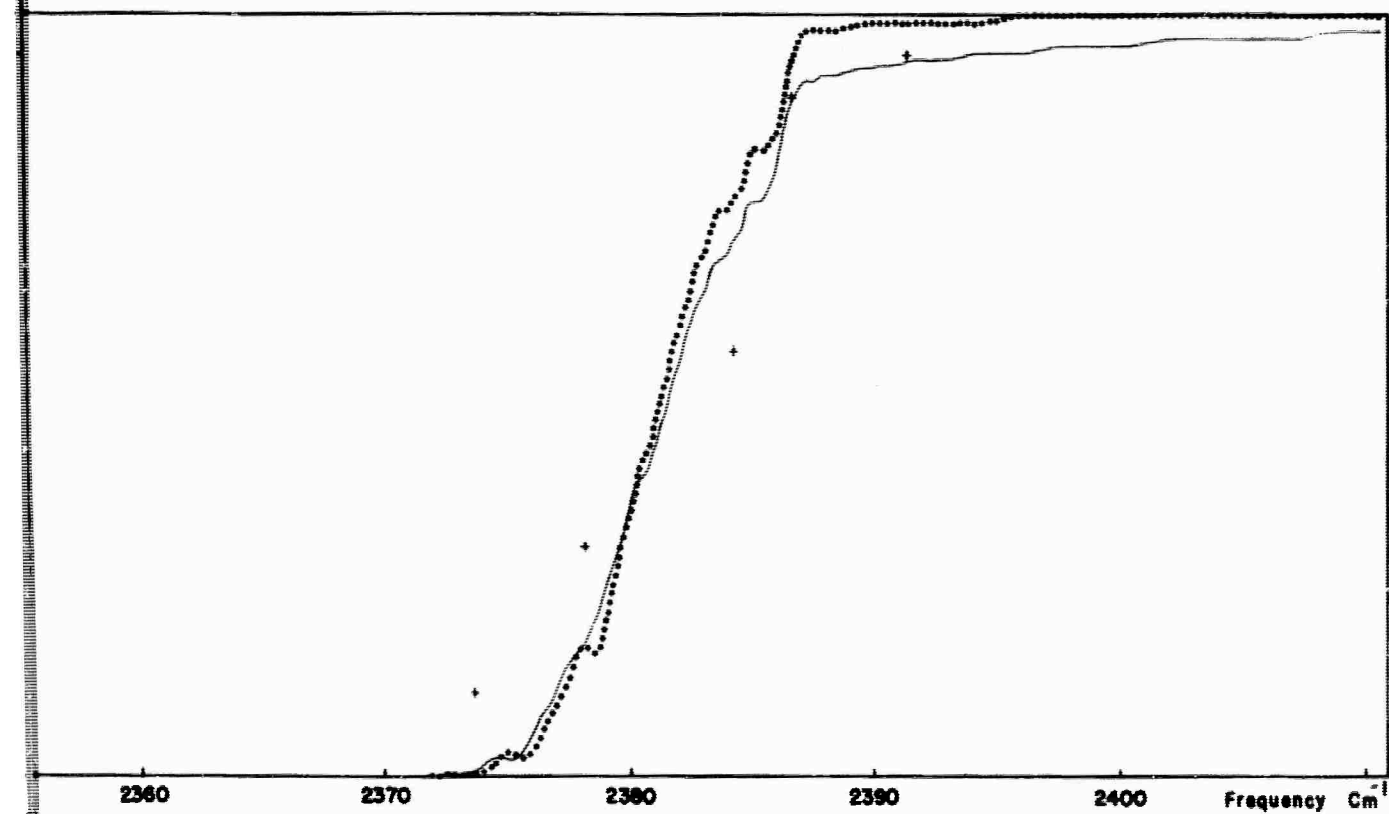
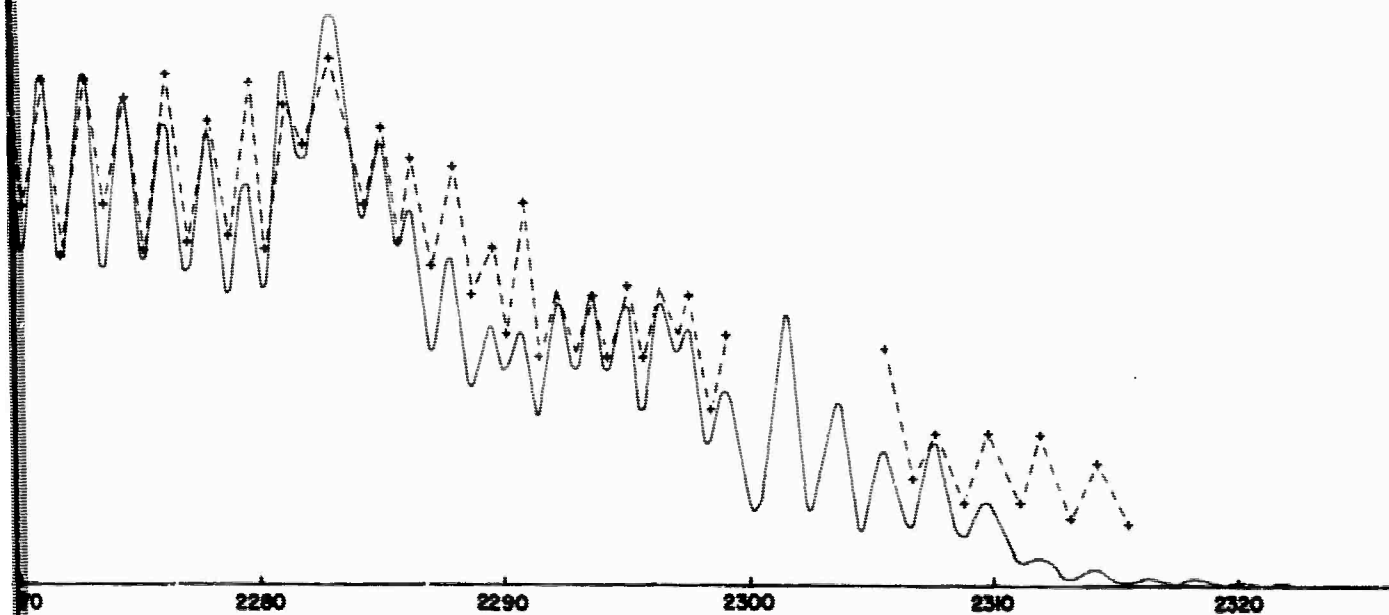
Figure 6. (Record 26) Comparison between Experimental and Calculated Values for the 4.3μ CO_2 Band at an Altitude of 18.3 km and 1000 mb. (— calculated; +---+ experimental; \cdots Benedict)



Experimental and Theoretical Spectral Transmittance Data
 and altitude of 18.3 km and a Solar Elevation of 22.71 Degrees.
 (Experimental; ···· Benedict modification)
 Benedict



Experimental and Theoretical Spectral Transmittance Data
 at an altitude of 18.8 km and a Solar Elevation of 27.33 Degrees.
 (— Experimental; ···· Benedict modification)



Comparison of Experimental and Theoretical Spectral Transmittance Data
at an Altitude of 19.7 km and a Solar Elevation of 24.58 Degrees.
(Solid line: Experimental; Benedict modification)

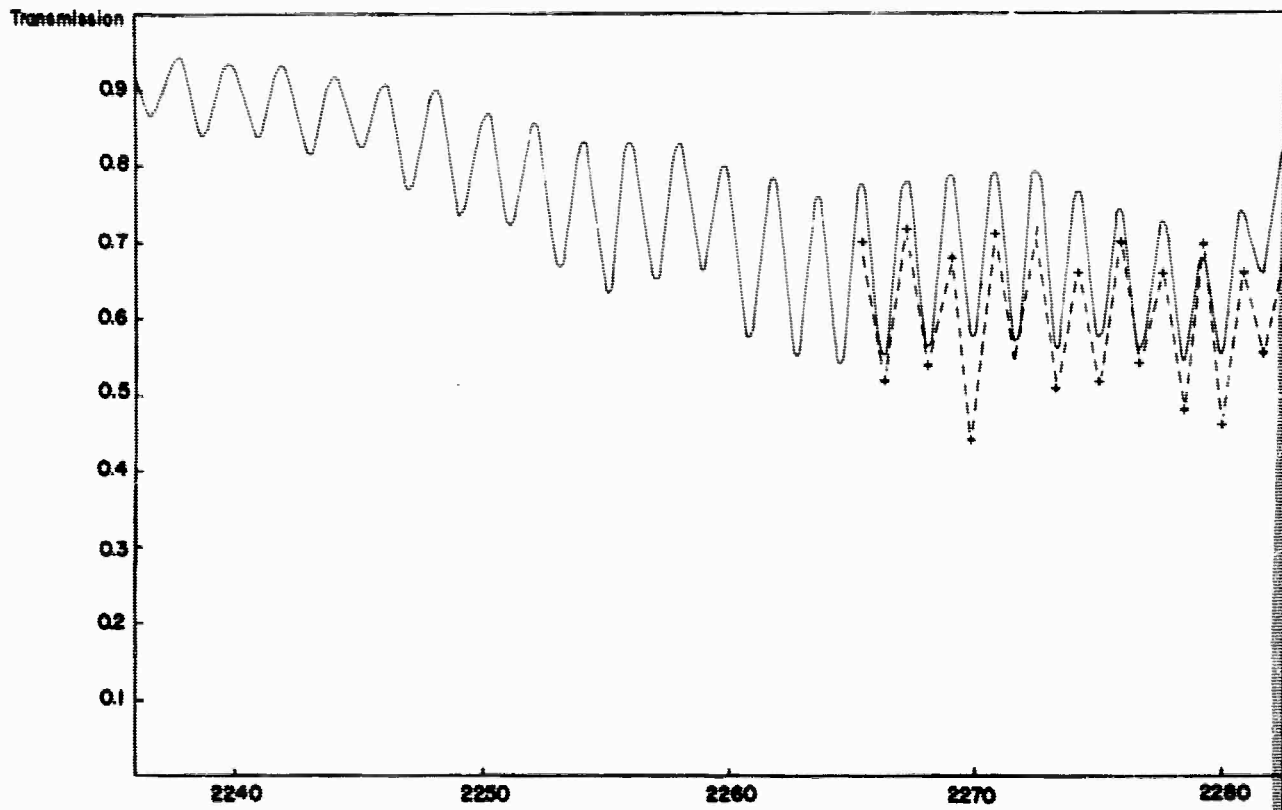
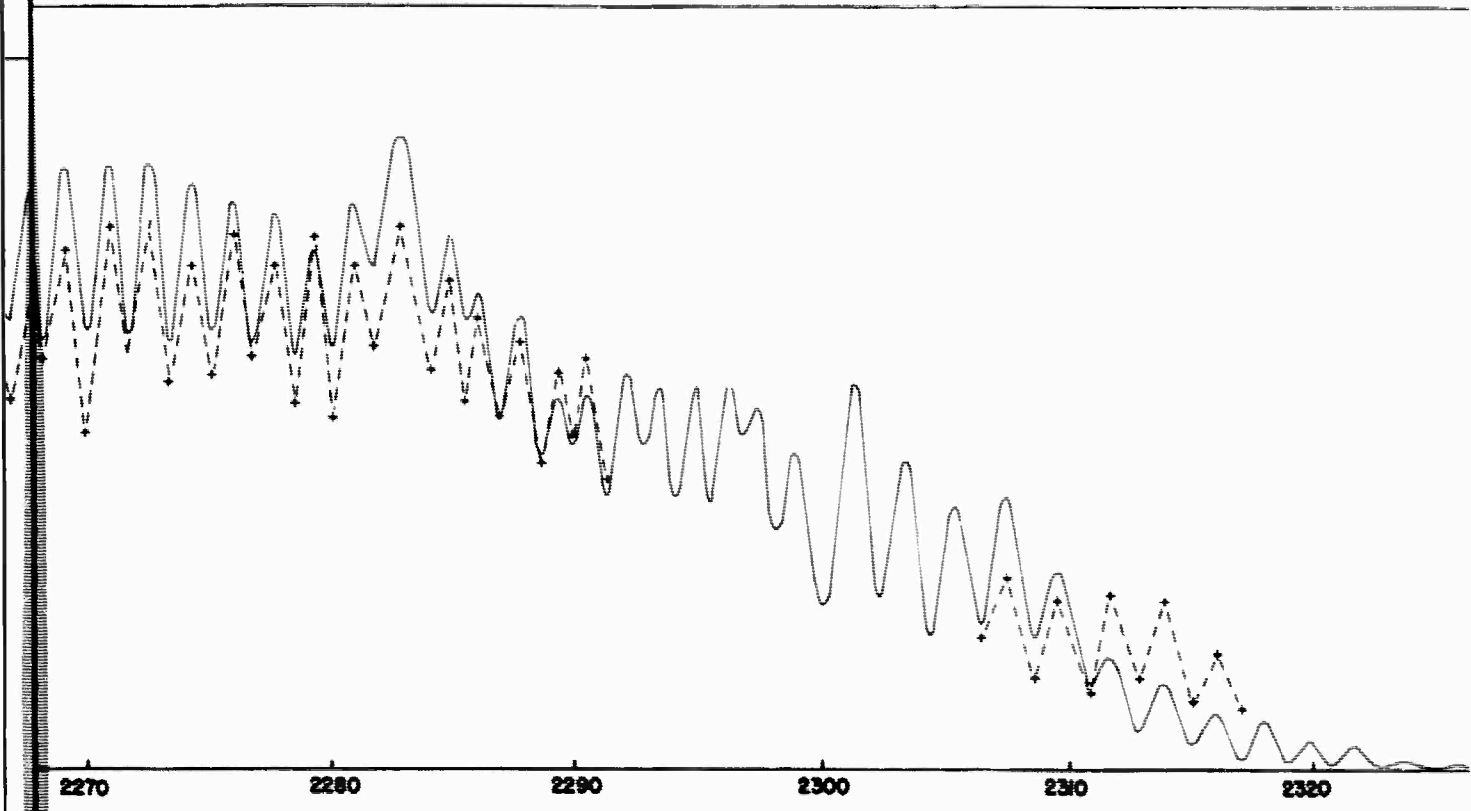
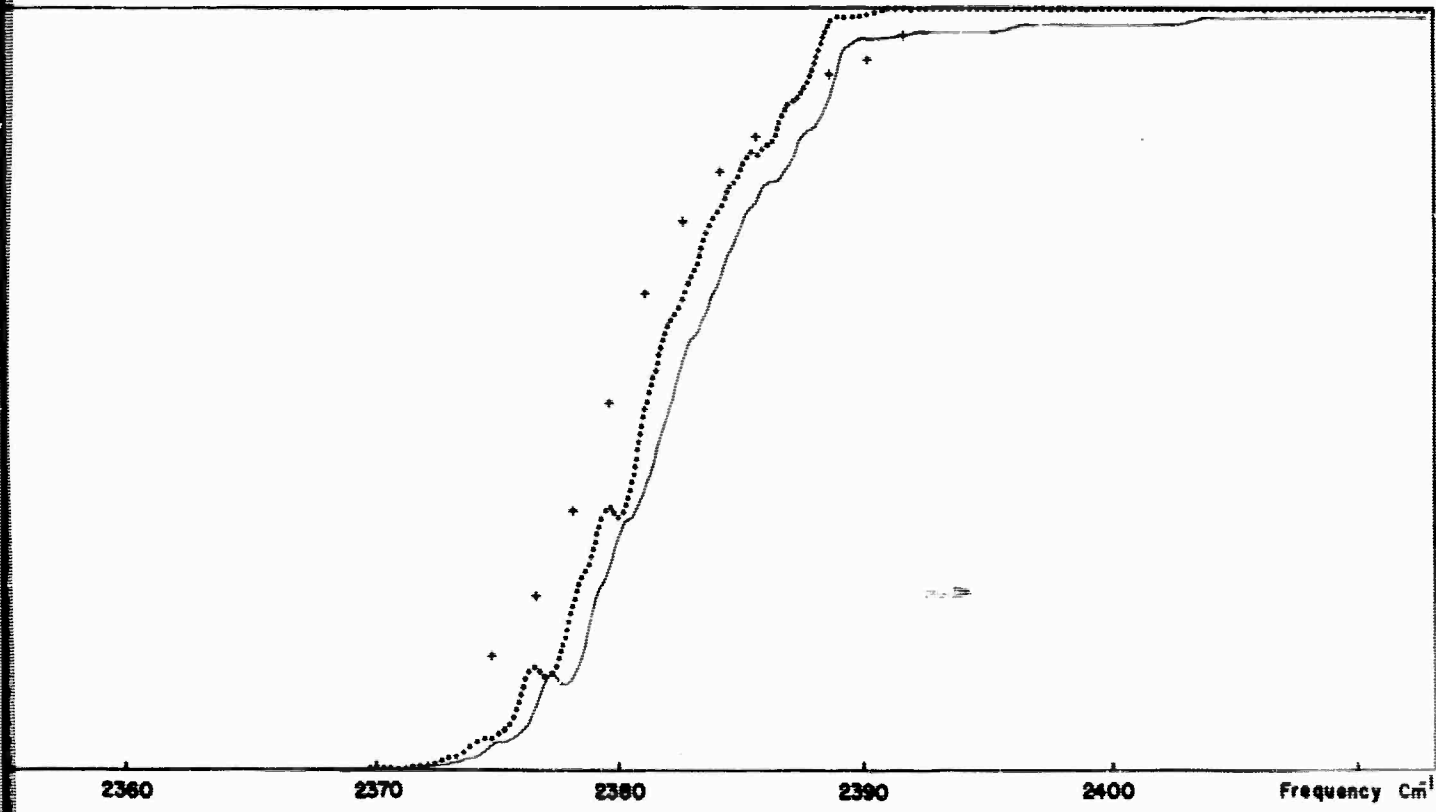


Figure 9. (Record 33) Comparison between Experimental and Calculated Transmission for the 4.3μ CO_2 Band at an Altitude of 21.6 km. (— calculated; +---+ experimental; Experimental)



2270 2280 2290 2300 2310 2320



2360 2370 2380 2390 2400 Frequency cm^{-1}

Comparison of Experimental and Theoretical Spectral Transmittance Data
 at an Altitude of 21.6 km and a Solar Elevation of 27.09 Degrees.
 (— Experimental; ···· Benedict modification)

B

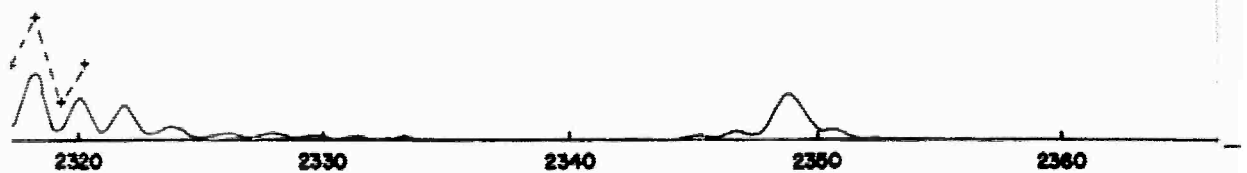
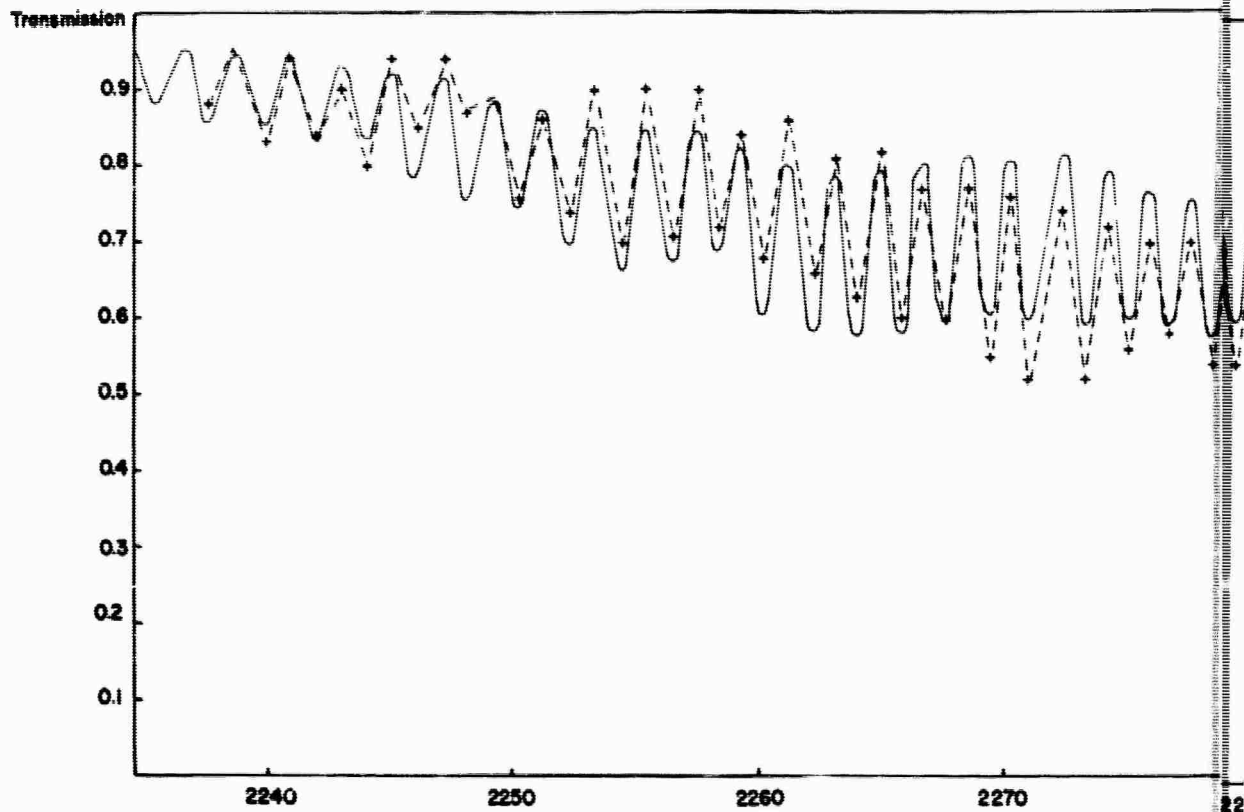
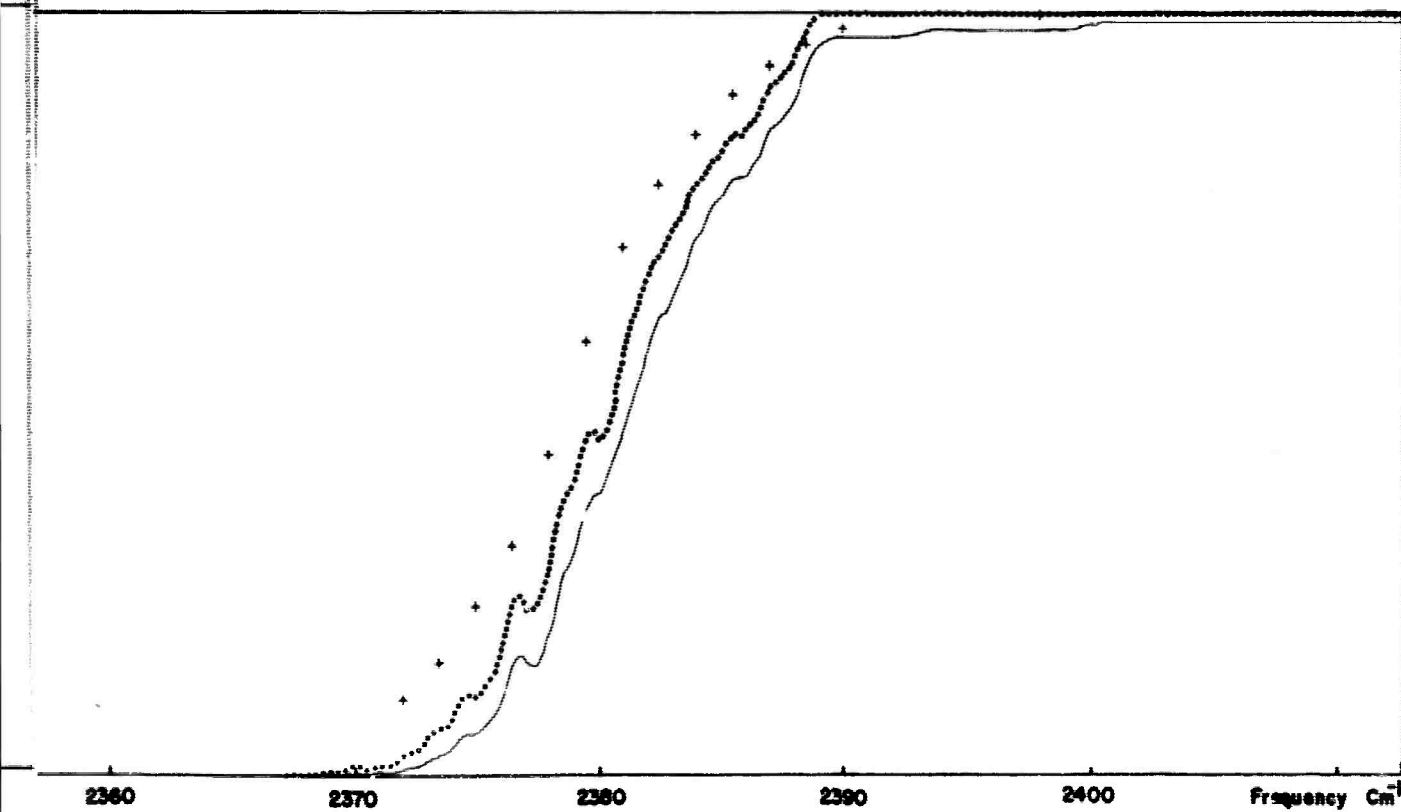
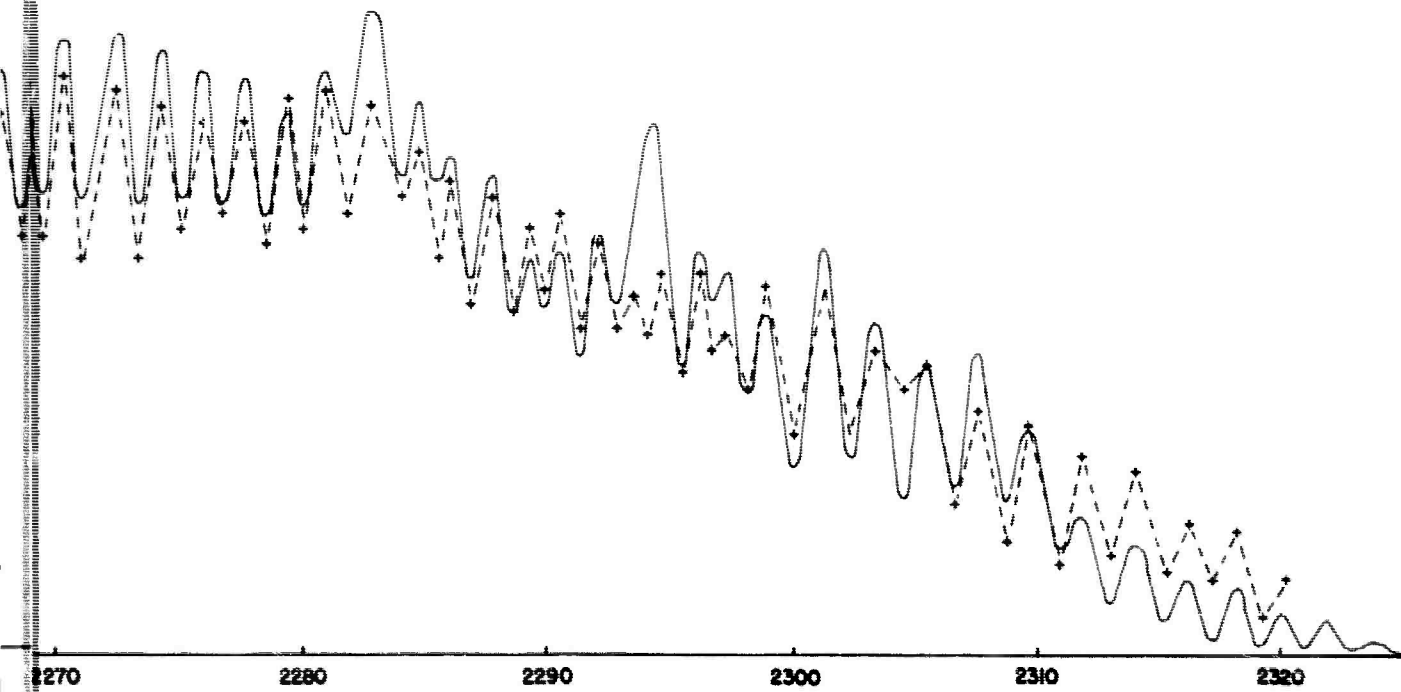


Figure 10. (Record 34) Comparison between Experimental and Calculated Transmission for the 4.3μ CO_2 Band at an Altitude of 22,000 ft. (— calculated; +---+ experimental; ····· experimental)



Comparison of Experimental and Theoretical Spectral Transmittance Data

2. Altitude of 22.0 km and a Solar Elevation of 27.72 Degrees.

(--- Experimental; ···· Benedict modification)

B

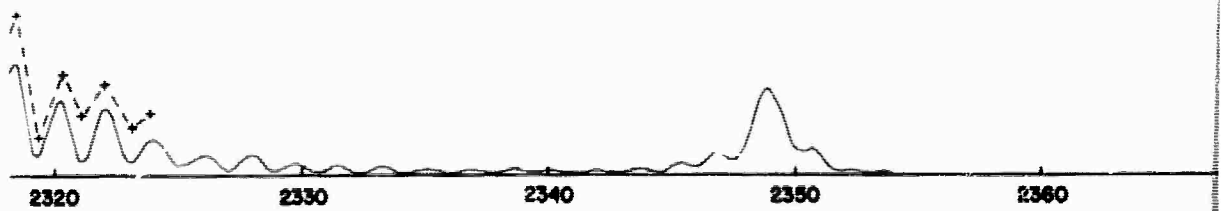
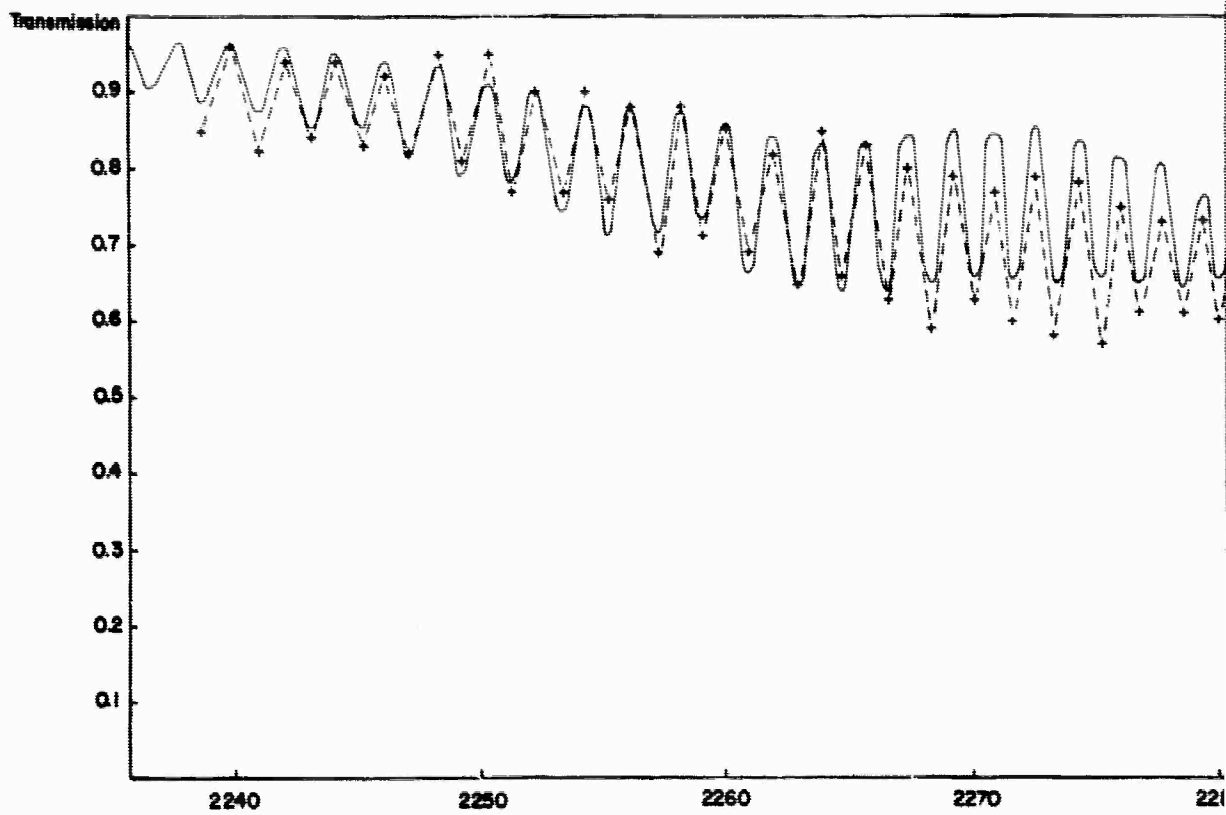
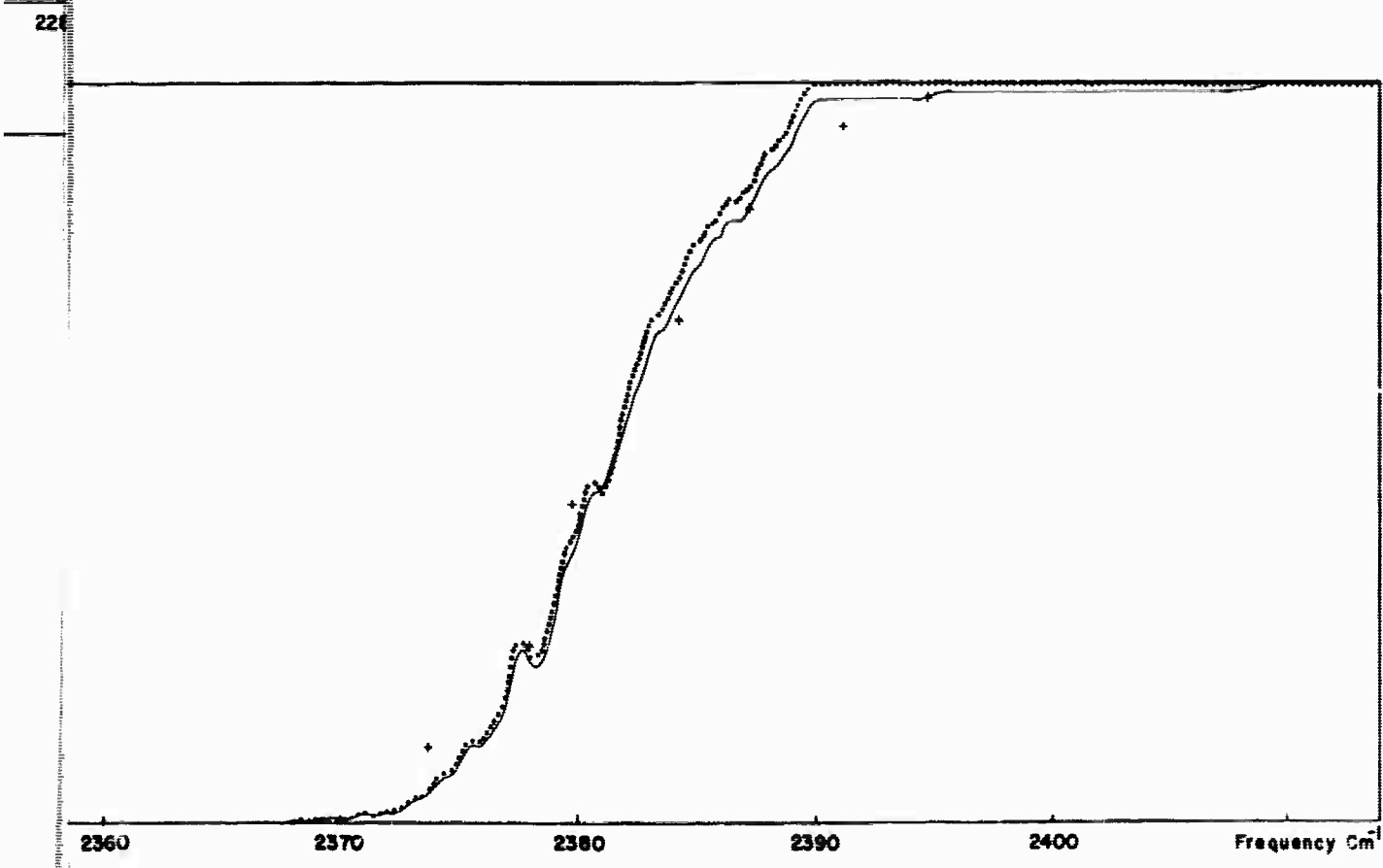
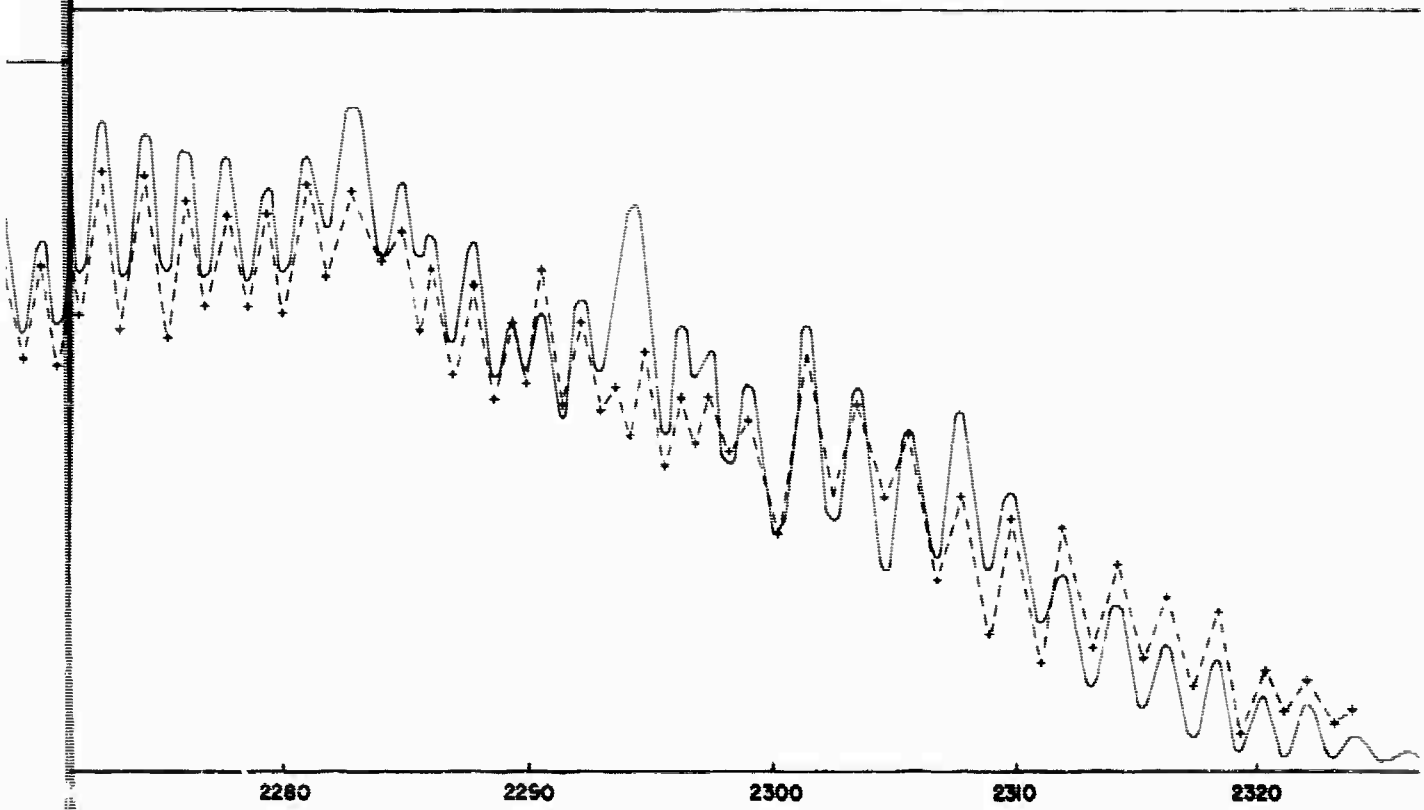


Figure 11. (Record 36) Comparison between Experiment and Calculation for the 4.3μ CO_2 Band at an Altitude of 23,000 ft. (— calculated; +---+ experimental; ...



... Experimental and Theoretical Spectral Transmittance Data
... altitude of 23.0 km and a Solar Elevation of 28.97 Degrees.
... Experimental; Benedict modification)
.....

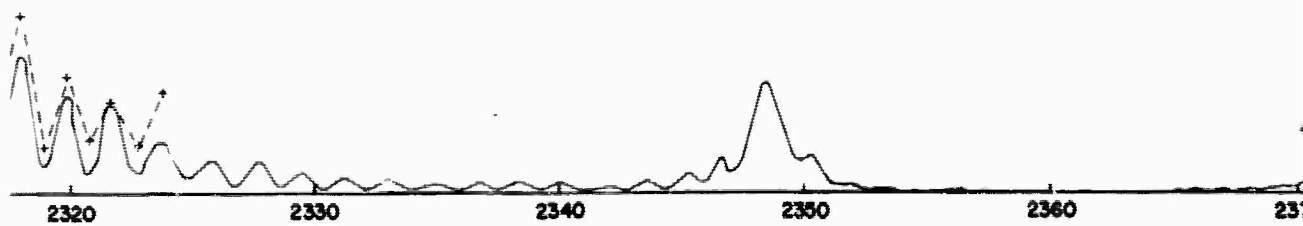
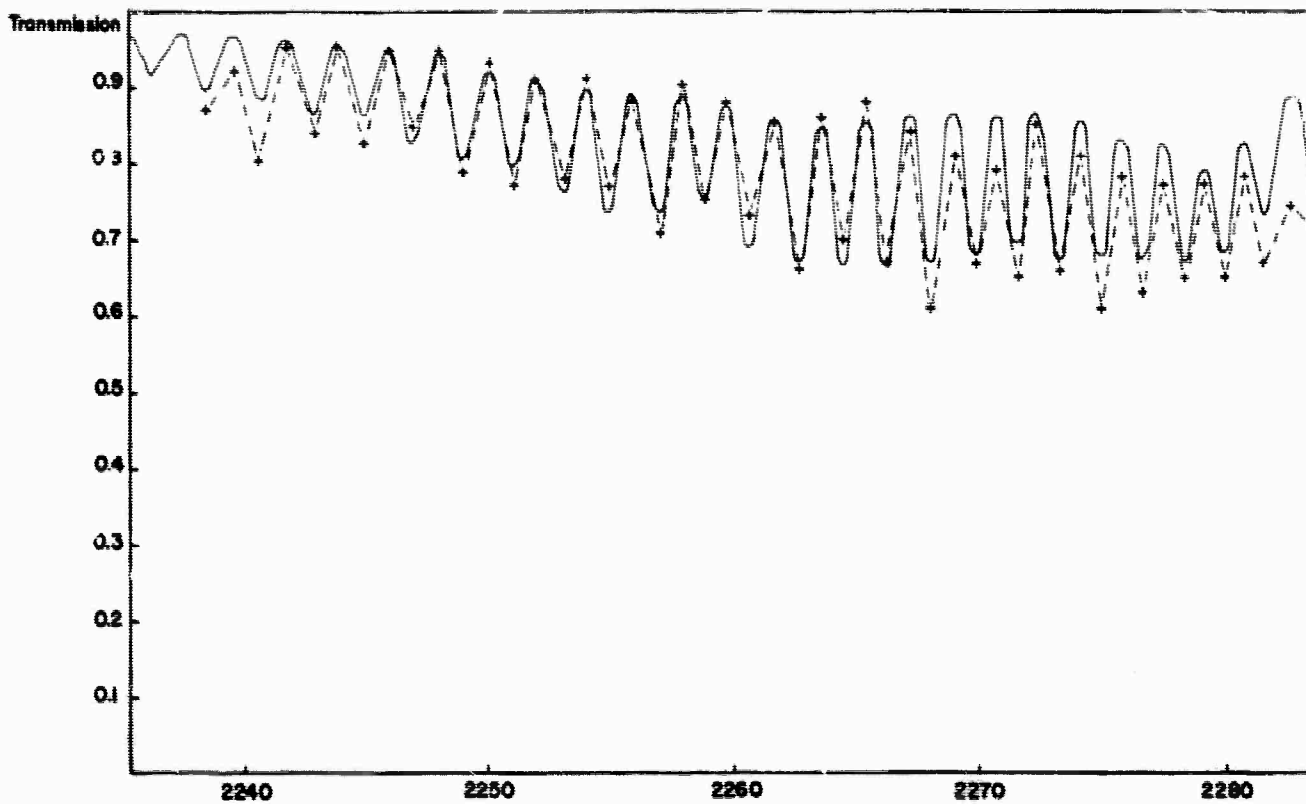
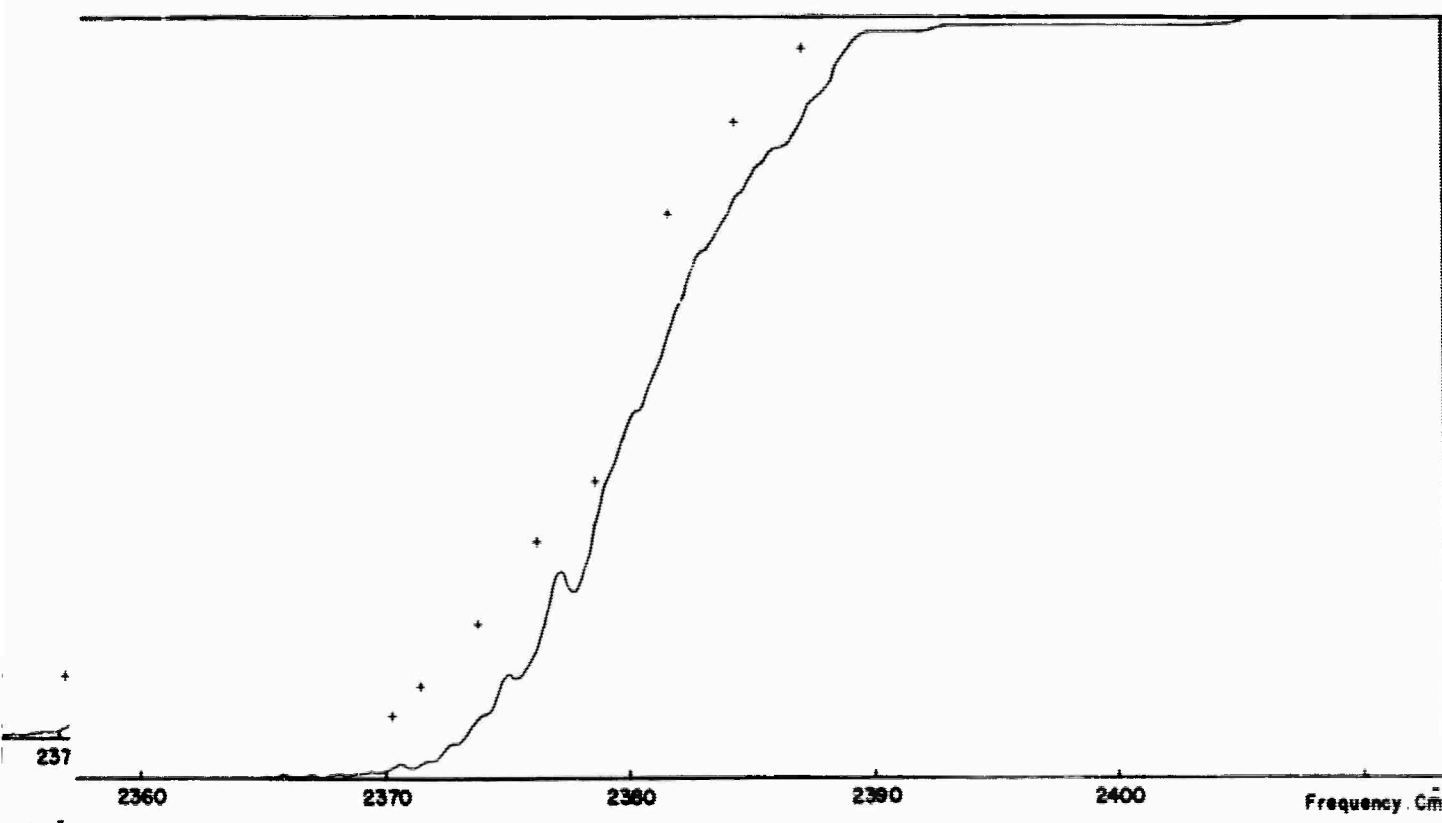
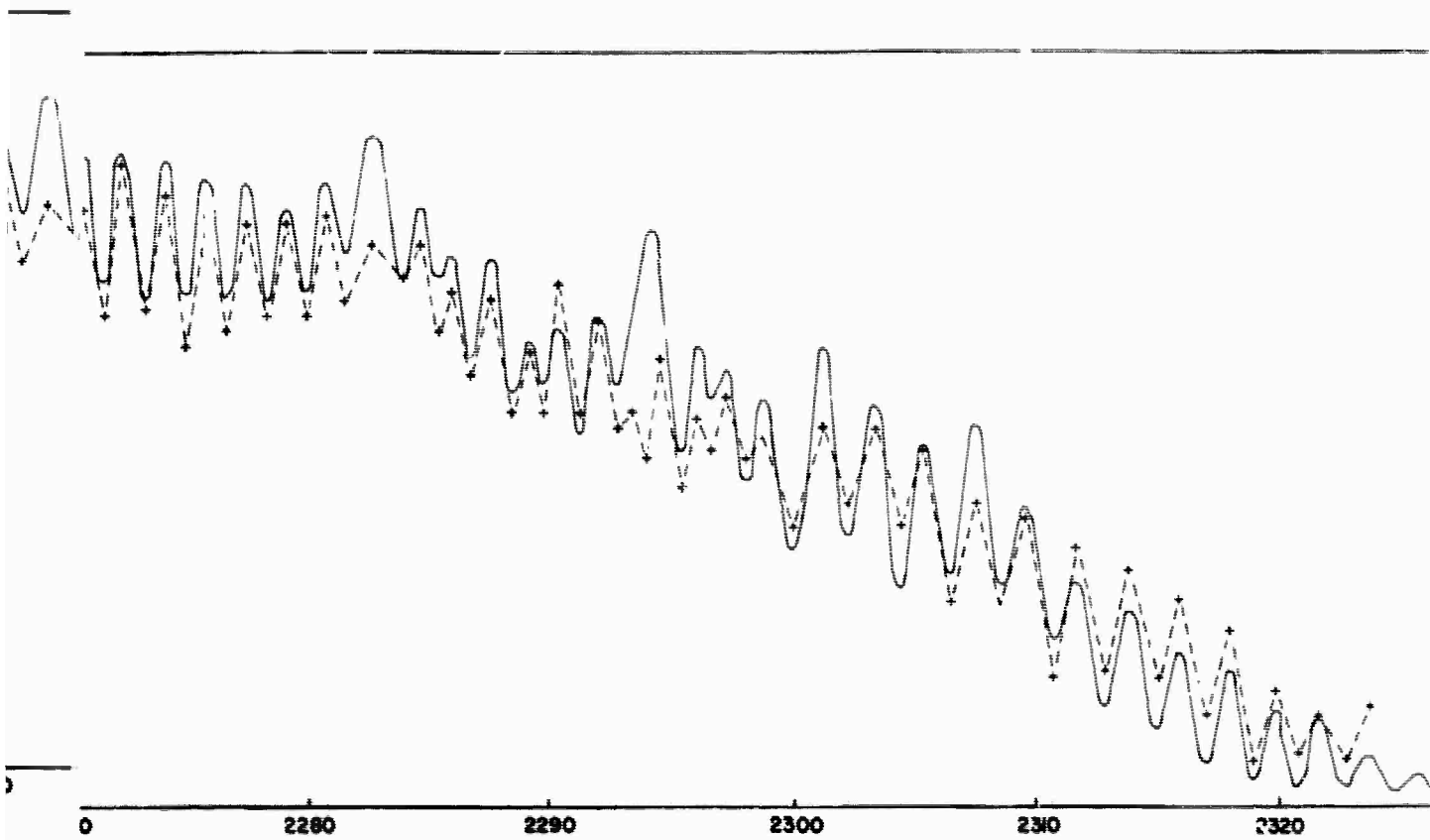


Figure 12. (Record 37) Comparison between Experimental for the 4.3μ CO_2 Band at an Altitude of 23.4 km (— calculated; +---+ experimental)



Known Experimental and Theoretical Spectral Transmittance Data
Altitude of 23.4 km and a Solar Elevation of 29.60 Degrees.
(Experimental)

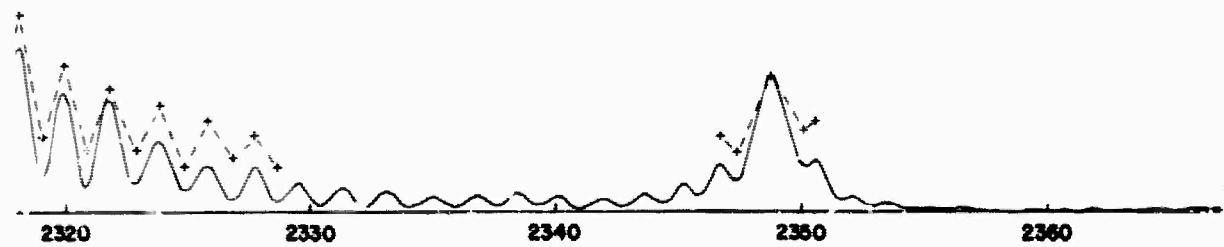
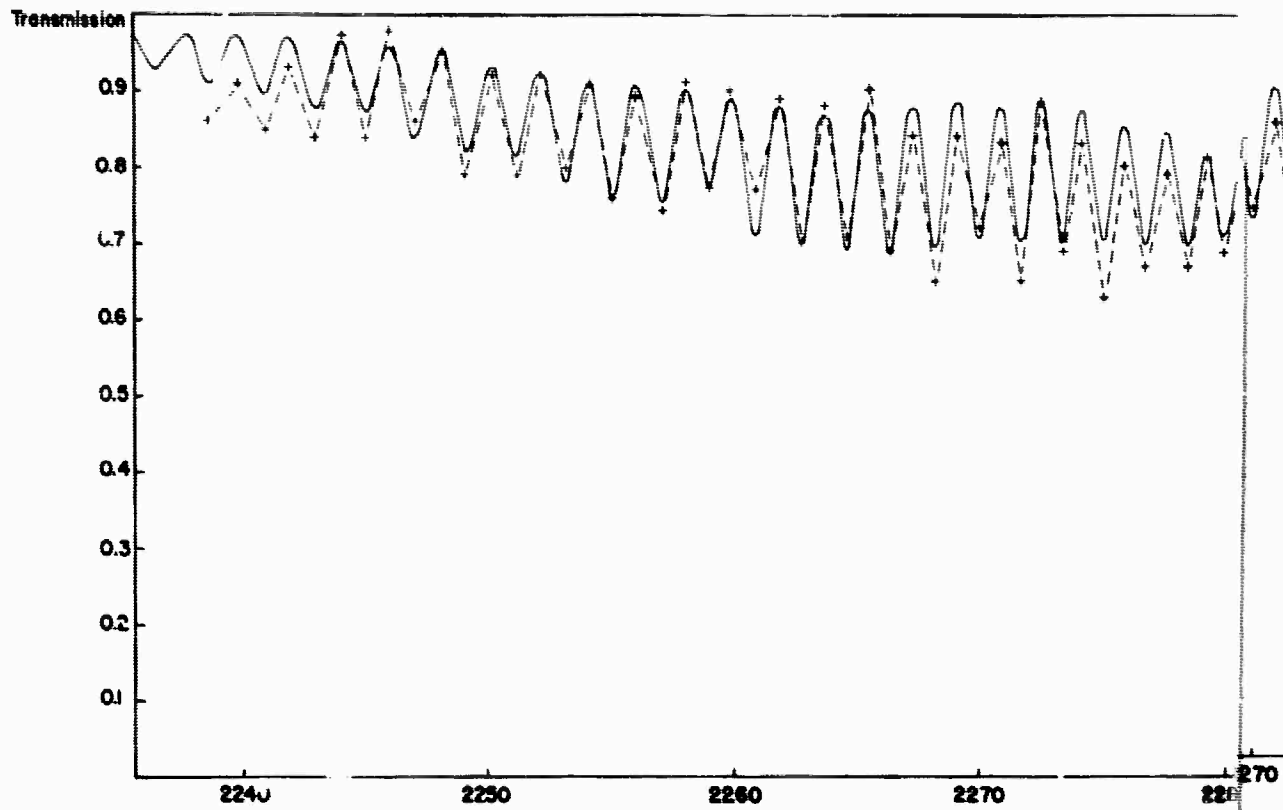
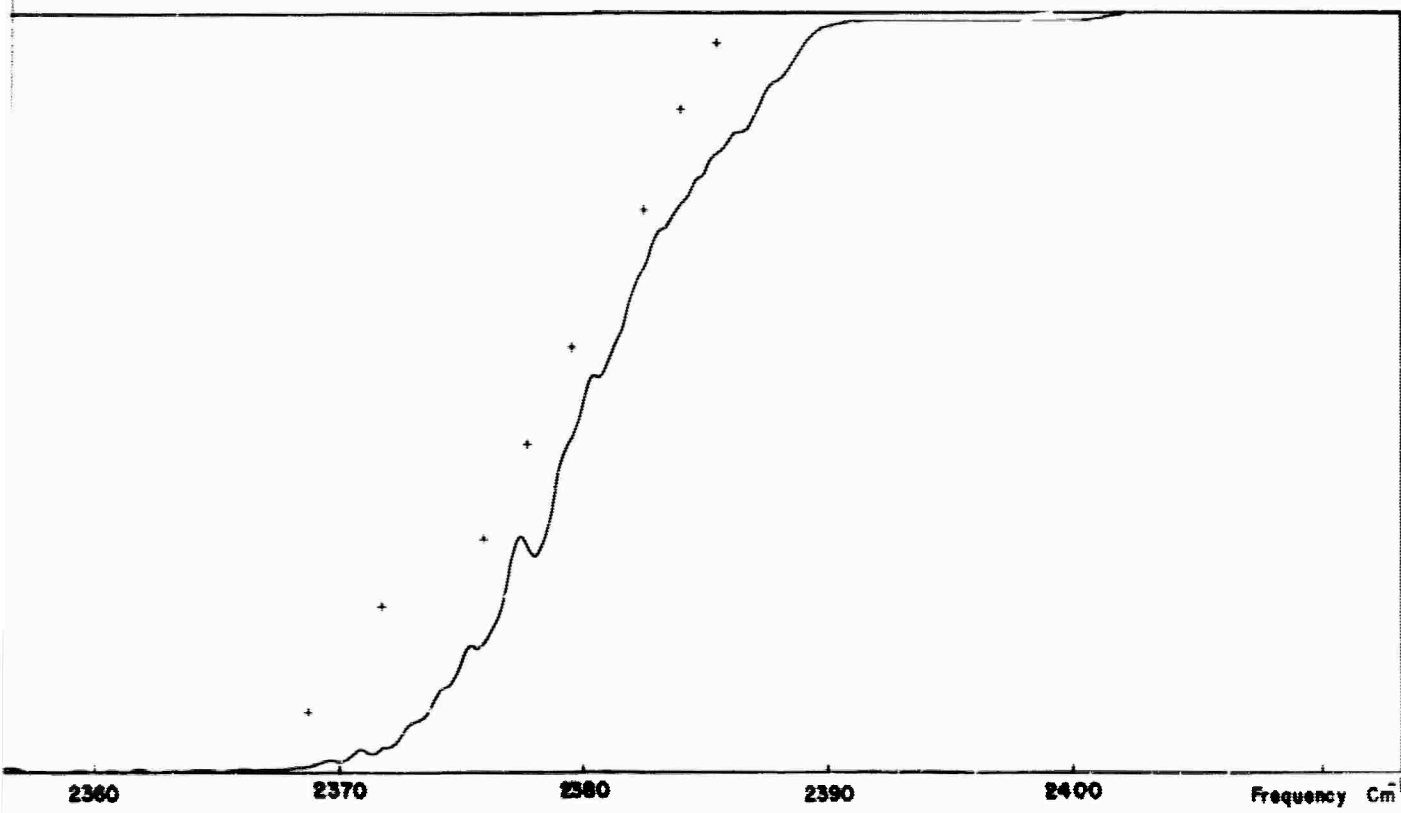
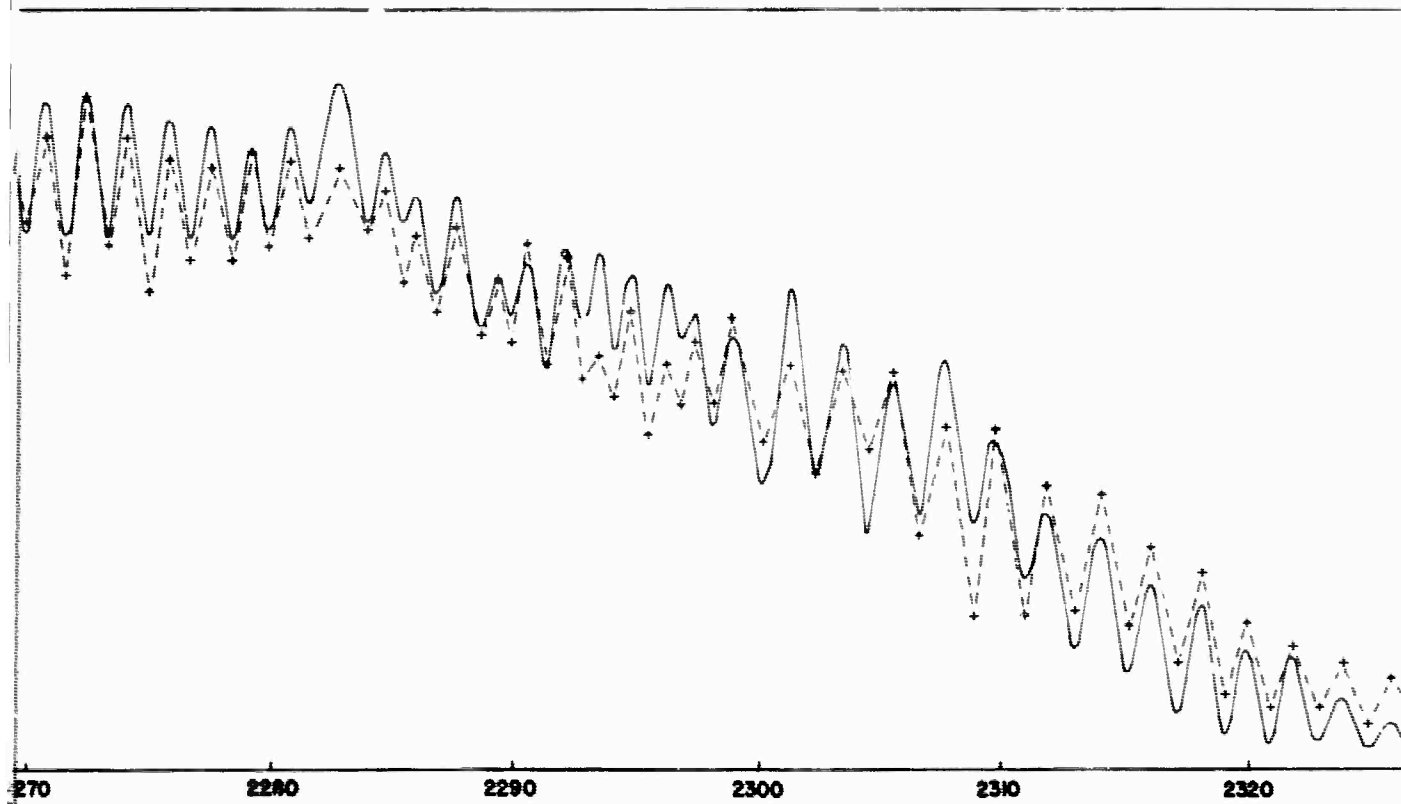


Figure 13. (Record 38) Comparison between Experimental and Calculated Transmission for the 4.3μ CO_2 Band at an Altitude of 23,000 Feet. (— calculated; +---+ experimental)



between Experimental and Theoretical Spectral Transmittance Data
at an Altitude of 23.8 km and a Solar Elevation of 30.23 Degrees.
(Experimental)

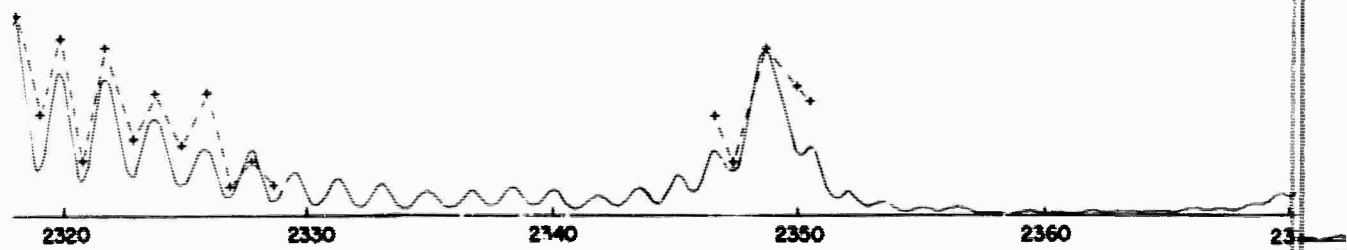
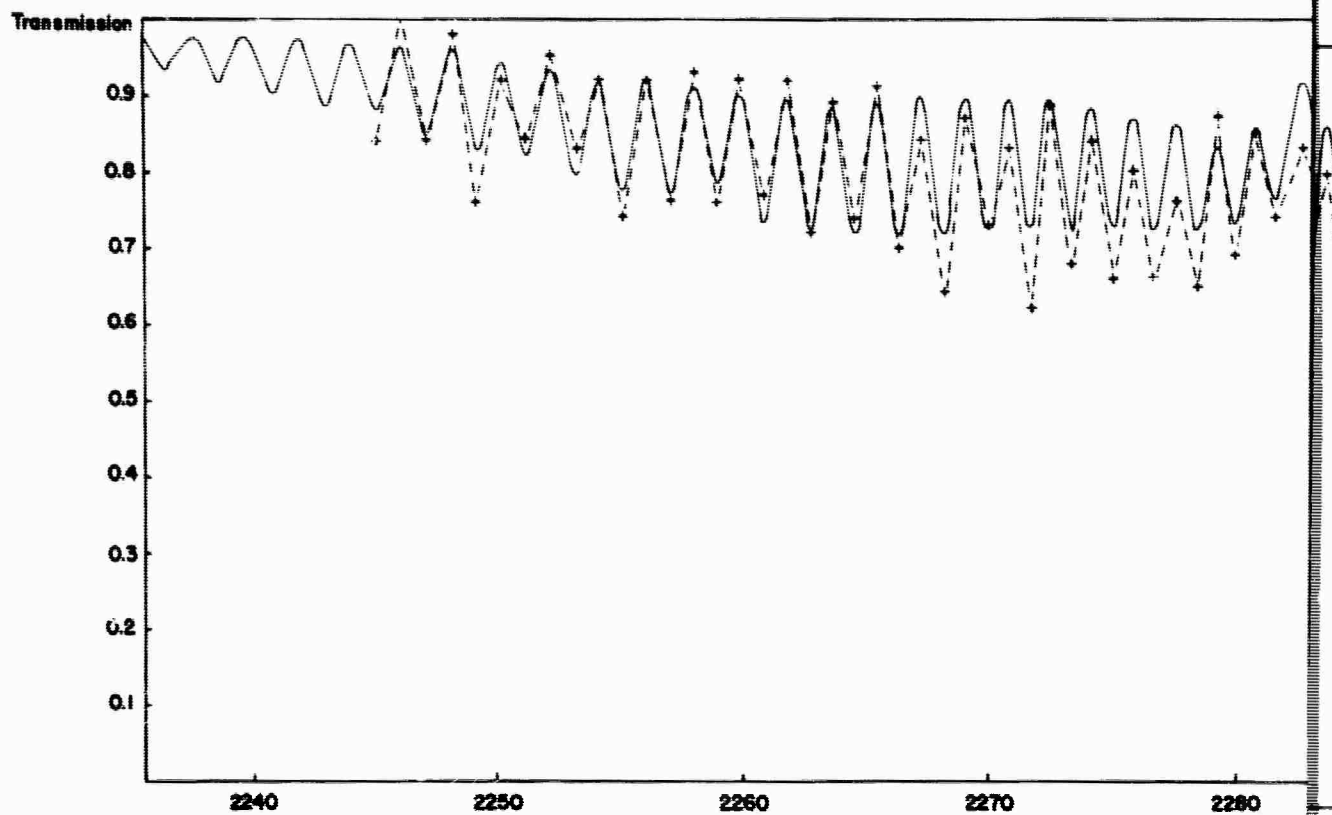
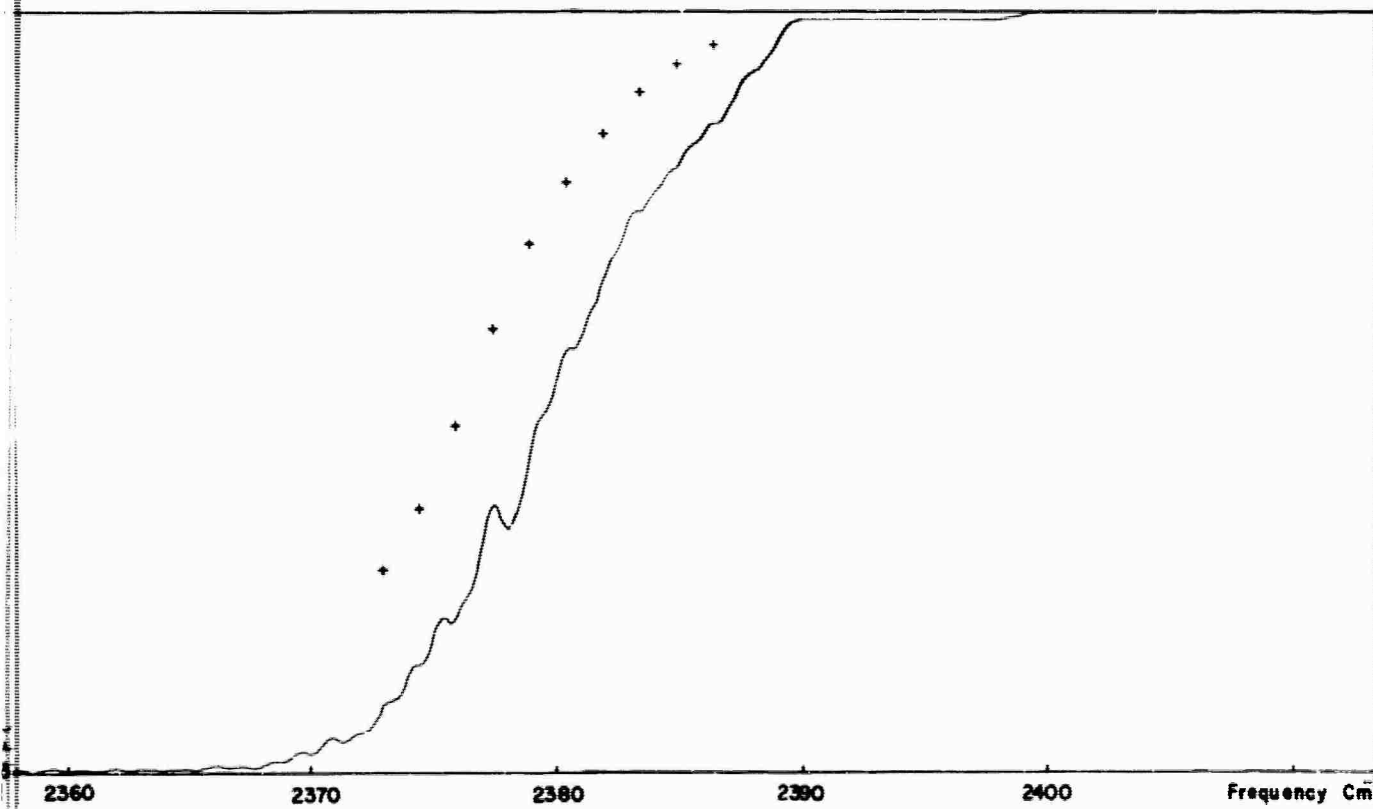
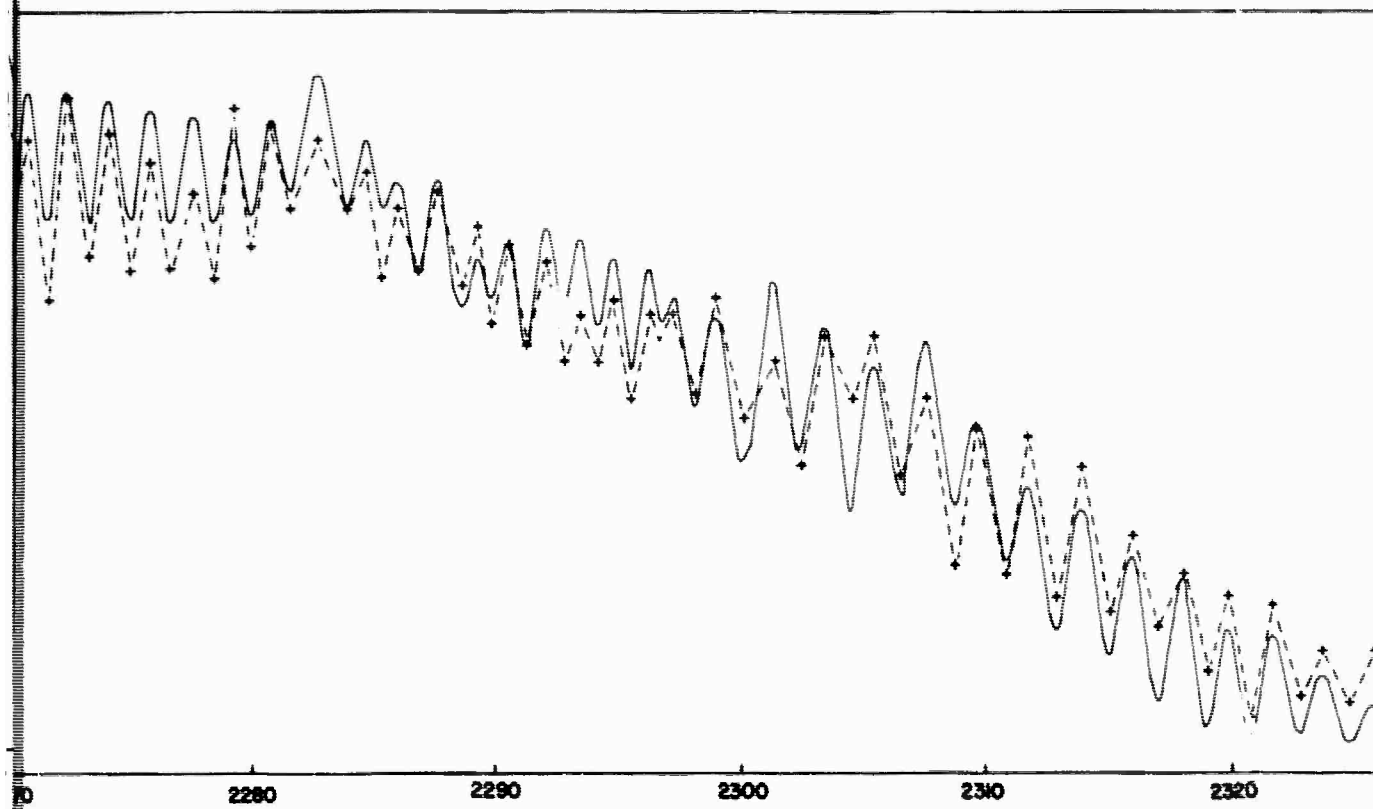


Figure 14. (Record 39) Comparison between Experimental and Calculated Transmission for the 4.3μ CO_2 Band at an Altitude of 24.3 km (— calculated; +---+ experimental)

ven
Alti
rin



Comparison of Experimental and Theoretical Spectral Transmittance Data
at an Altitude of 24.3 km and a Solar Elevation of 30.86 Degrees.
(Experimental)

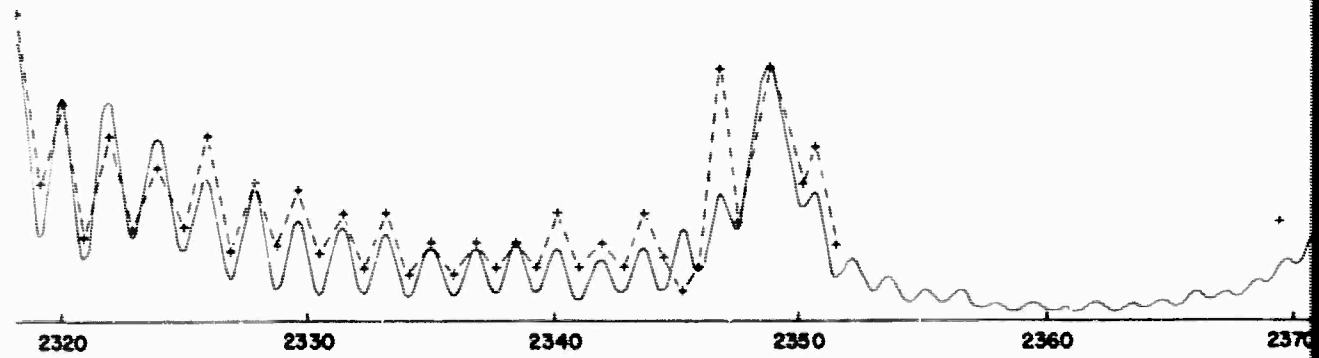
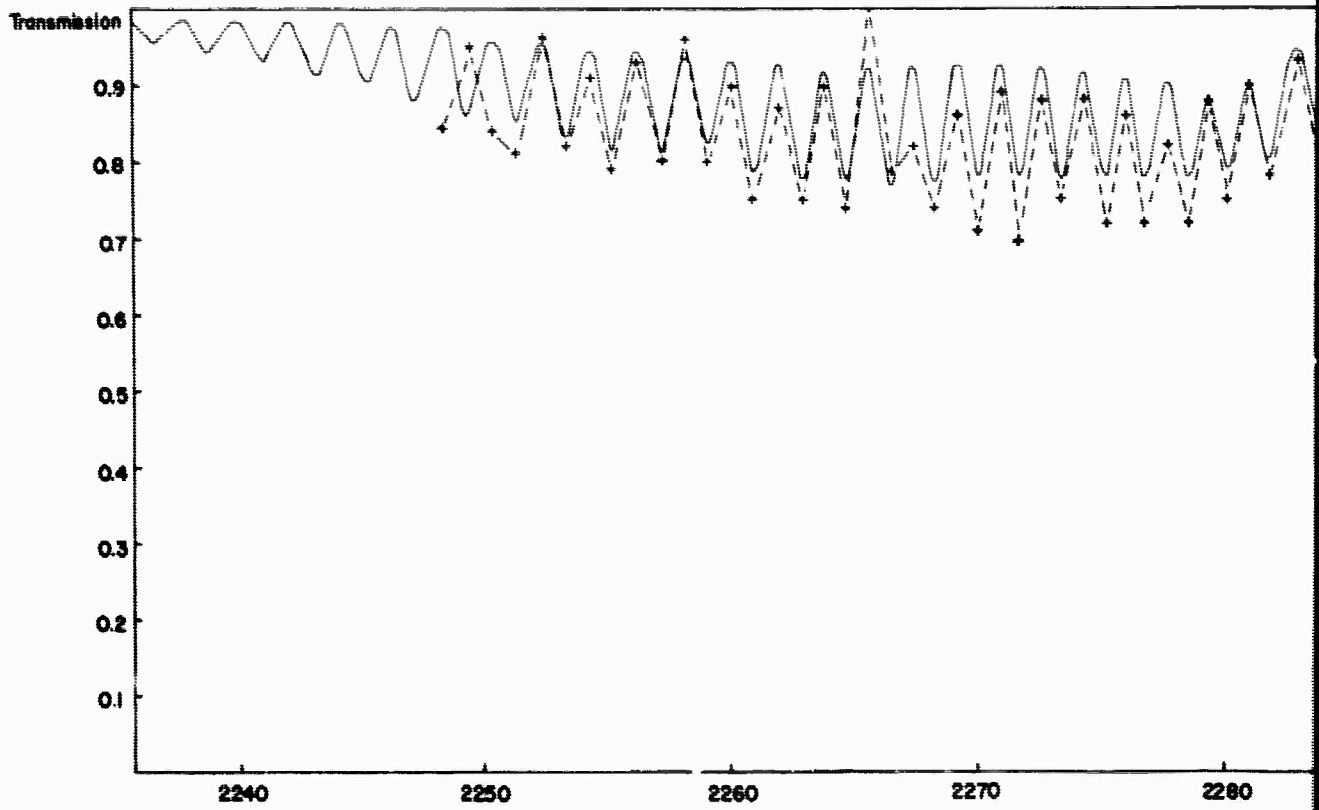
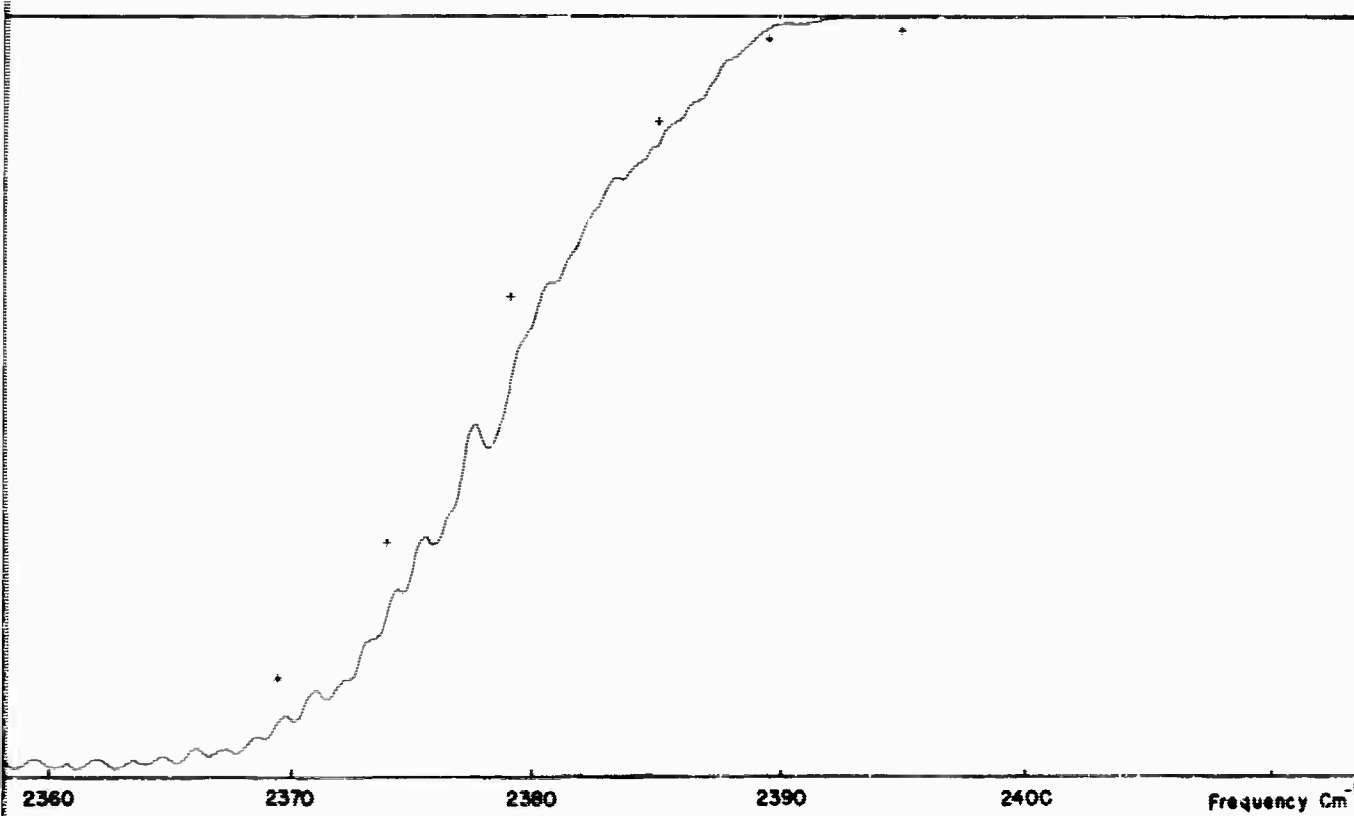
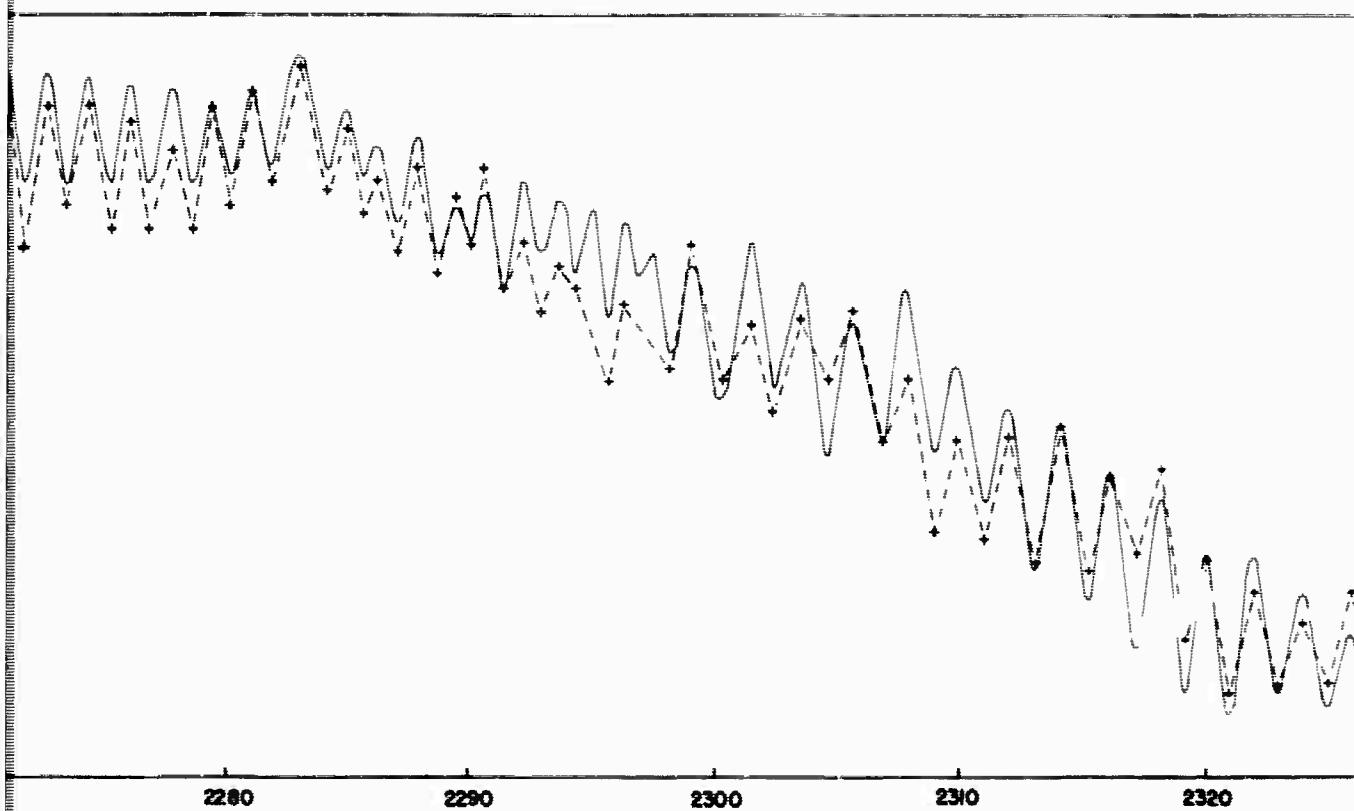


Figure 15. (Record 42) Comparison between Experimental
 for the 4.3μ CO_2 Band at an Altitude of 25.6 km
 (— calculated; +---+ experimental)



Comparison of Experimental and Theoretical Spectral Transmittance Data
at an Altitude of 25.6 km and a Solar Elevation of 32.75 Degrees.
(Theoretical Data is shown as a solid line, and Experimental Data is shown as a dashed line)

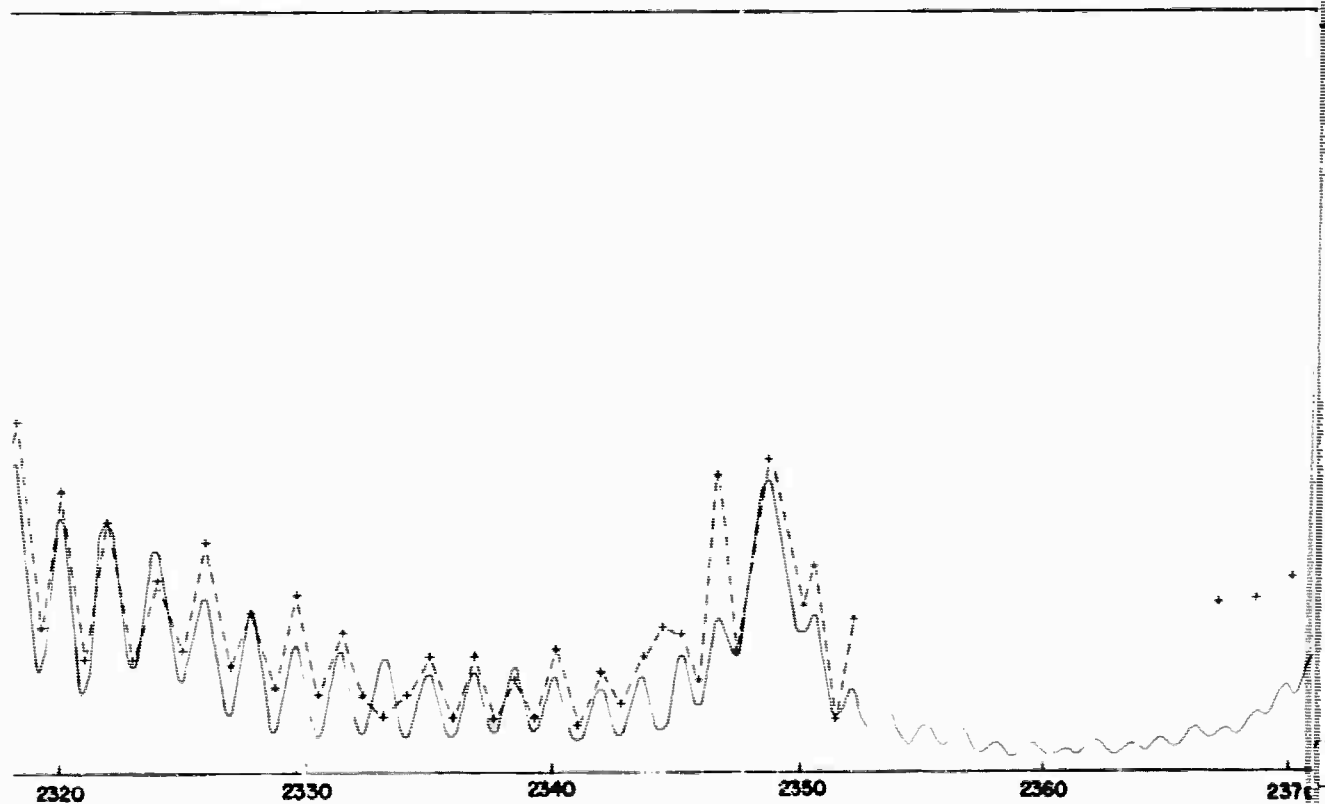
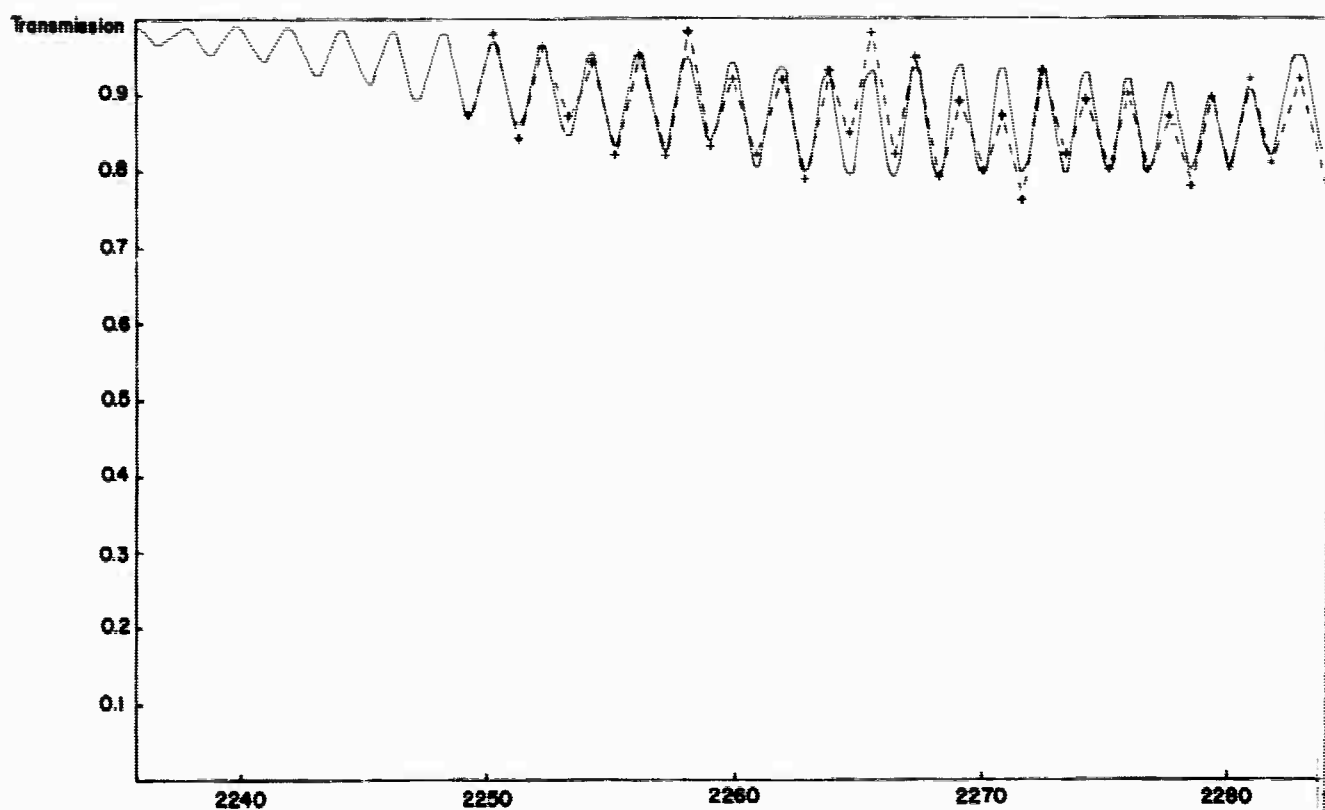
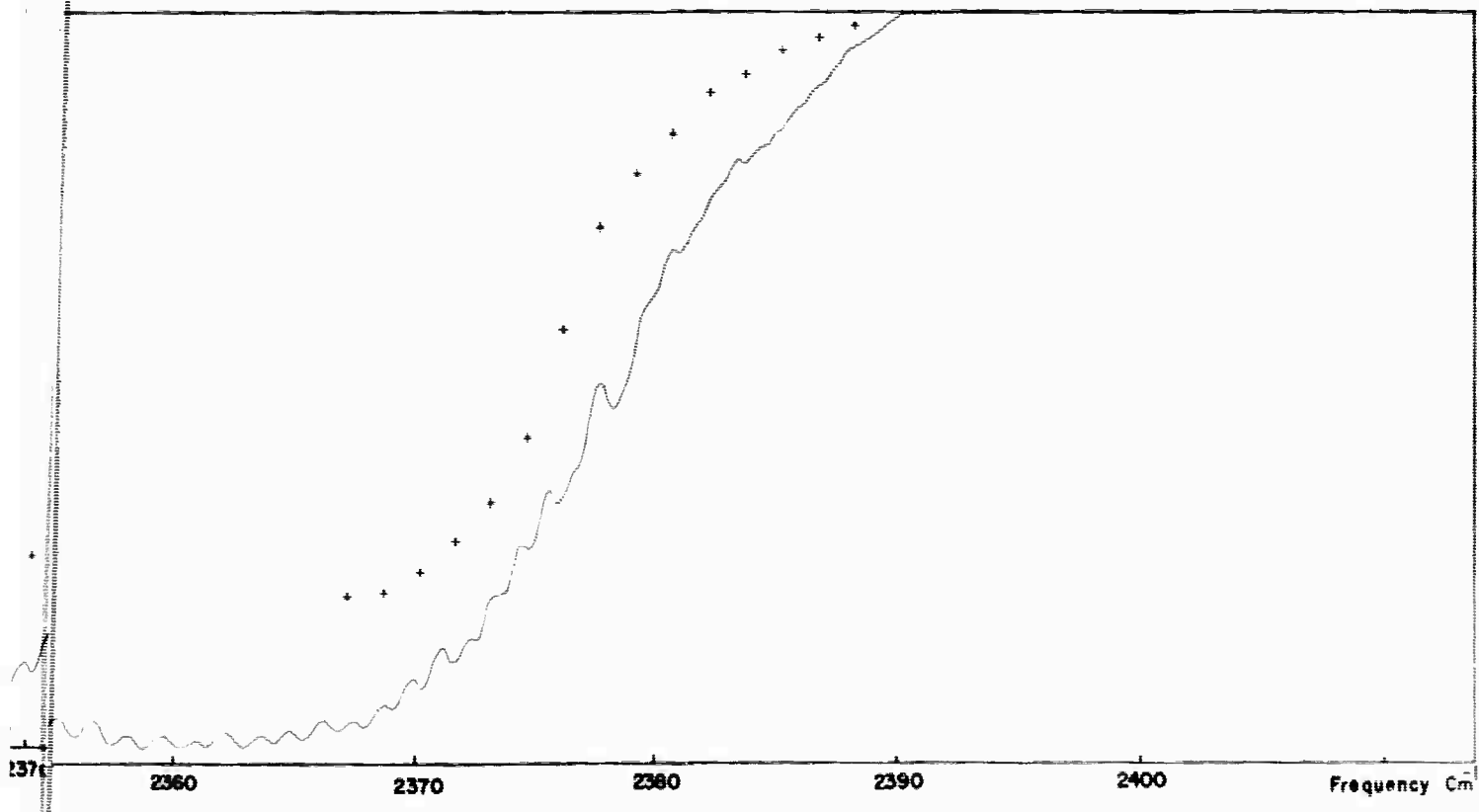
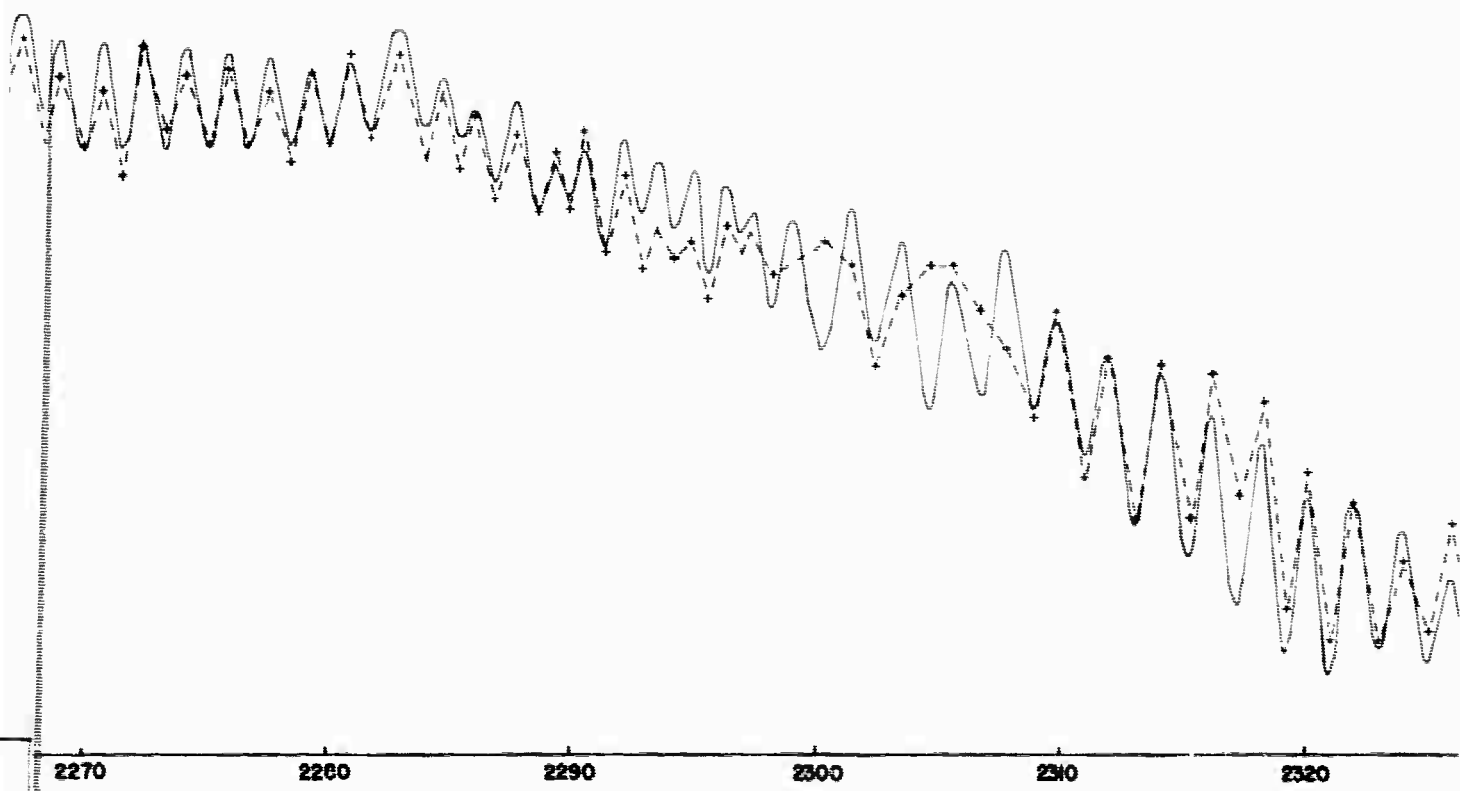


Figure 16. (Record 43) Comparison between Experimental for the 4.3 μ CO₂ Band at an Altitude of 26.1 km (— calculated; +---+ experimental)



al
cm
between Experimental and Theoretical Spectral Transmittance Data
an Altitude of 26.1 km and a Solar Elevation of 33.38 Degrees.
(experimental)

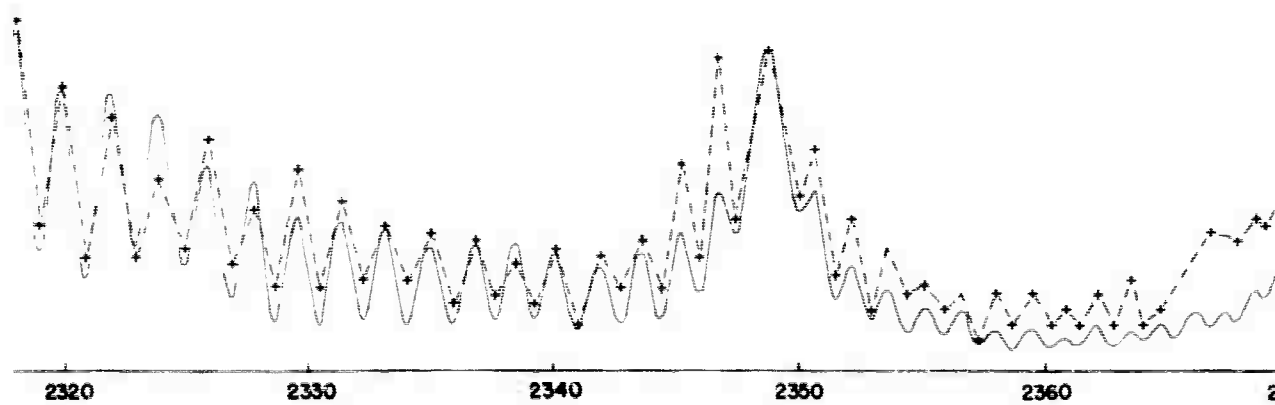
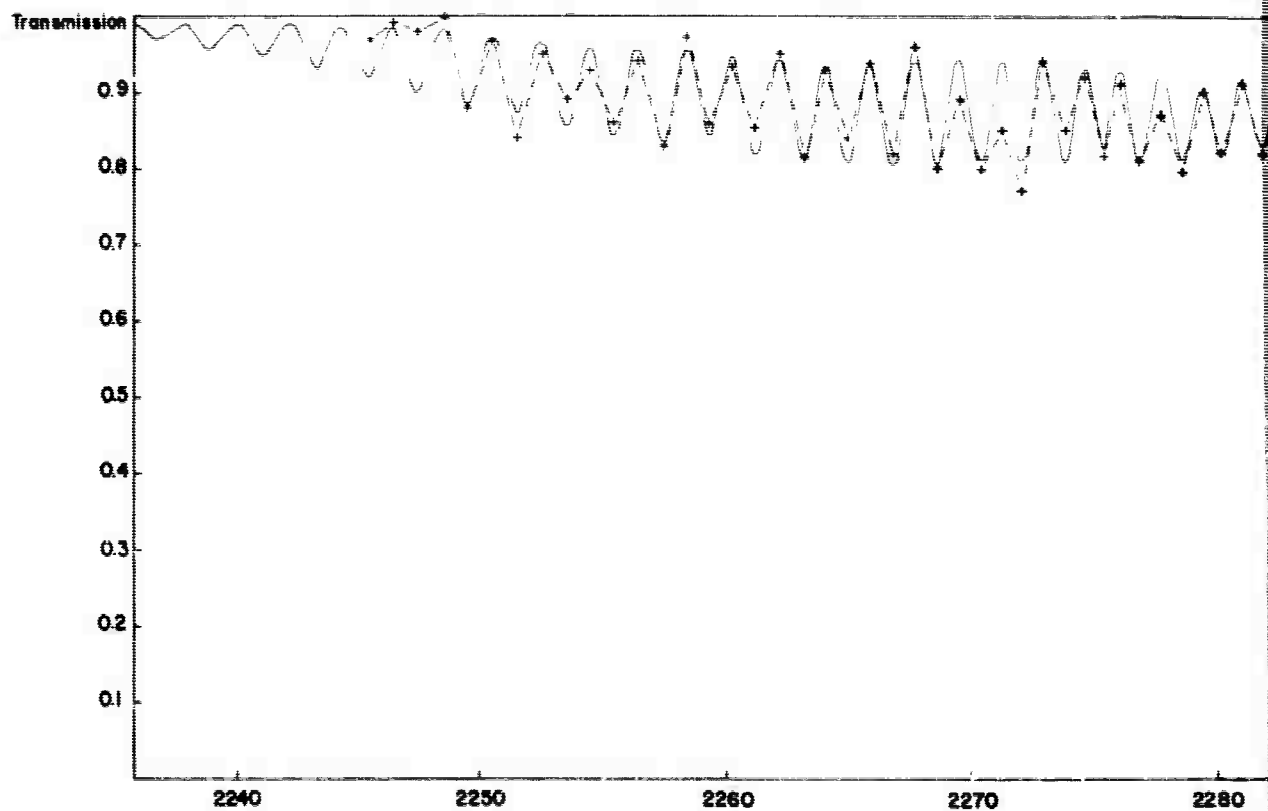
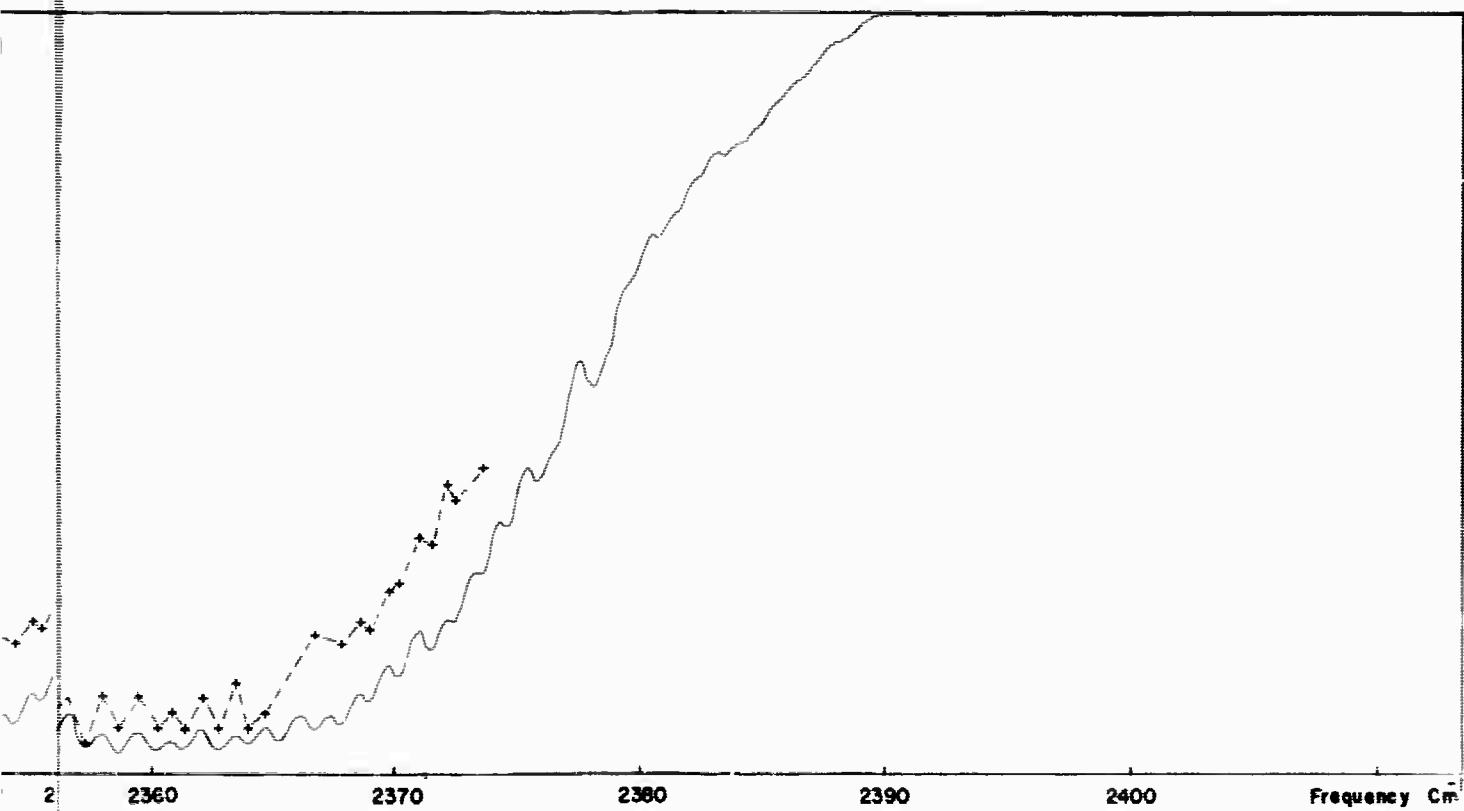
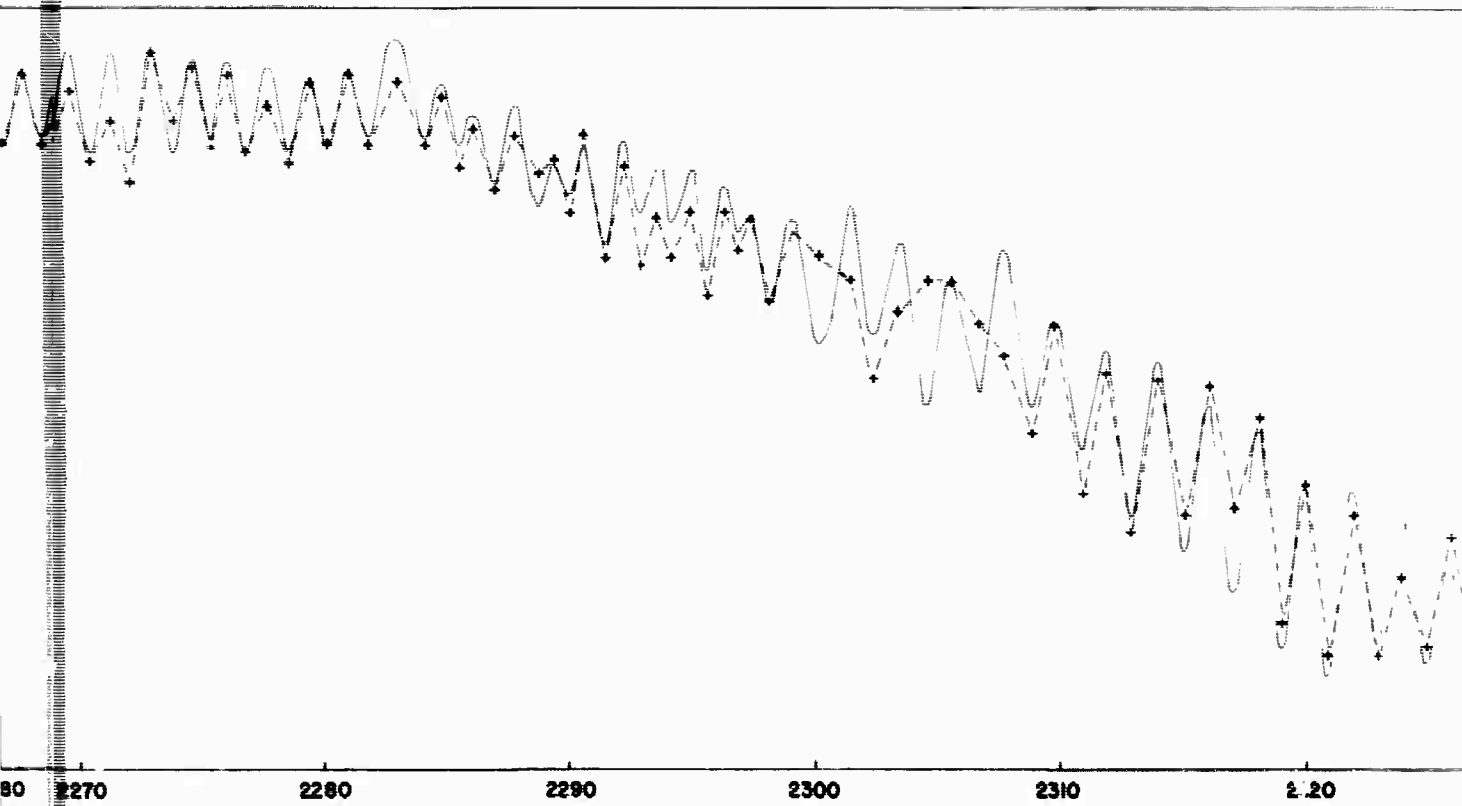


Figure 17. (Record 44) Comparison between Experimental and Calculated Transmission for the 4.3μ CO_2 Band at an Altitude of 26.6 km (— calculated; +---+ experimental)



Comparison between Experimental and Theoretical Spectral Transmittance Data
 at an Altitude of 26.6 km and a Solar Elevation of 34.01 Degrees.
 (Theoretical and Experimental)

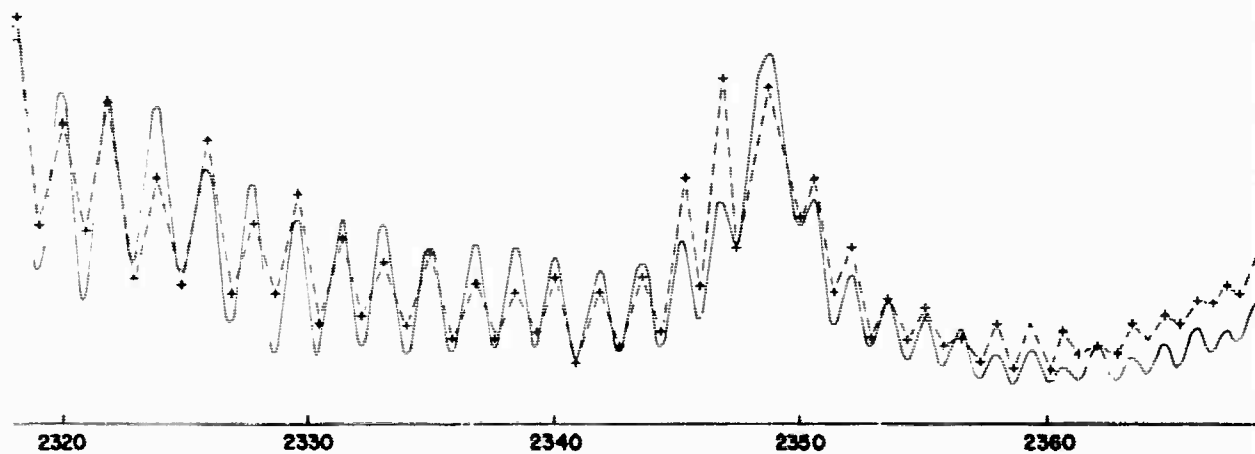
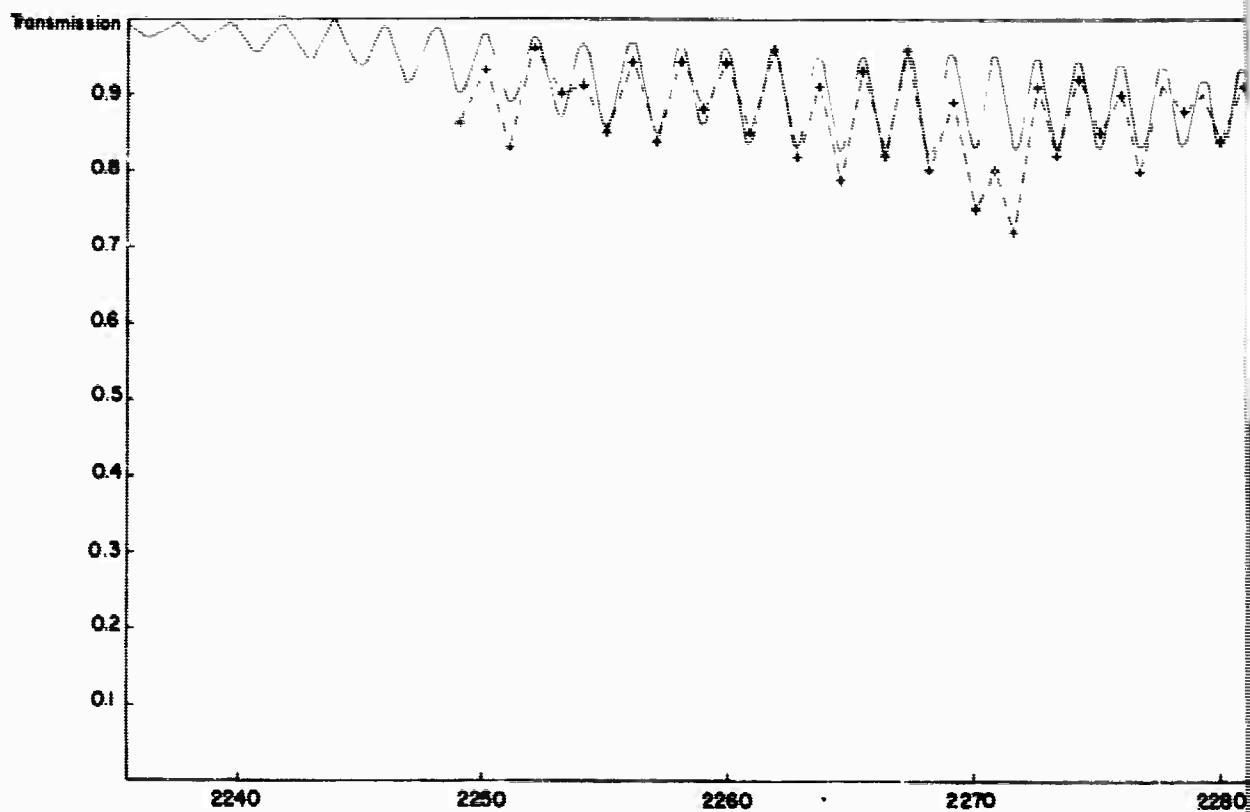
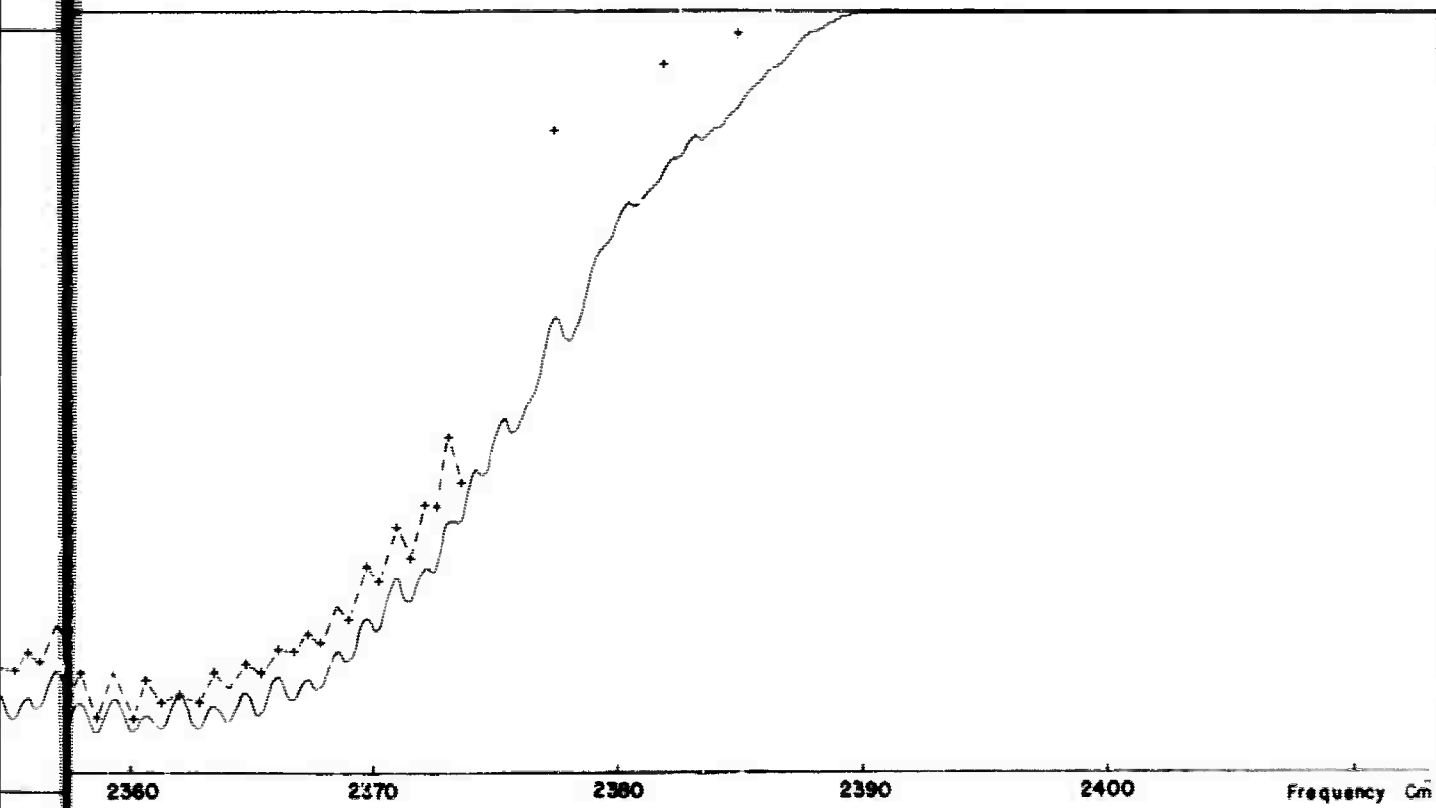
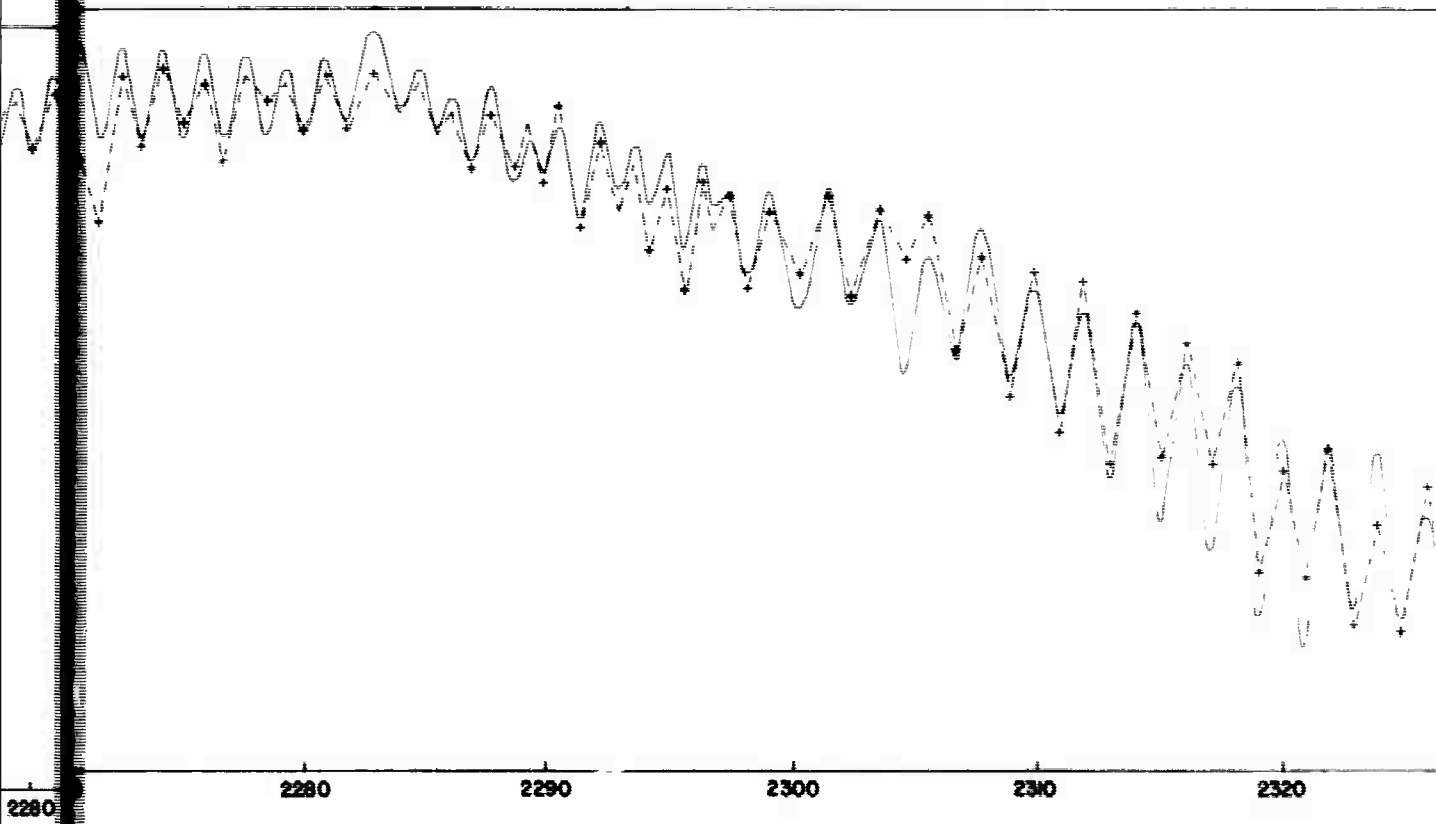


Figure 18. (Record 45) Comparison between Experimental and Calculated Transmission for the 4.3 μm CO₂ Band at an Altitude of 27.0 (— calculated; +---+ experimental);



Comparison between Experimental and Theoretical Spectral Transmittance Data
at an Altitude of 27.0 km and a Solar Elevation of 34.64 Degrees.
(Theoretical Data is shown as a dashed line with '+' markers and the experimental data as a solid line)

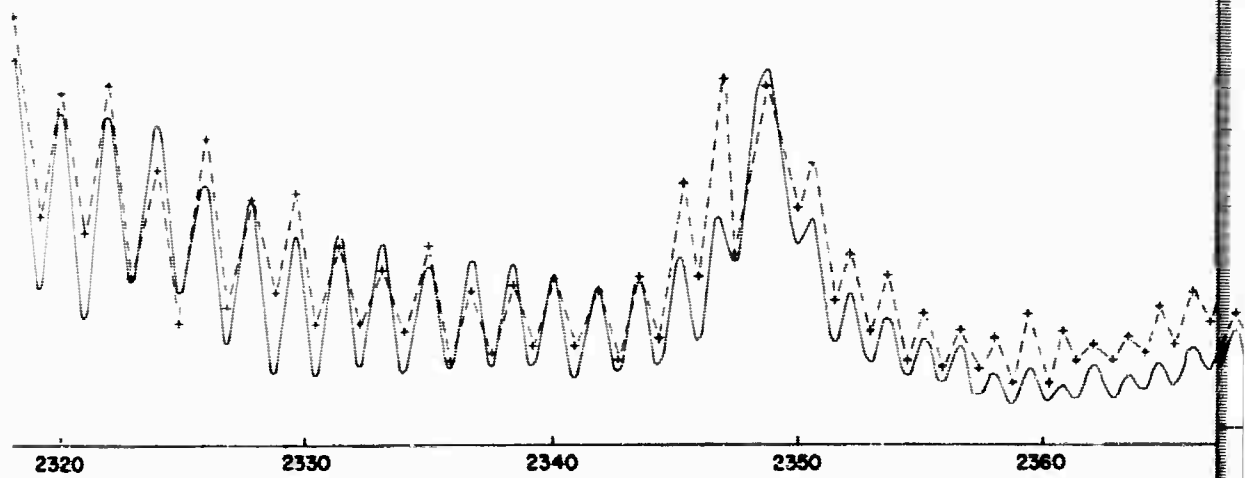
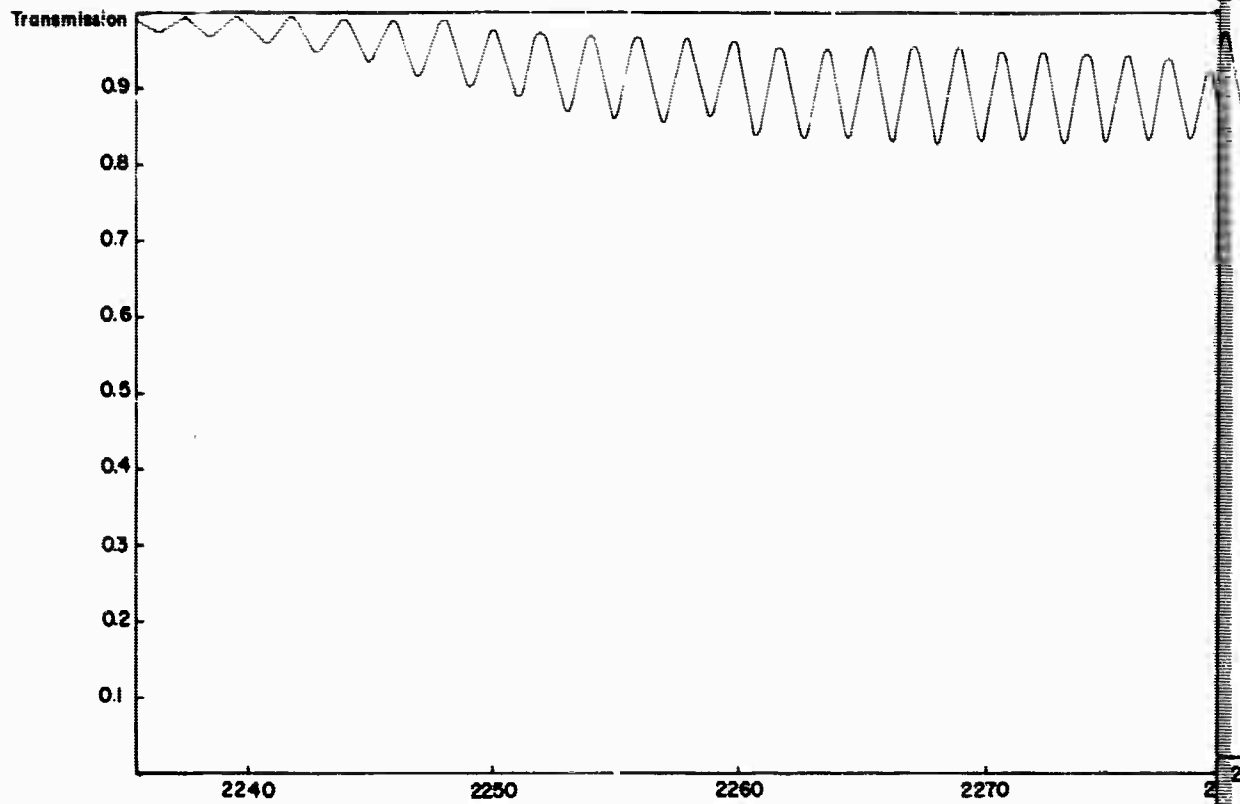
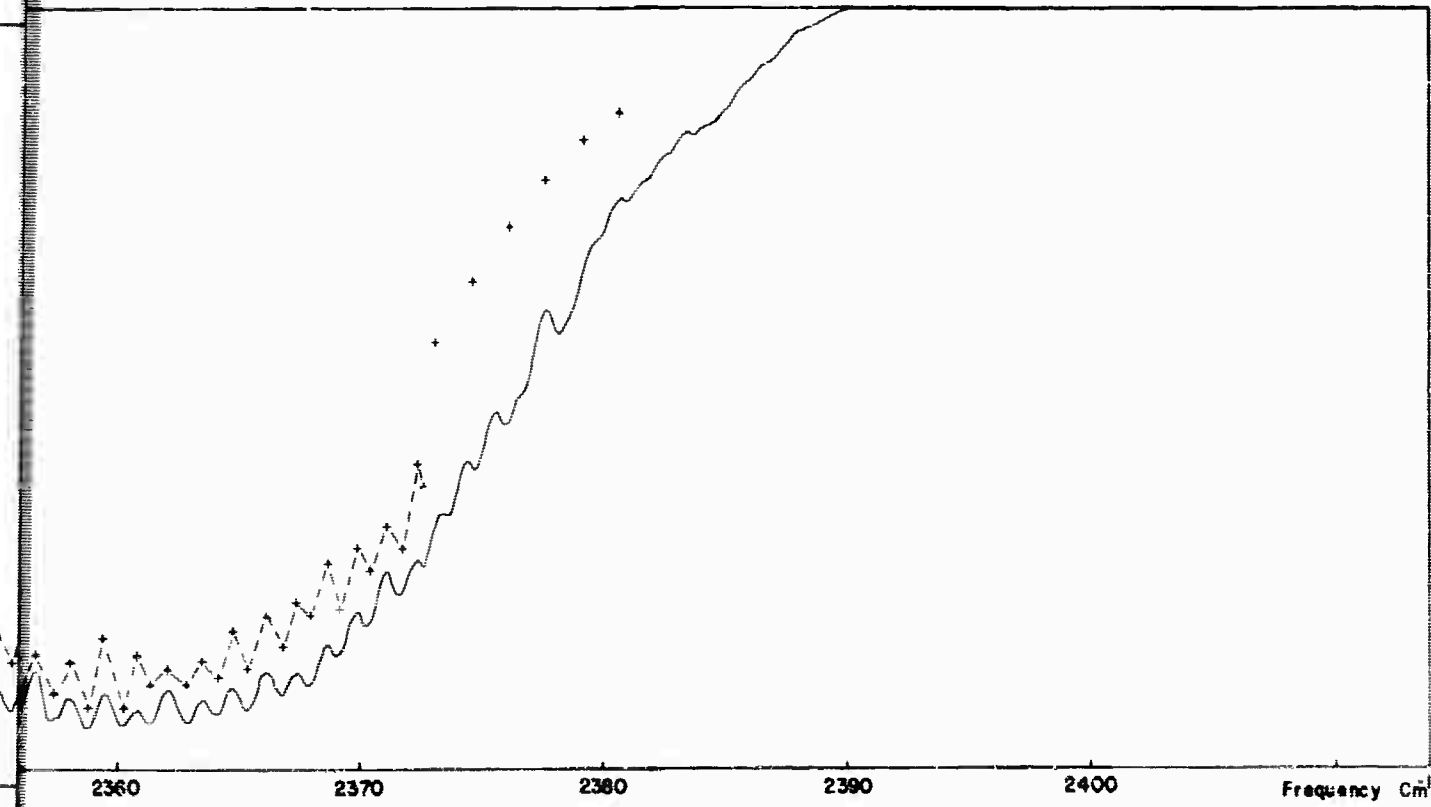
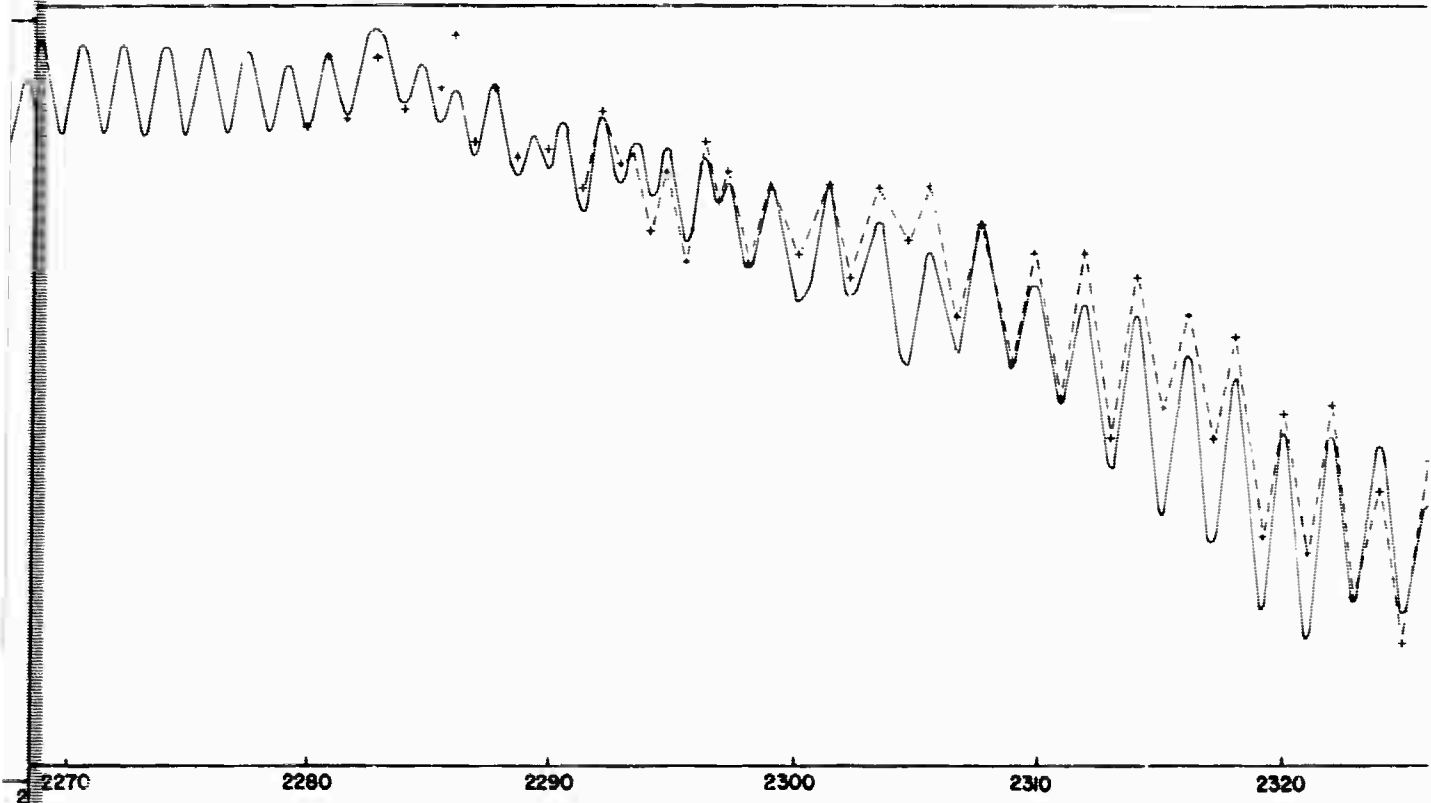


Figure 19. (Record 46) Comparison between Experimental and Calculated Data for the 4.3μ CO_2 Band at an Altitude of 27,000 ft. (— calculated; + - - - + experimental)



Comparison between Experimental and Theoretical Spectral Transmittance Data
at an Altitude of 27.4 km and a Solar Elevation of 35.27 Degrees.
(Experimental)

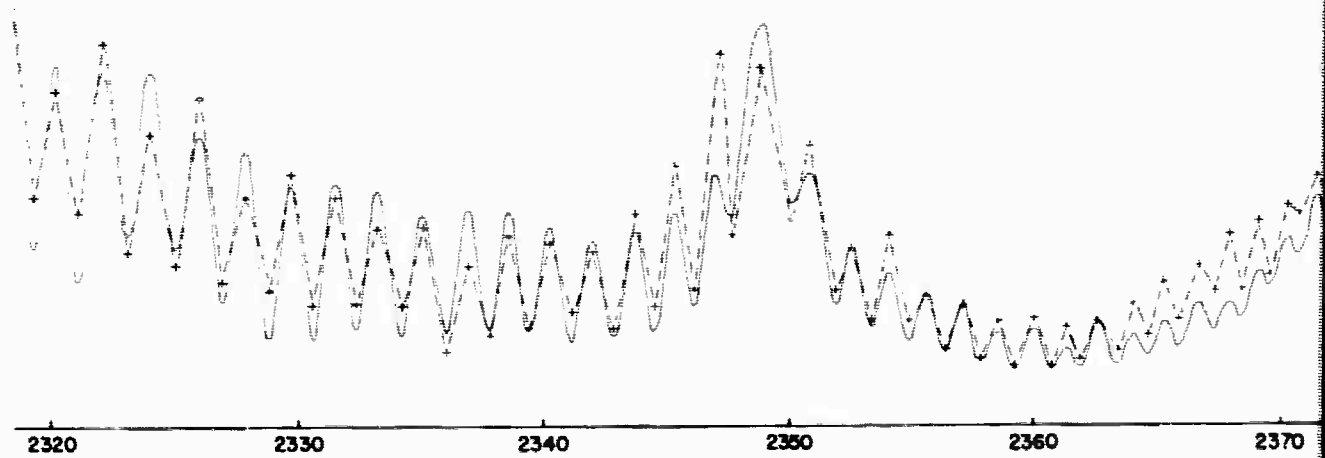
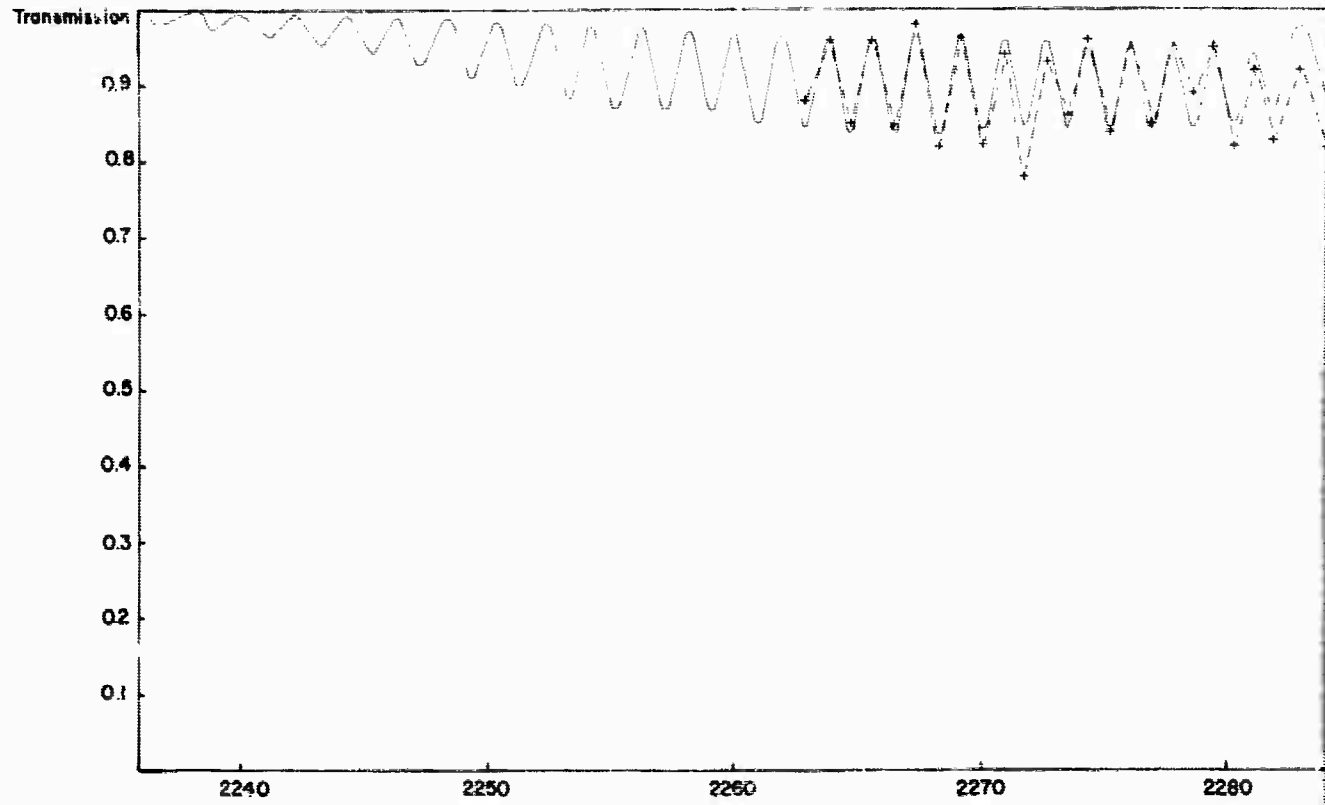
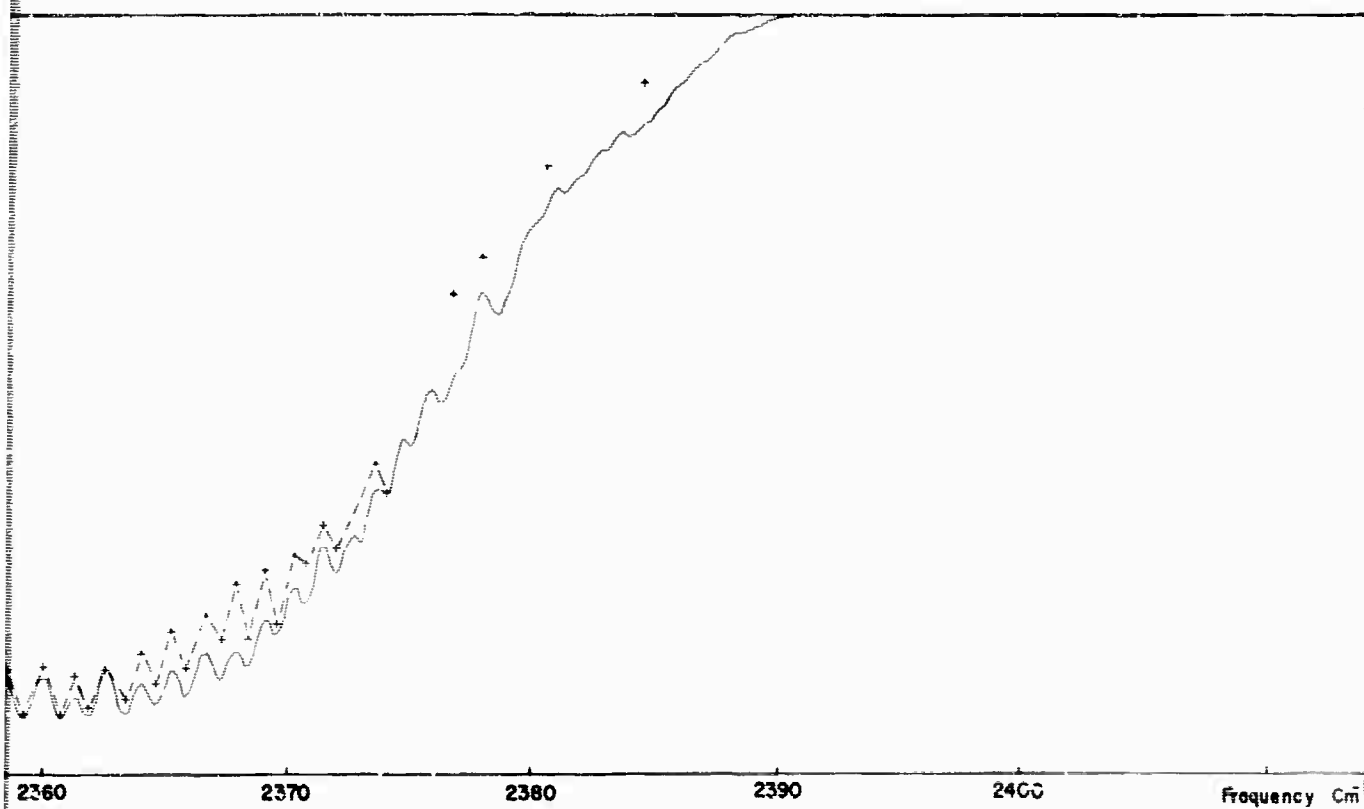
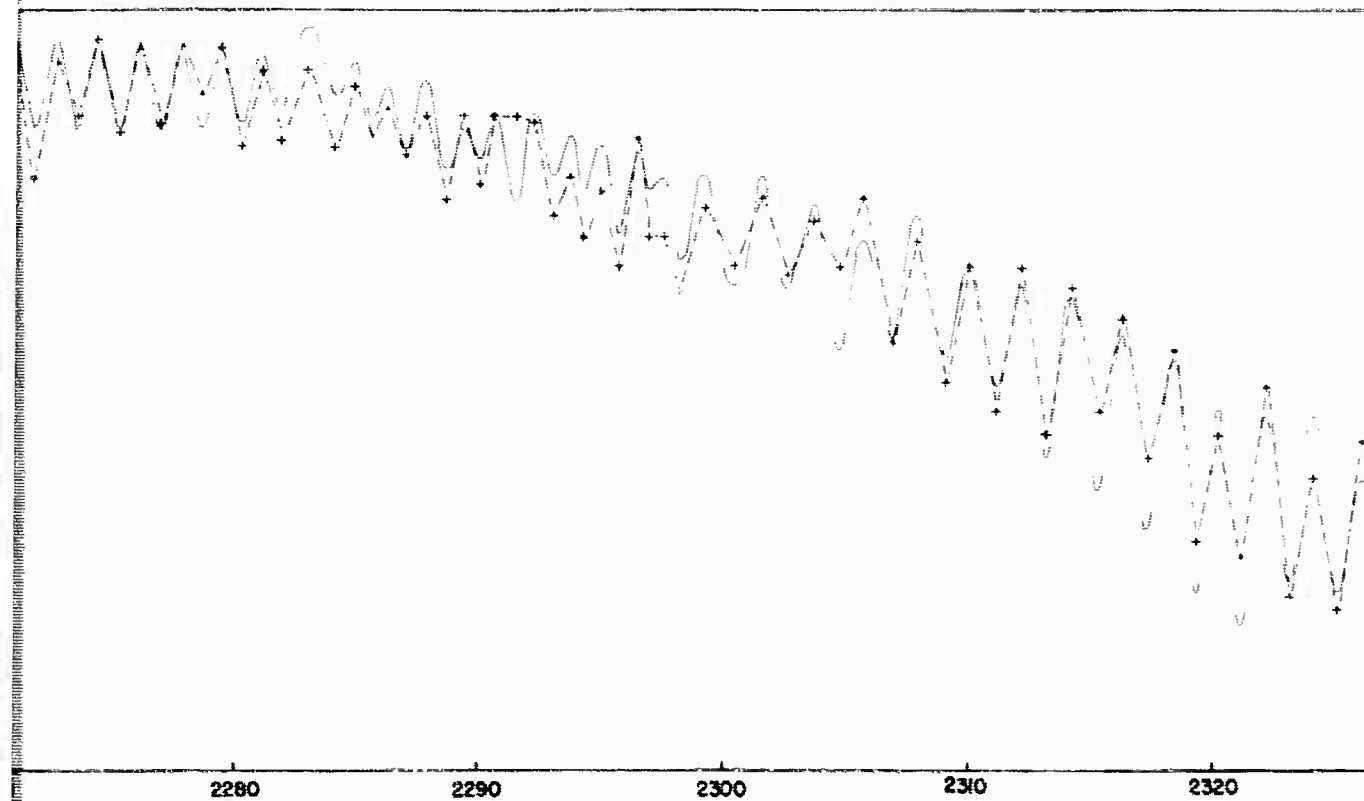


Figure 20. (Record 47) Comparison between Experimental for the 4.3μ CO_2 Band at an Altitude of 27.9 km (— calculated; +---+ experimental)



Experimental and Theoretical Spectral Transmittance Data
Altitude of 27.9 km and a Solar Elevation of 35.90 Degrees.
(Experimental)

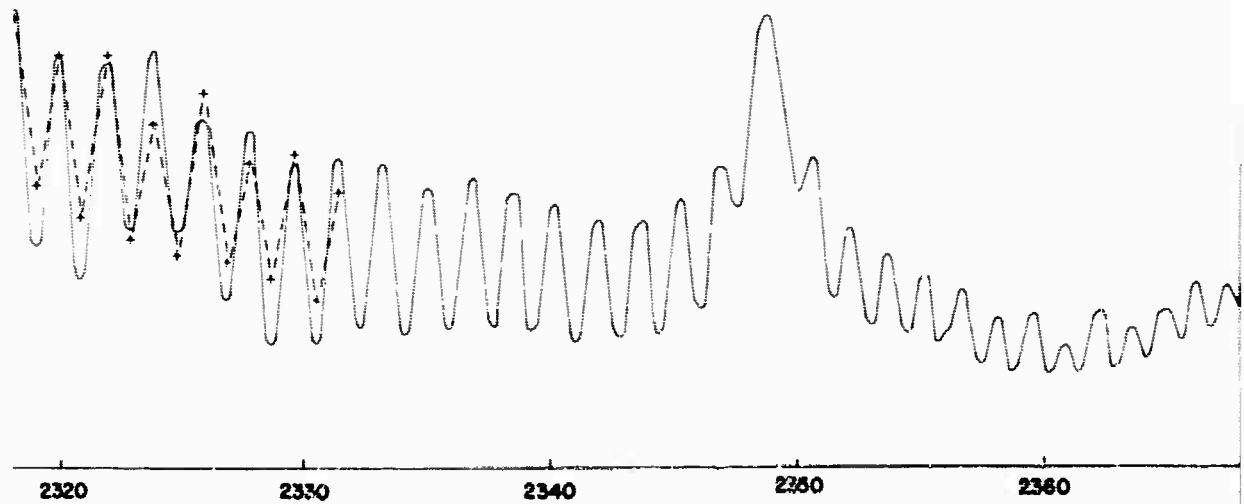
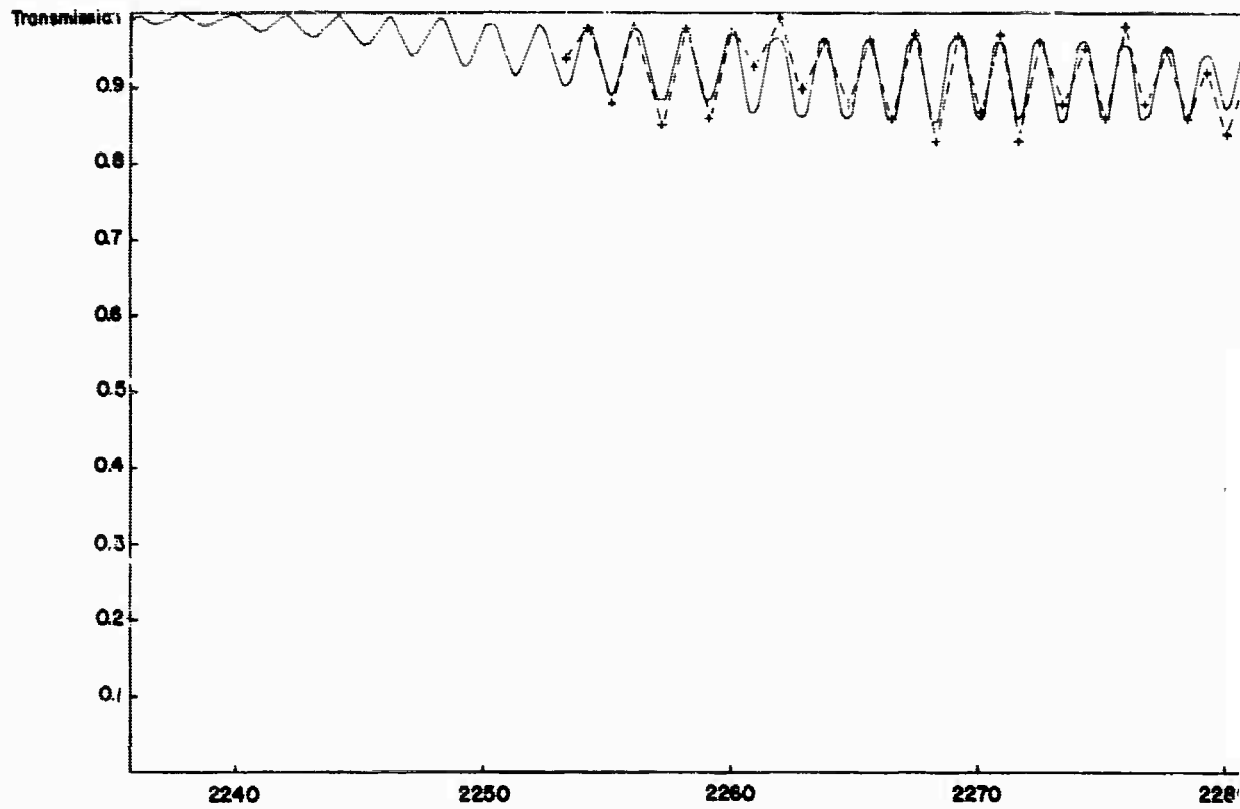
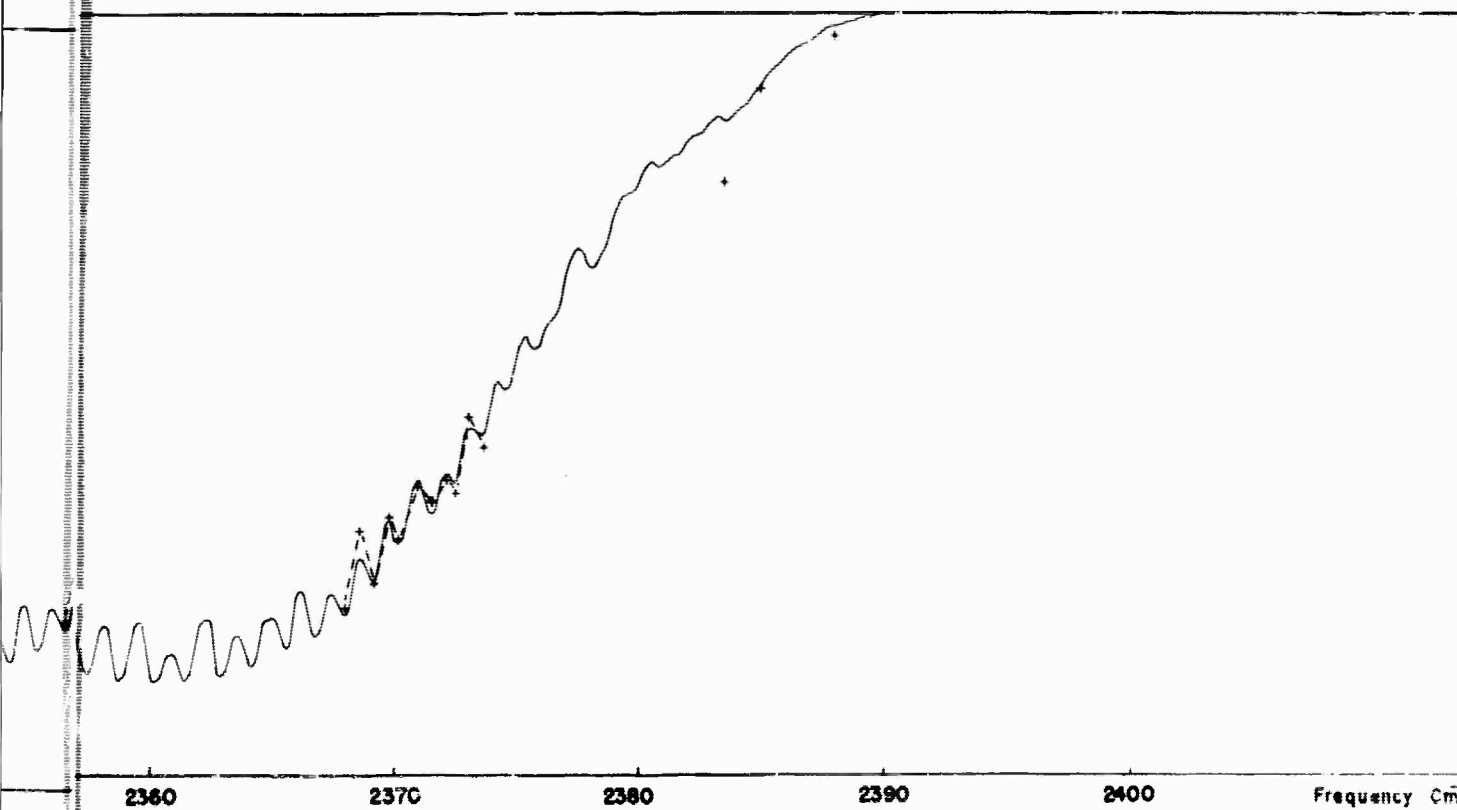
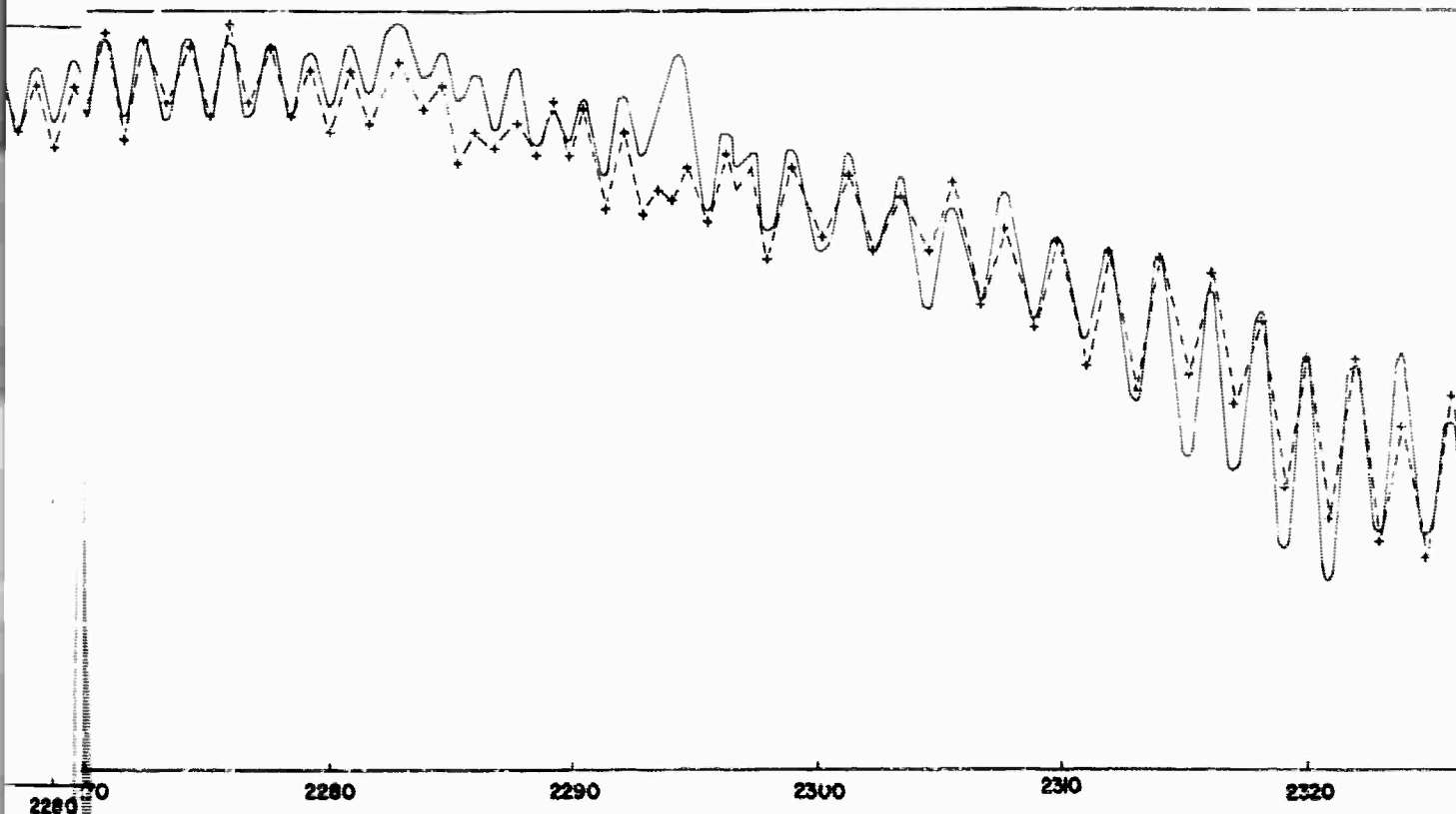


Figure 21. (Record 49) Comparison between Experimental and Calculated Transmission for the 4.3μ CO_2 Band at an Altitude of 28,000 ft. (— calculated; +---+ experimental)



Comparison between Experimental and Theoretical Spectral Transmittance Data
at an Altitude of 28.8 km and a Solar Elevation of 37.16 Degrees.
(Experimental)

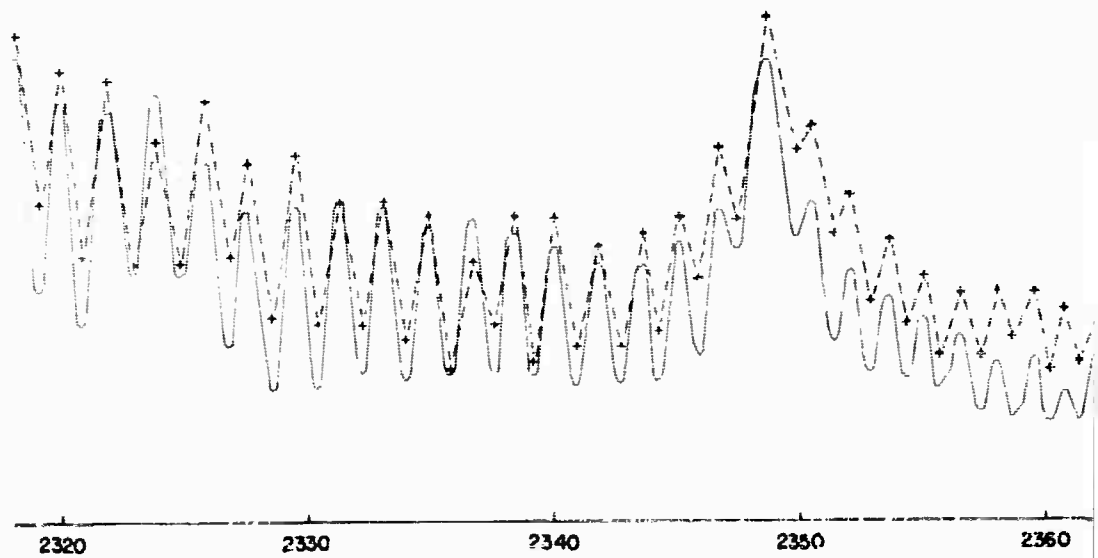
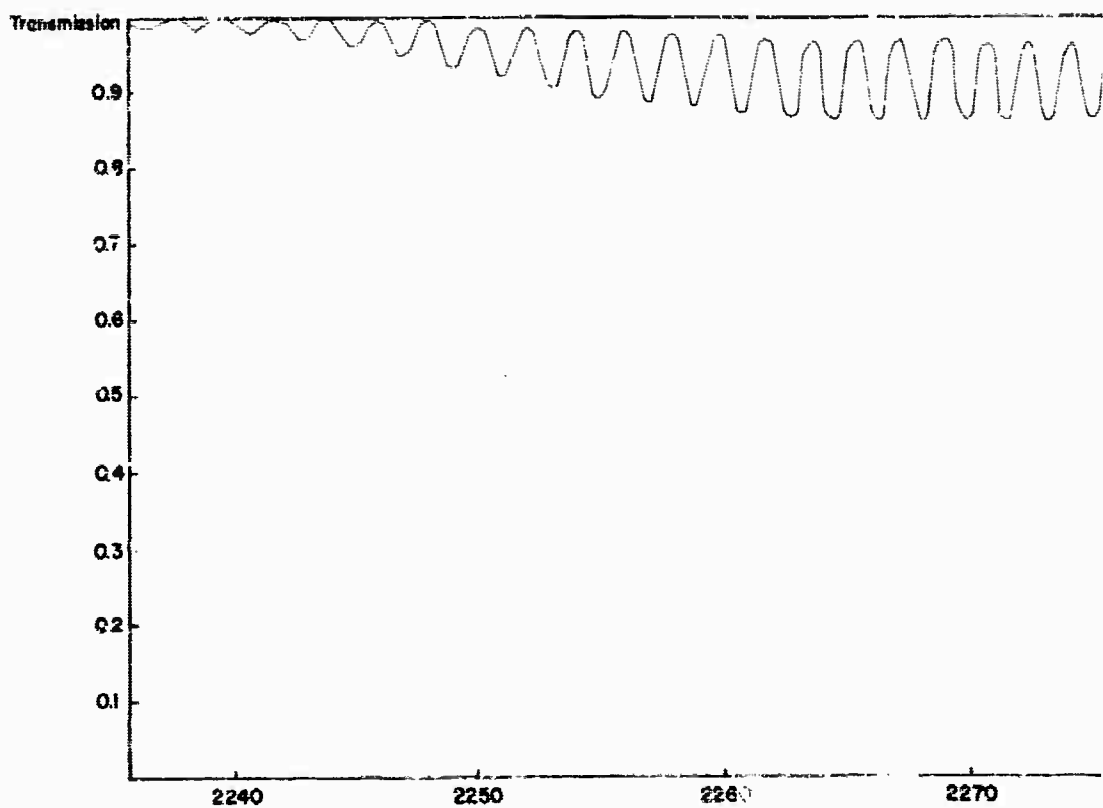
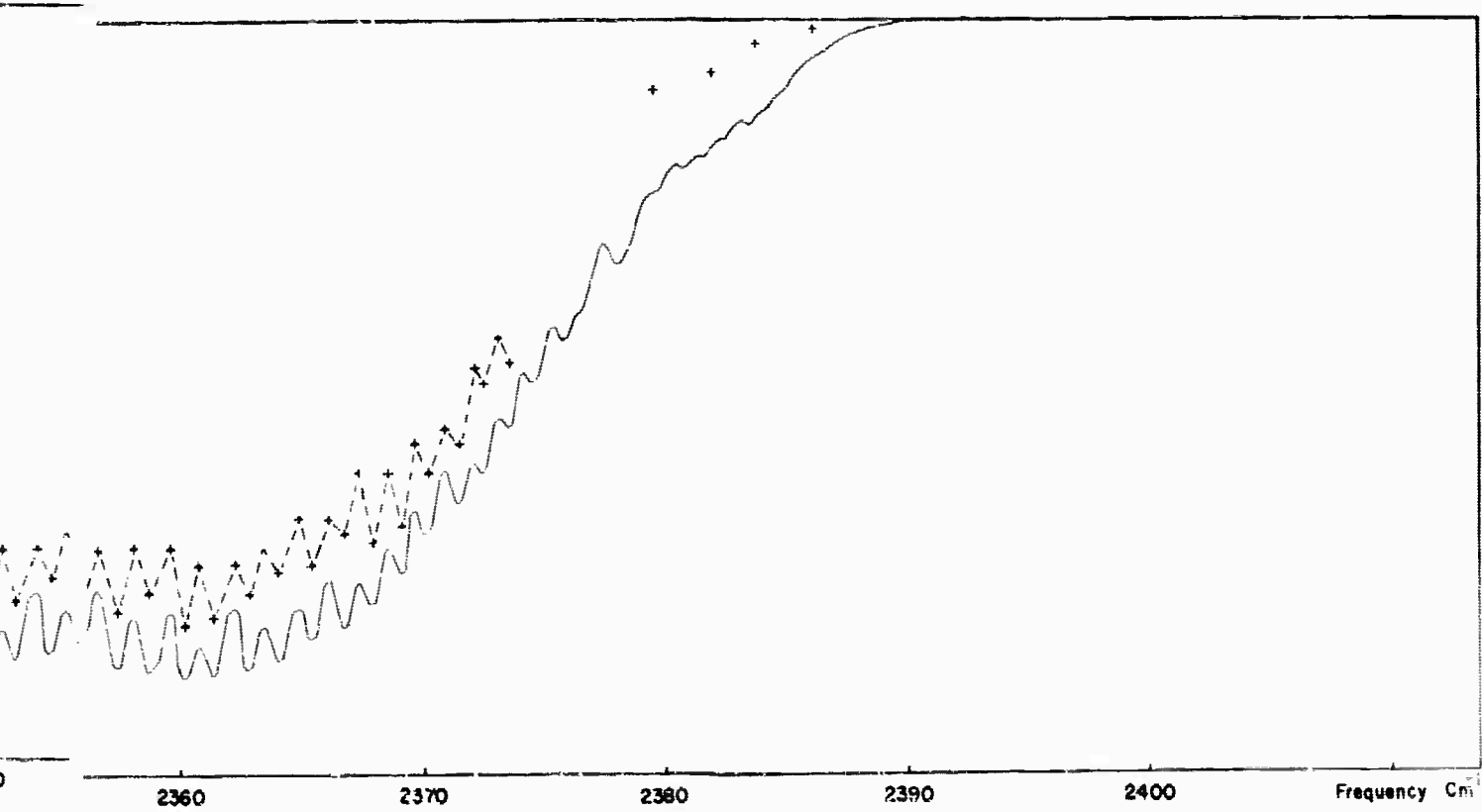
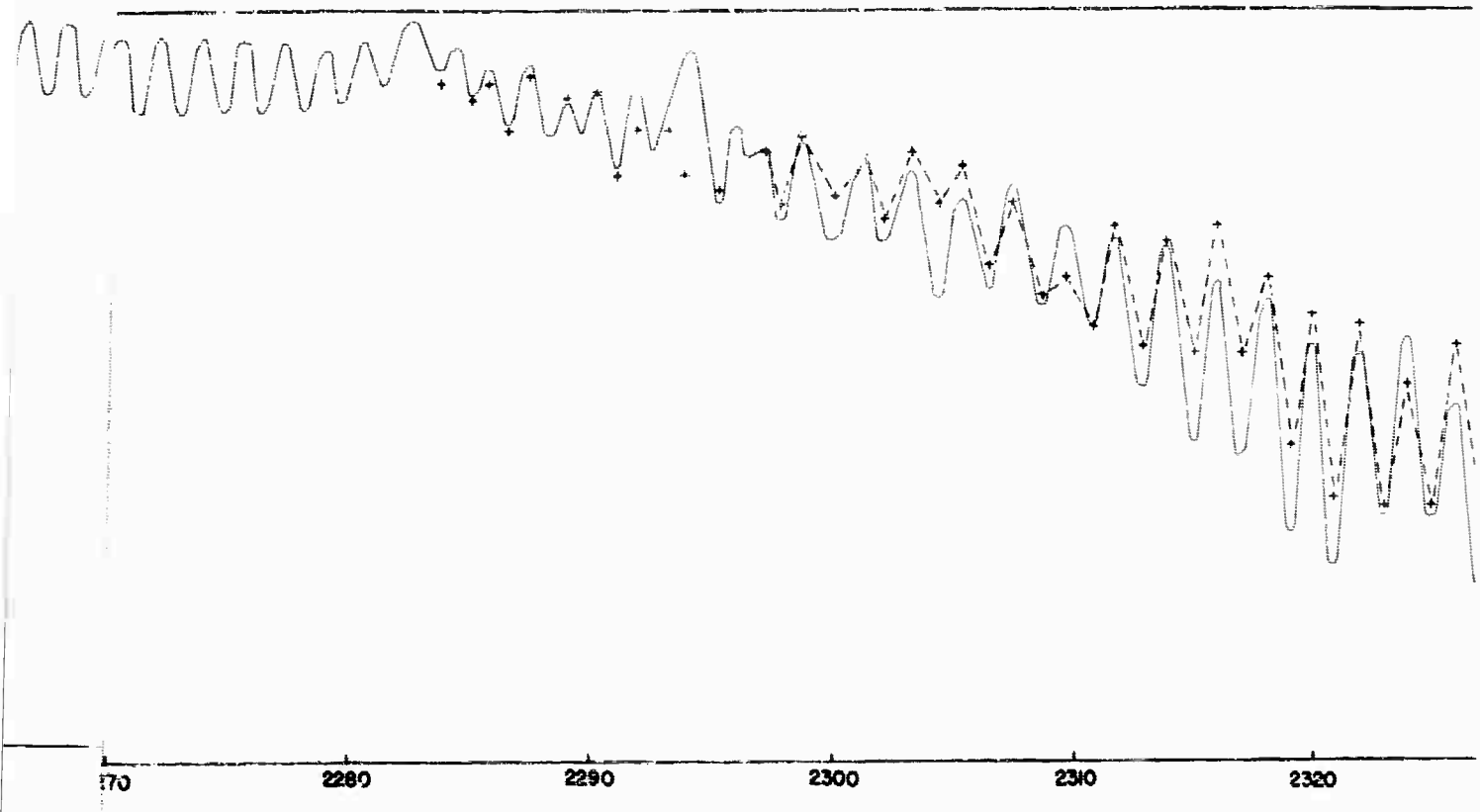


Figure 22. (Record 50) Comparison between calculated and experimental transmission for the 4.3 μ CO₂ Band at an Altitude of 10,000 Feet (— calculated; +----+ experimental)



Comparison between Experimental and Theoretical Spectral Transmittance Data
at an Altitude of 29.2 km and a Solar Elevation of 37.80 Degrees.
(Experimental)

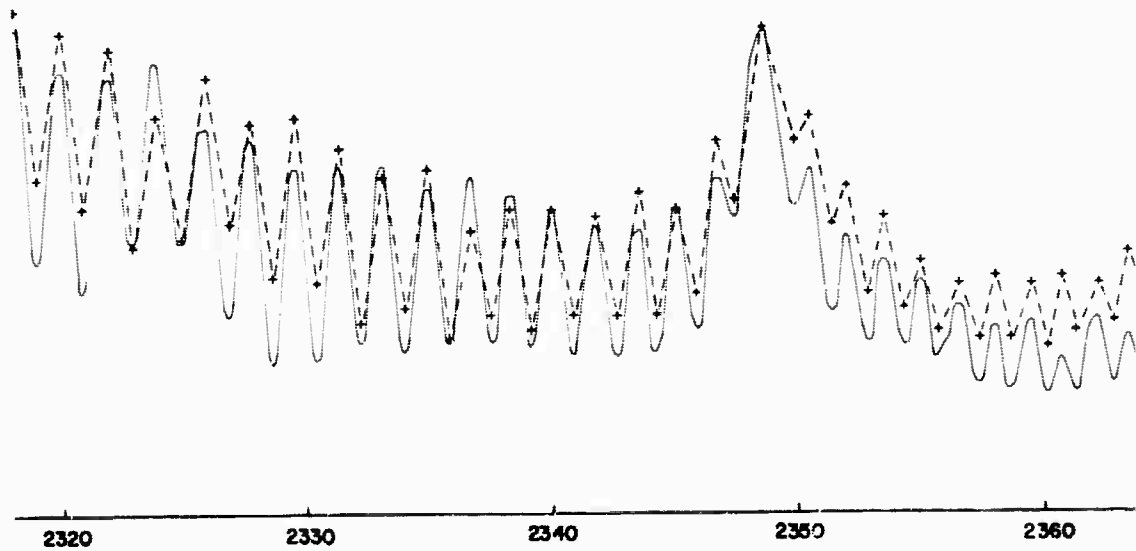
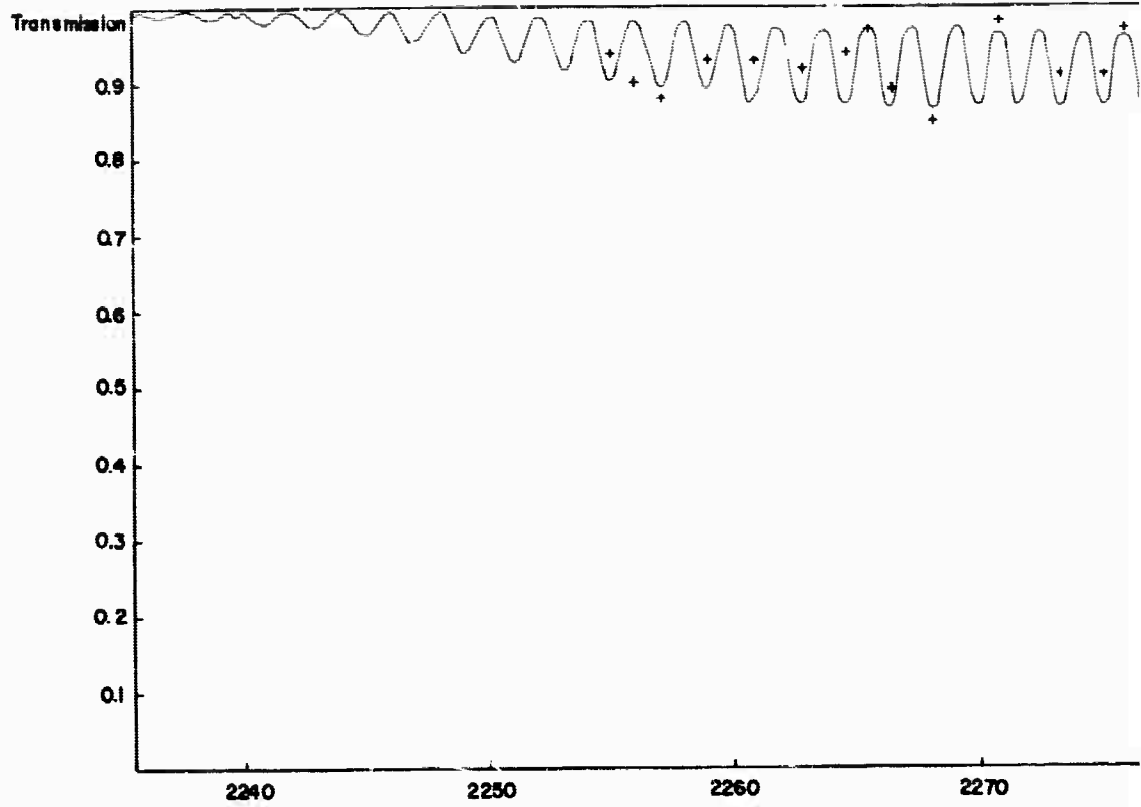
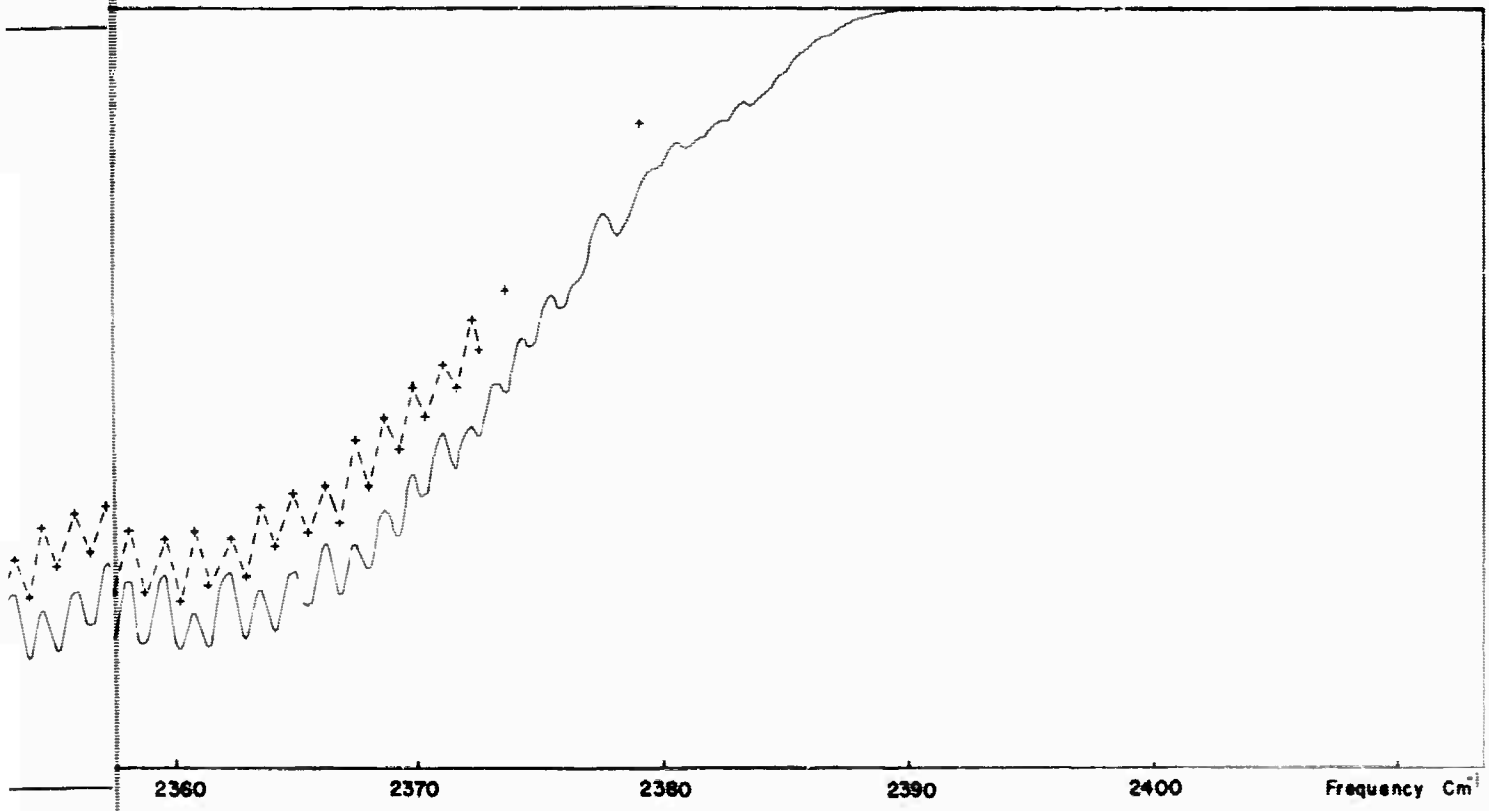
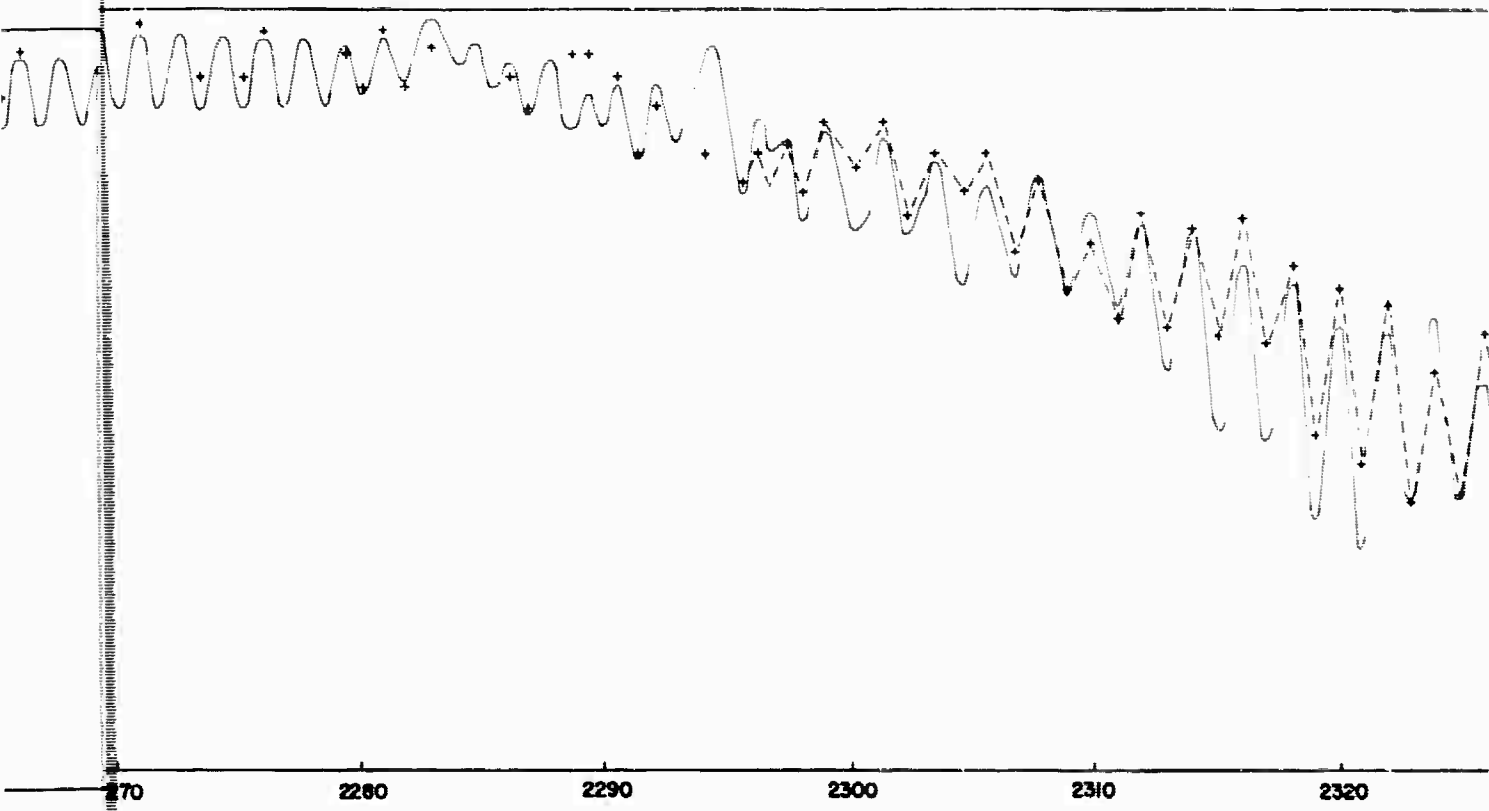


Figure 23. (Record 51) Comparison between Exp
for the 4.3 μ CO₂ Band at an Altitude of
(—— calculated; +---+ experimental)



Comparison Between Experimental and Theoretical Spectral Transmittance Data
Altitude of 29.6 km and a Solar Elevation of 38.43 Degrees.
(Experimental)

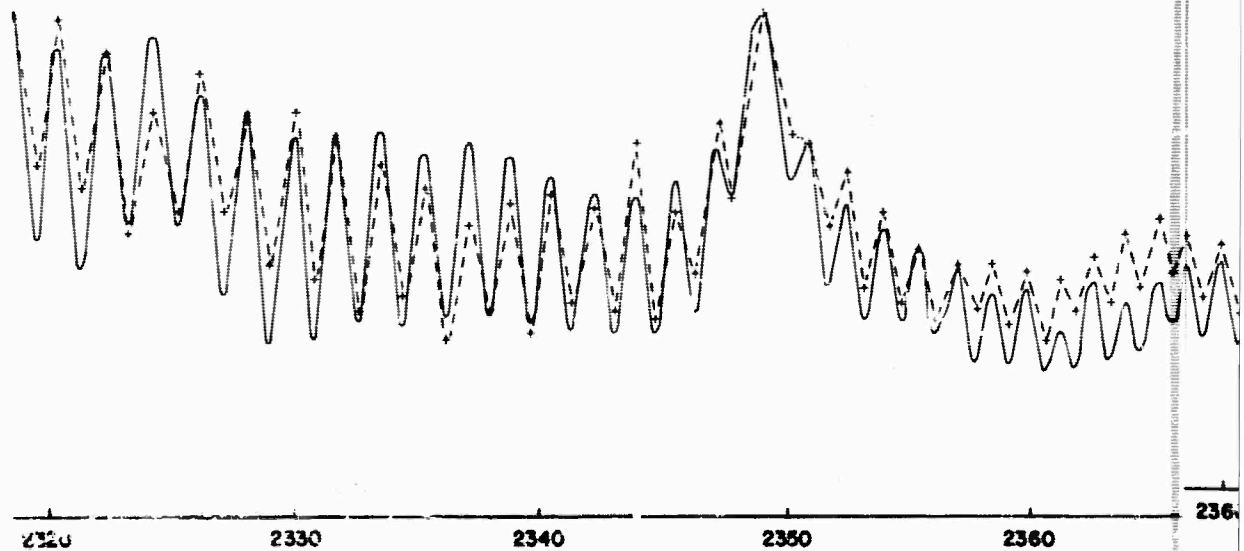
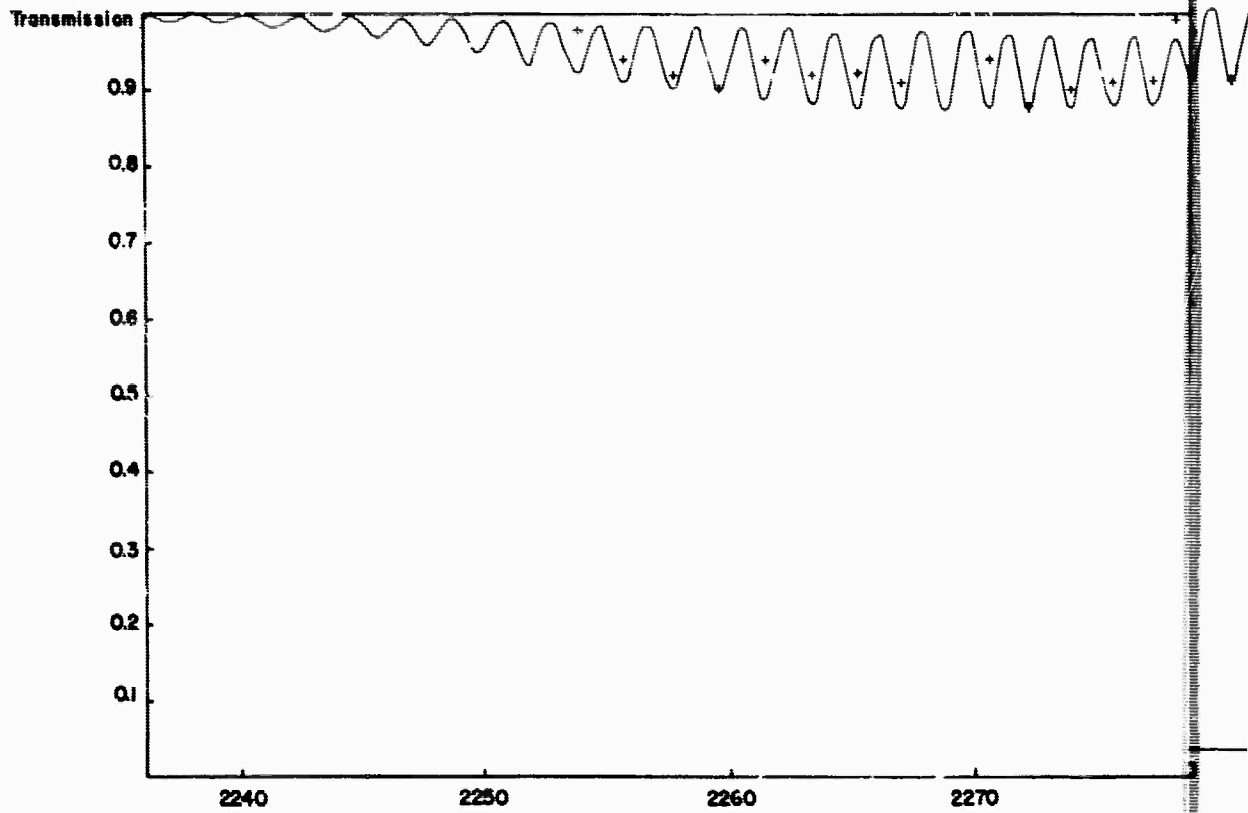
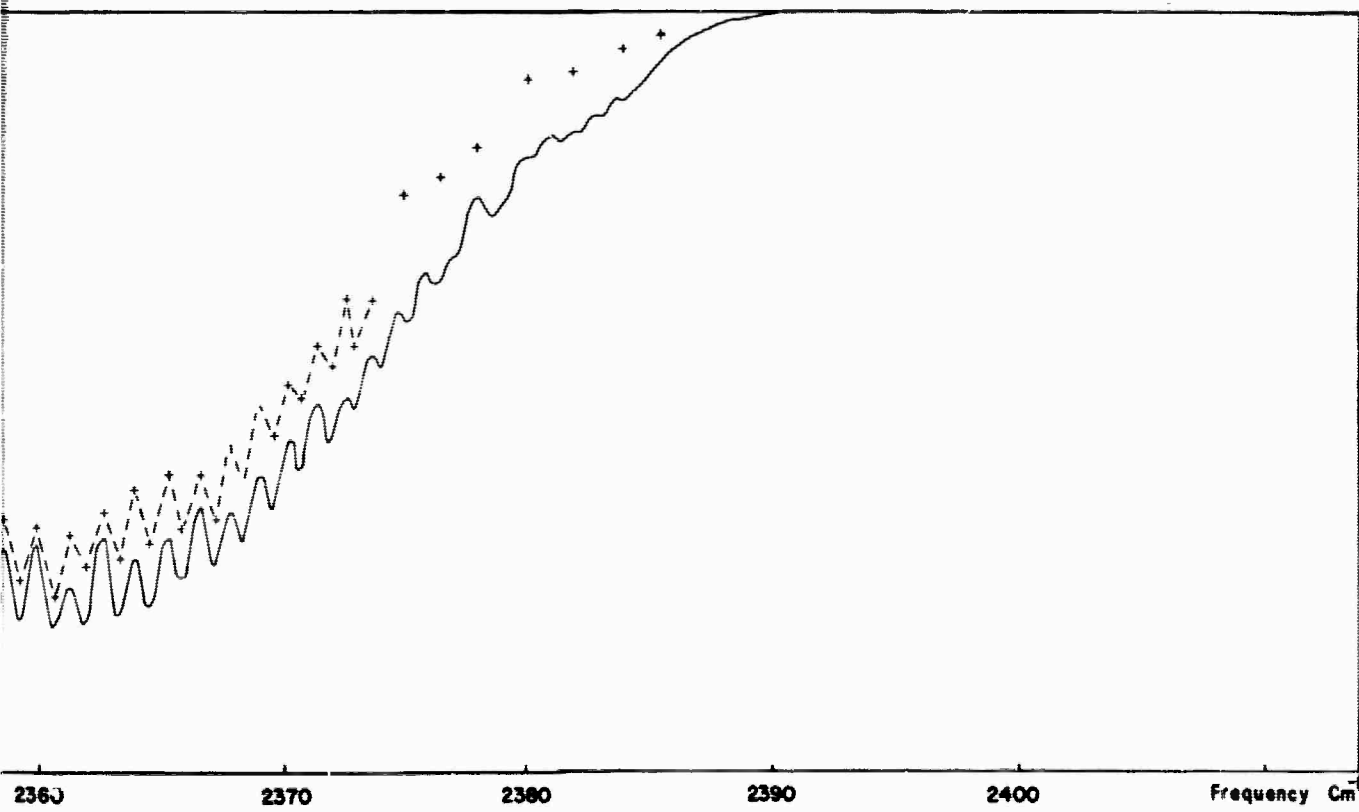
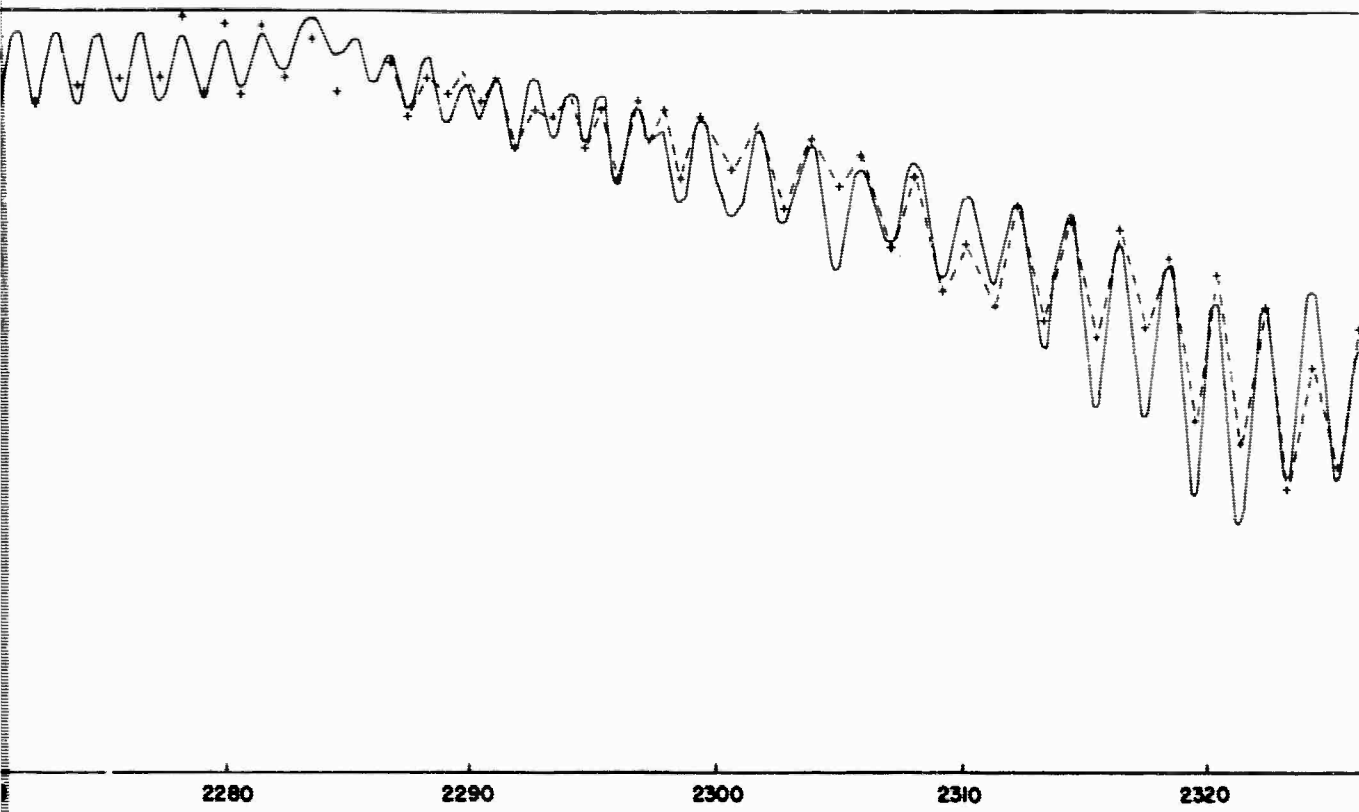


Figure 24. (Record 52) Comparison between Experimental and Calculated Transmission for the 4.3μ CO_2 Band at an Altitude of 10,000 ft. (— calculated; +---+ experimental)



Comparison of Experimental and Theoretical Spectral Transmittance Data
at an Altitude of 30.0 km and a Solar Elevation of 39.06 Degrees.
(Experimental)

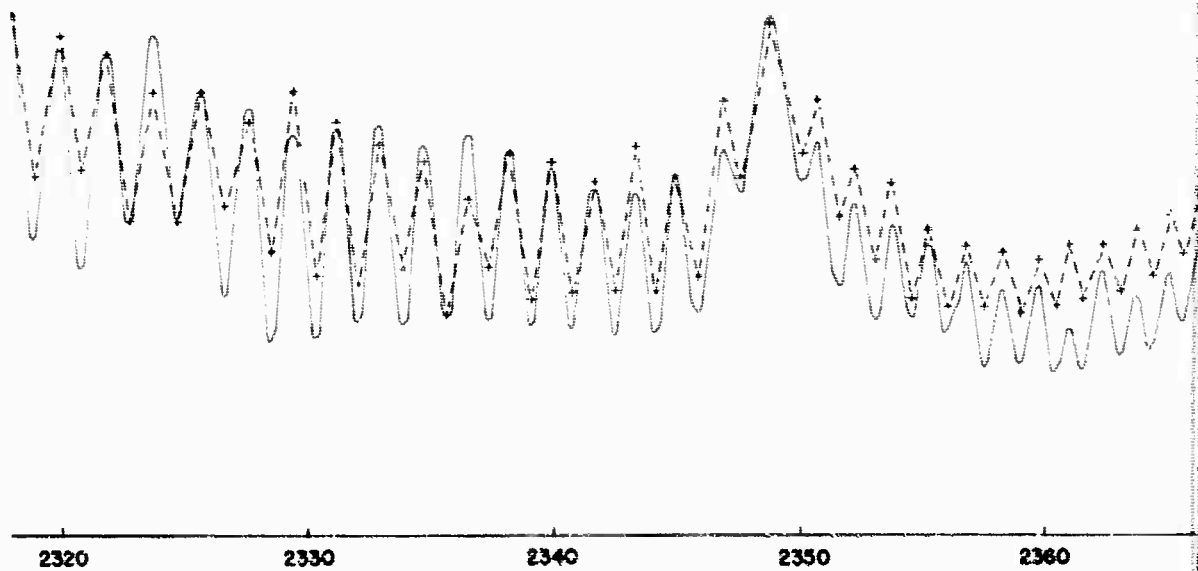
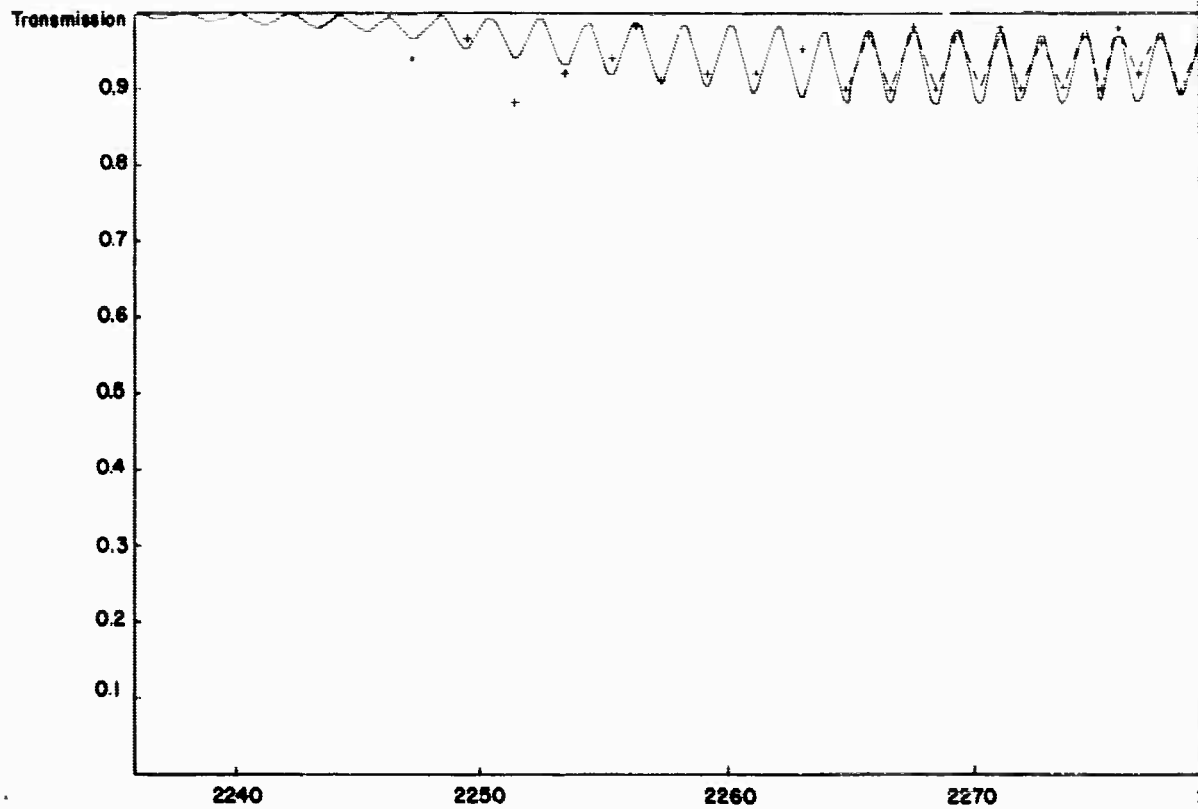
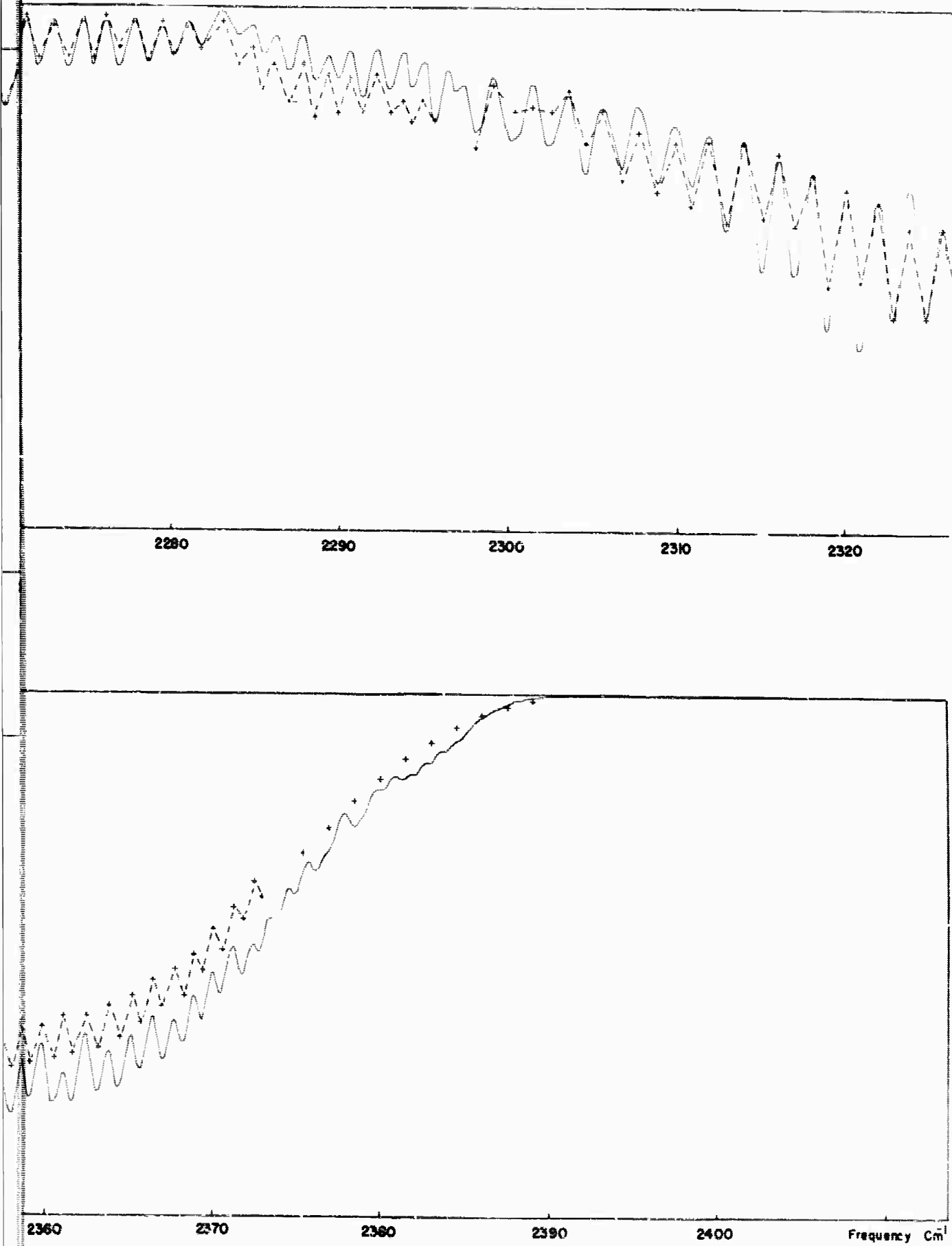


Figure 25. (Record 54) Comparison between Experimental and Calculated Transmission for the 4.3μ CO_2 Band at an Altitude of 30,000 ft. (— calculated; +---+ experimental)



Experimental and Theoretical Spectral Transmittance Data
at an Altitude of 30.4 km and a Solar Elevation of 40.32 Degrees.
(Experimental)

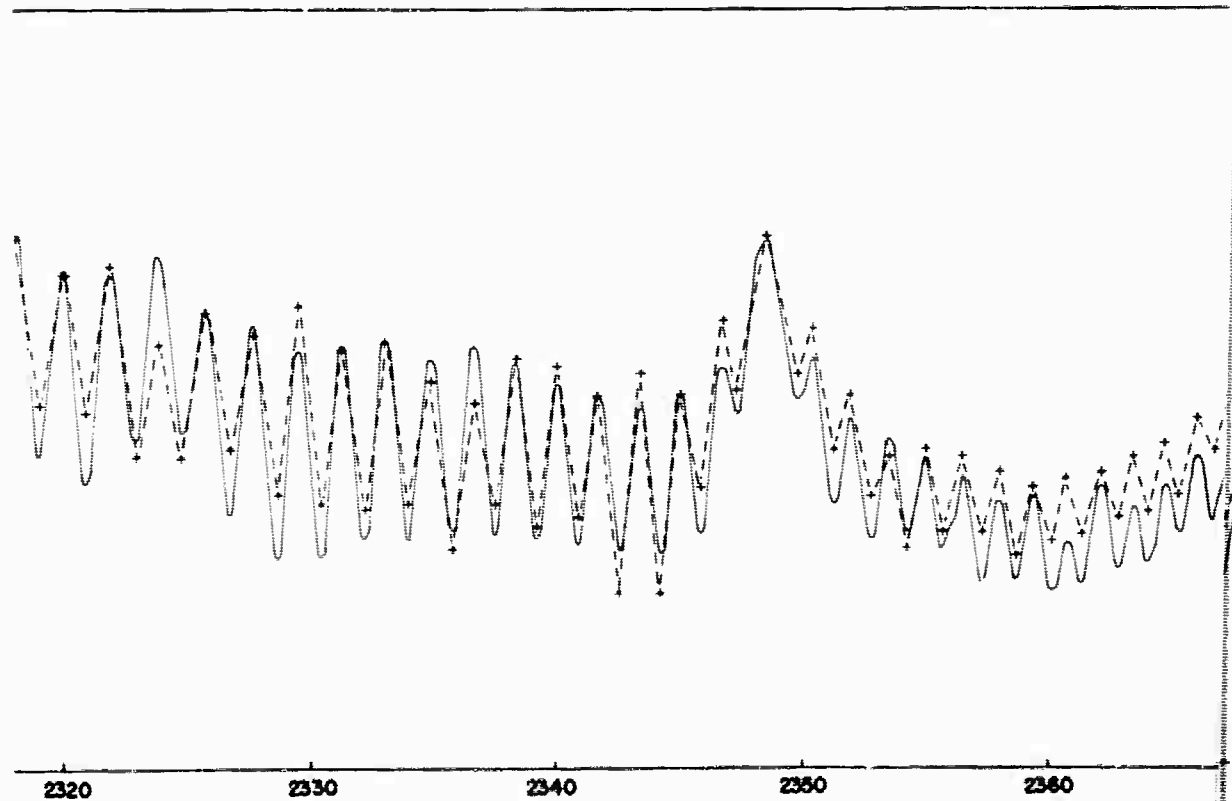
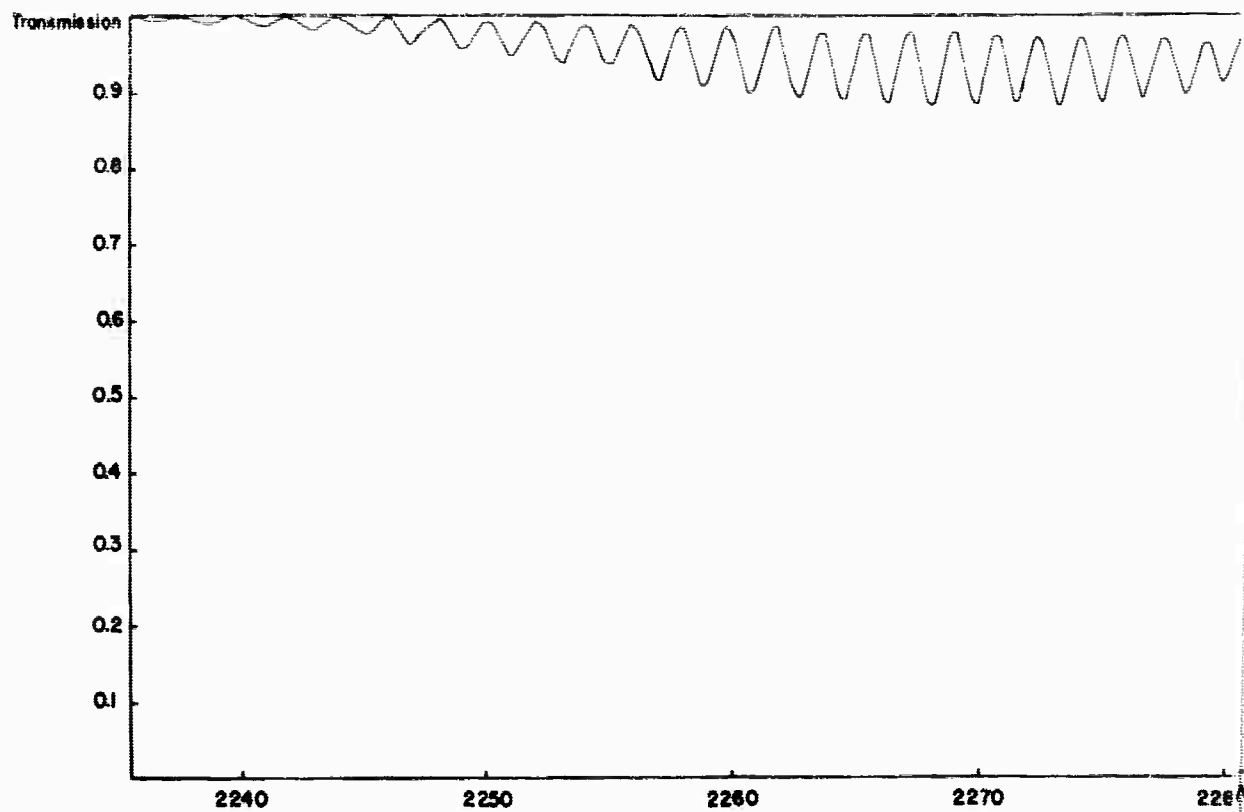
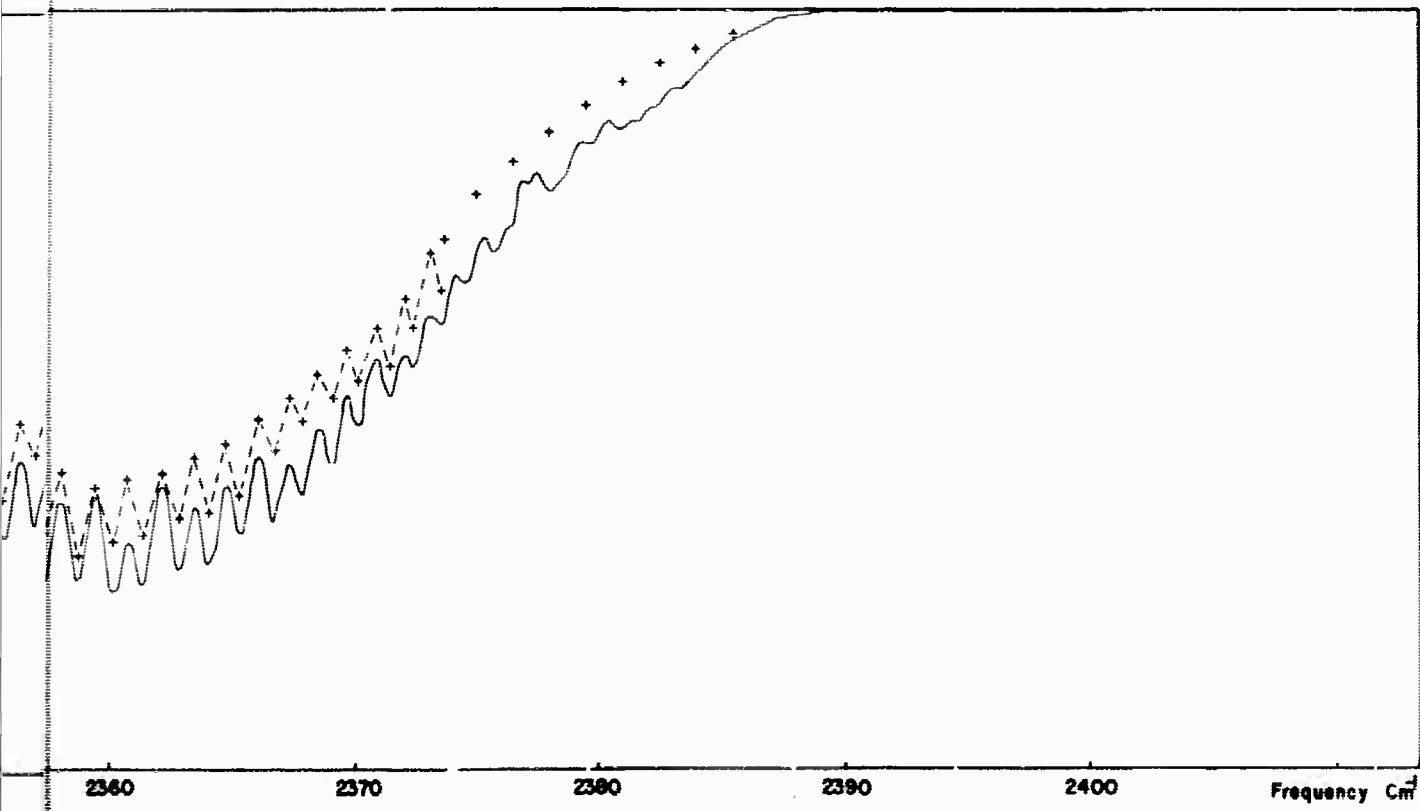
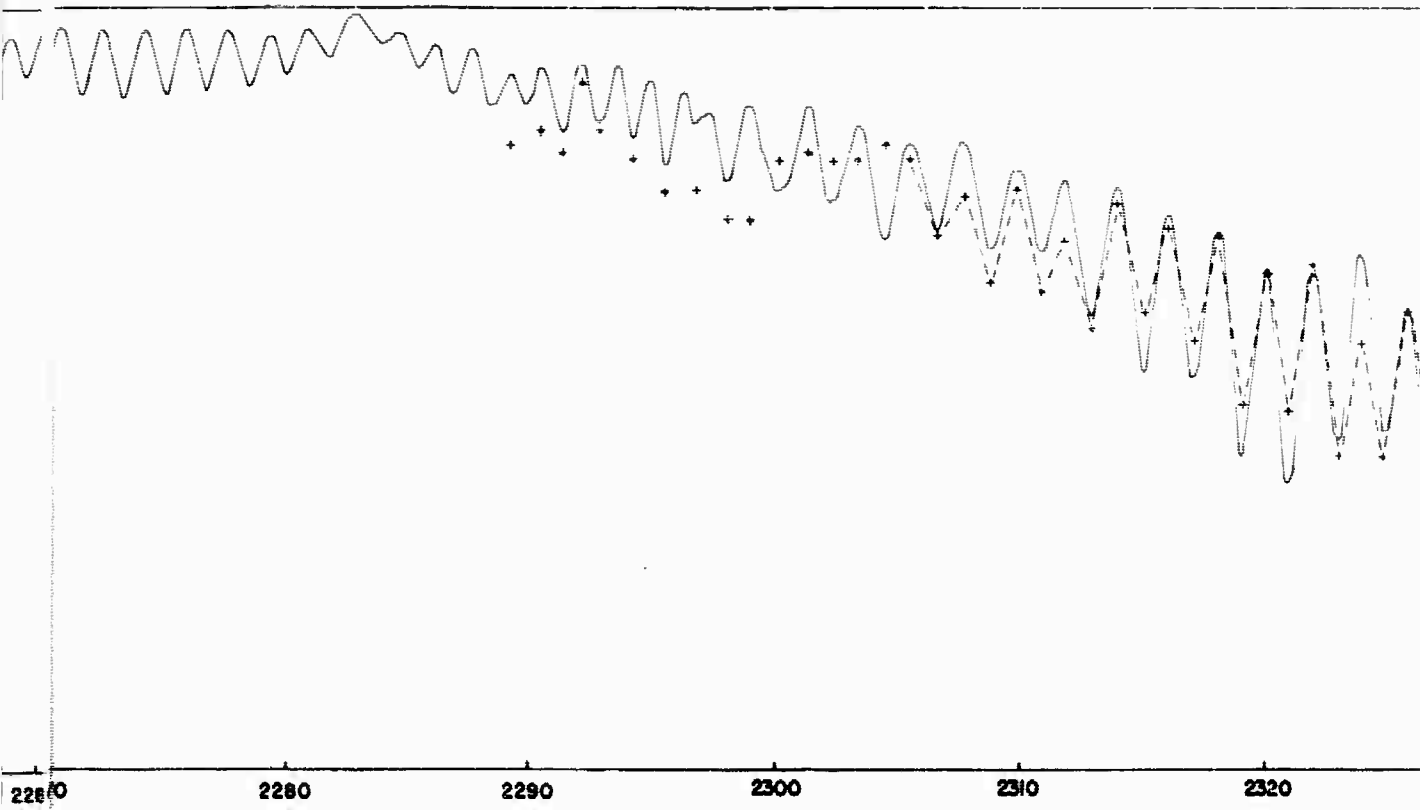


Figure 26. (Record 55) Comparison between Experiment and Calculation for the 4.3 μm CO₂ Band at an Altitude of 30,000 ft. (— calculated; +----+ experimental)



Comparison of Experimental and Theoretical Spectral Transmittance Data
at an Altitude of 30.8 km and a Solar Elevation of 40.95 Degrees.
(Experimental)

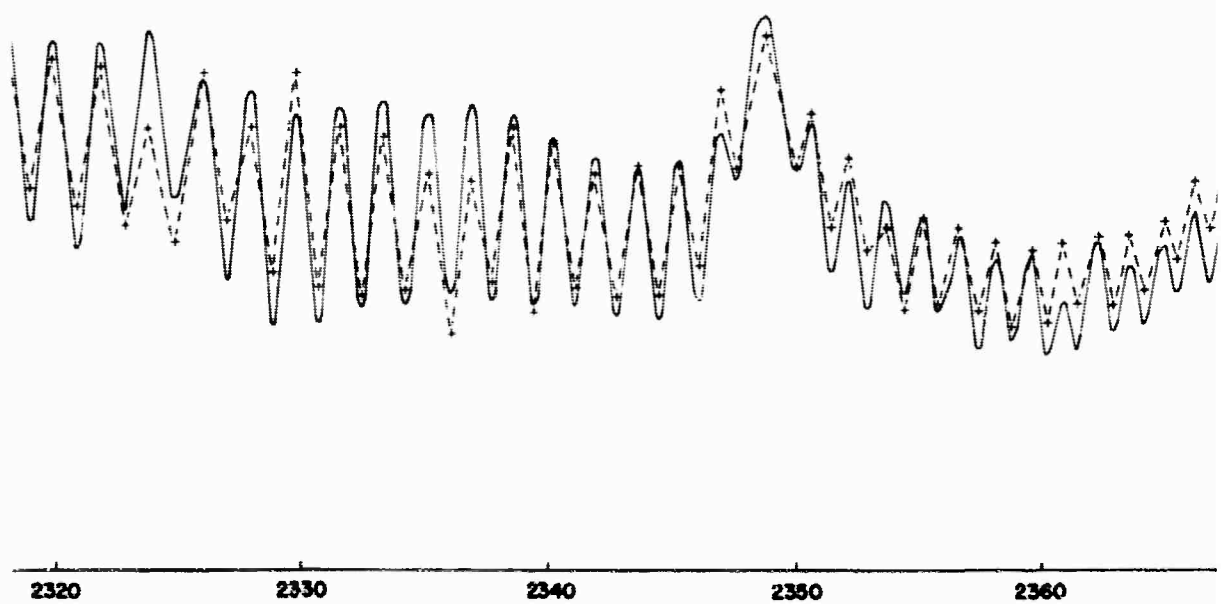
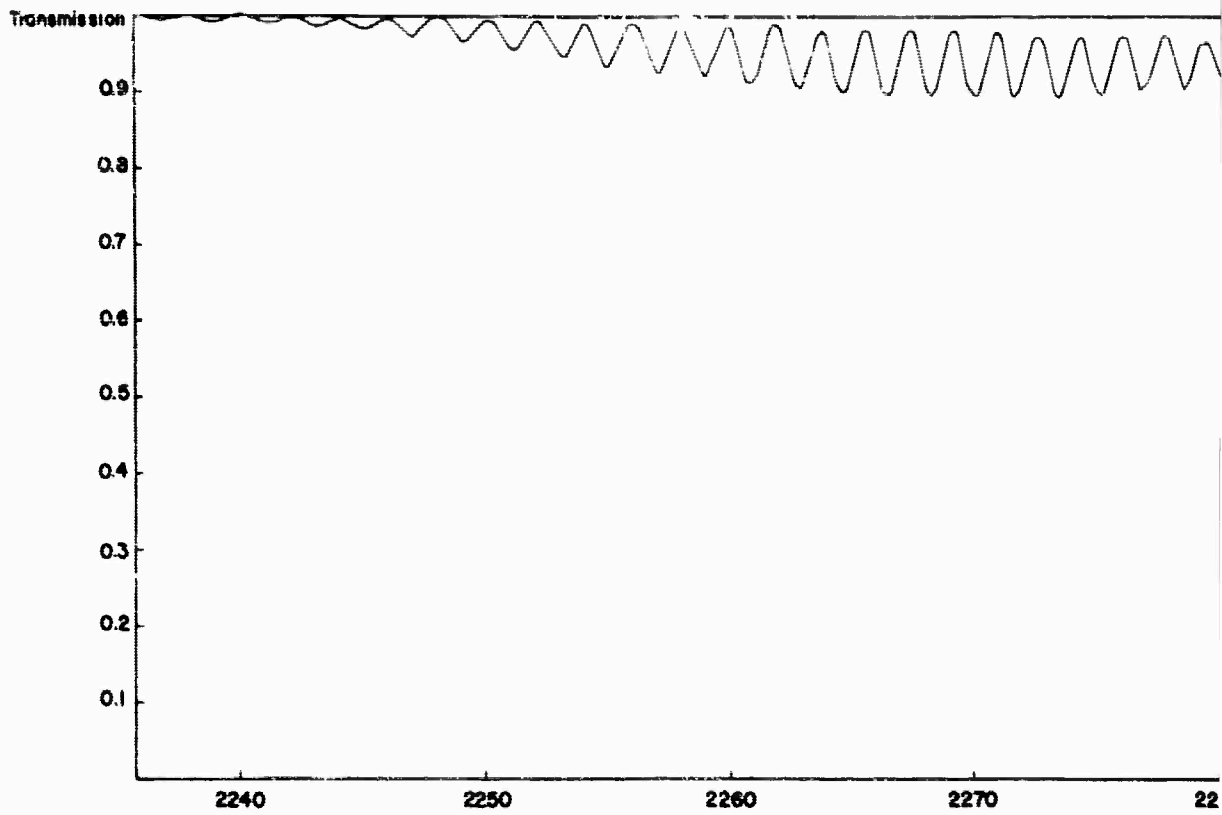
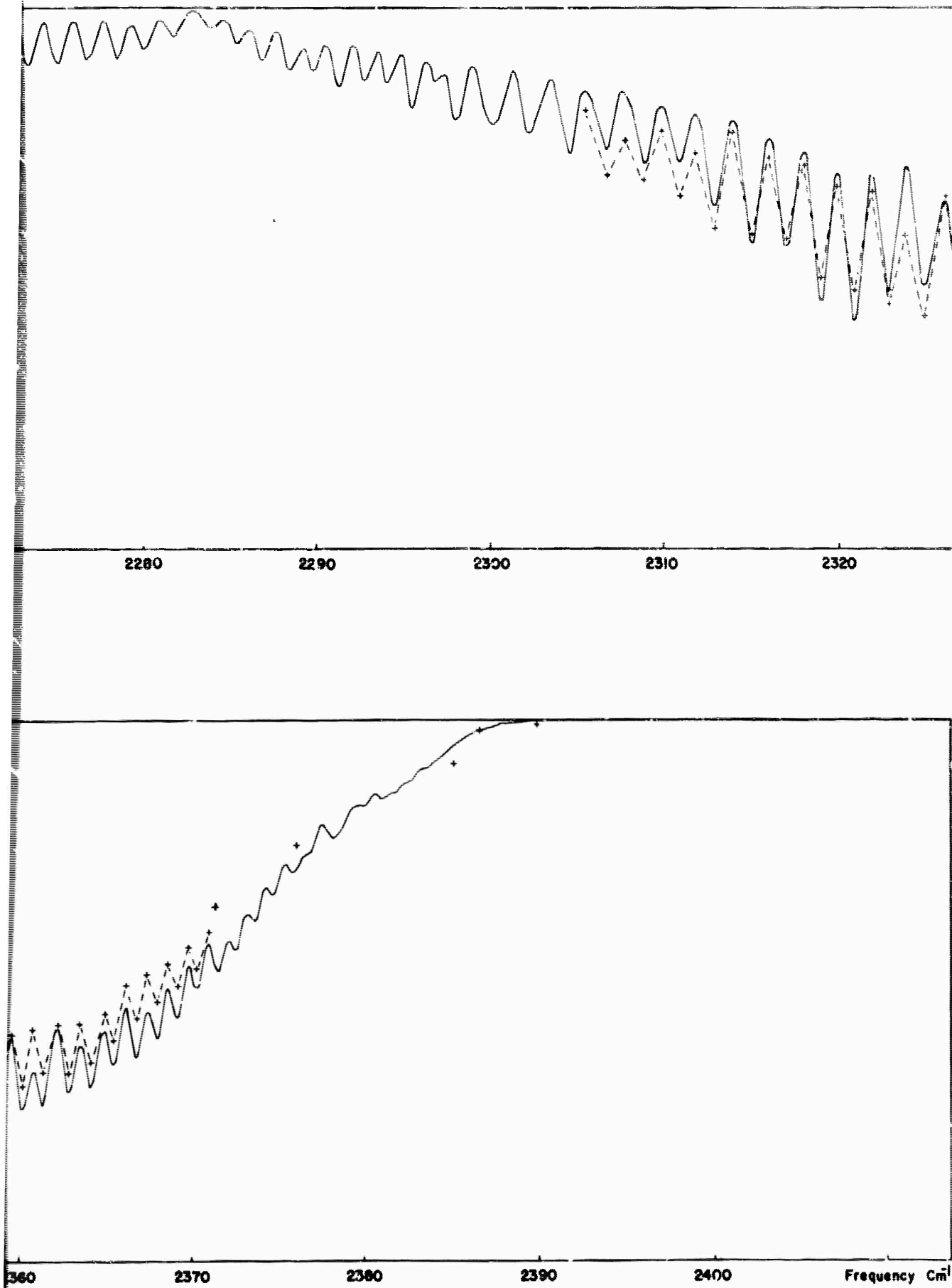


Figure 27. (Record 57) Comparison between Experimental and Calculated Transmission for the 4.3μ CO_2 Band at an Altitude of 31,000 ft. (— calculated; +---+ experimental)



Experimental and Theoretical Spectral Transmittance Data
at a Path Length of 31.4 km and a Solar Elevation of 42.21 Degrees.
(Experimental)

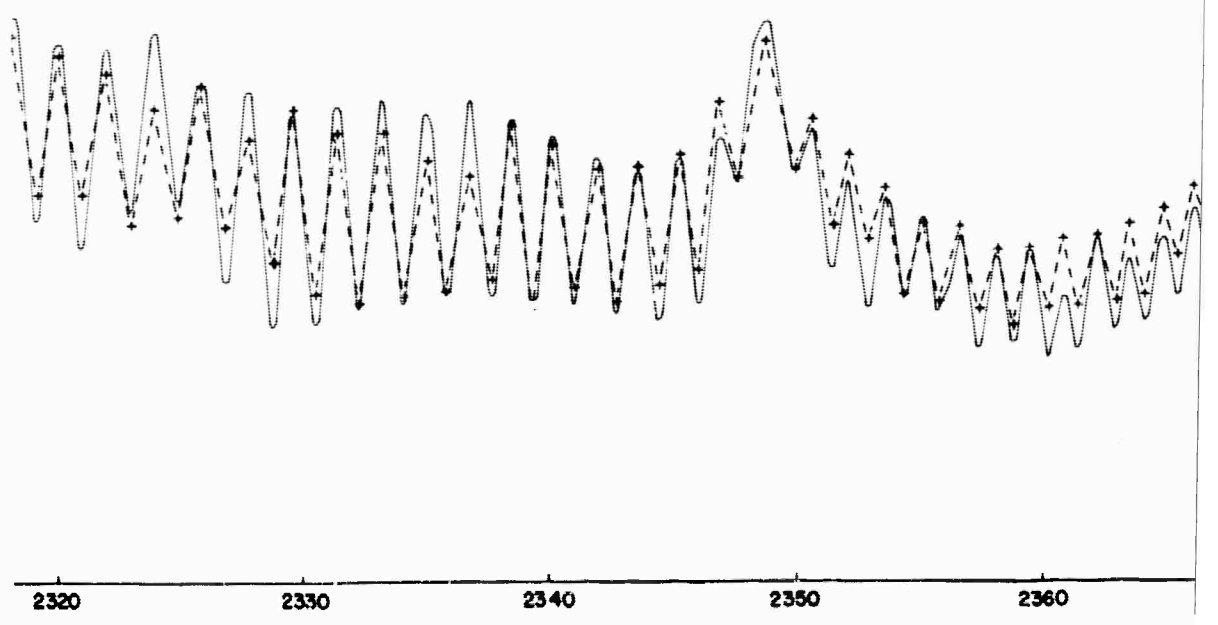
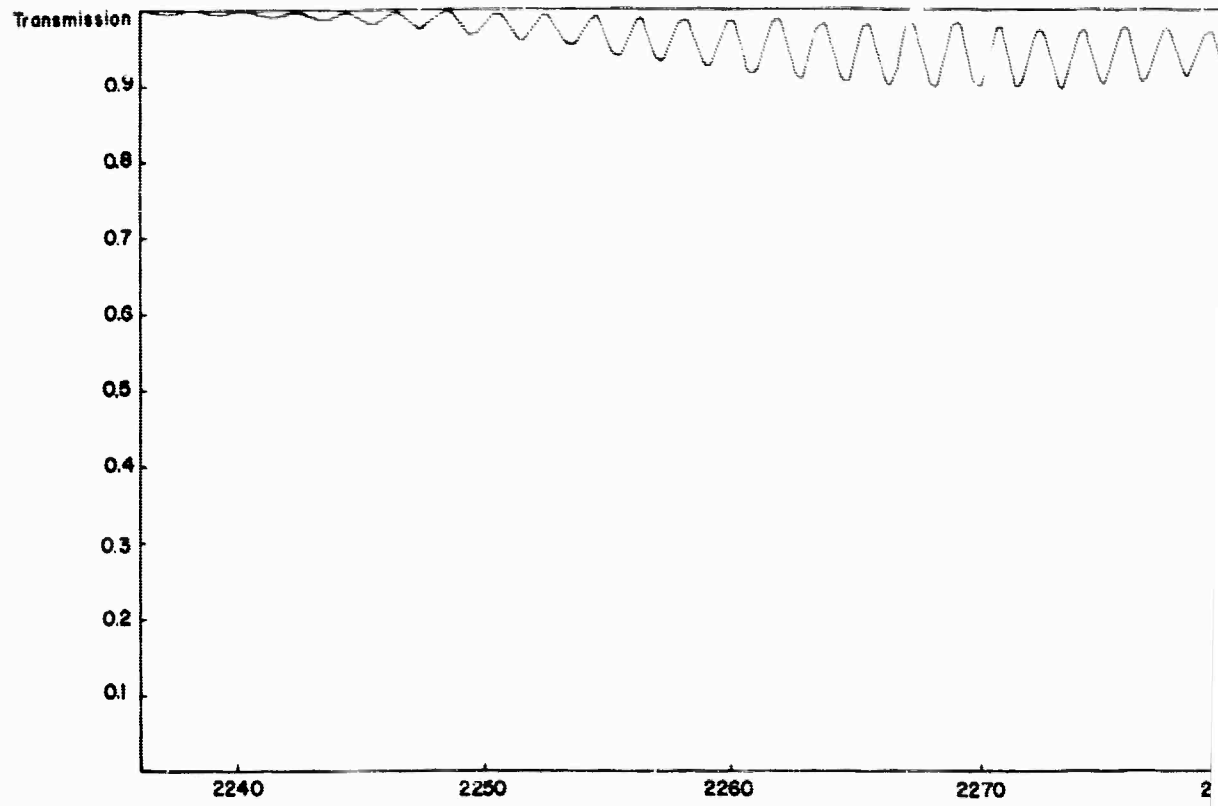


Figure 28. (Record 58) Comparison between Experiment and Calculation for the 4.3 μ CO₂ Band at an Altitude of 30,000 Feet. (— calculated; +----+ experimental)

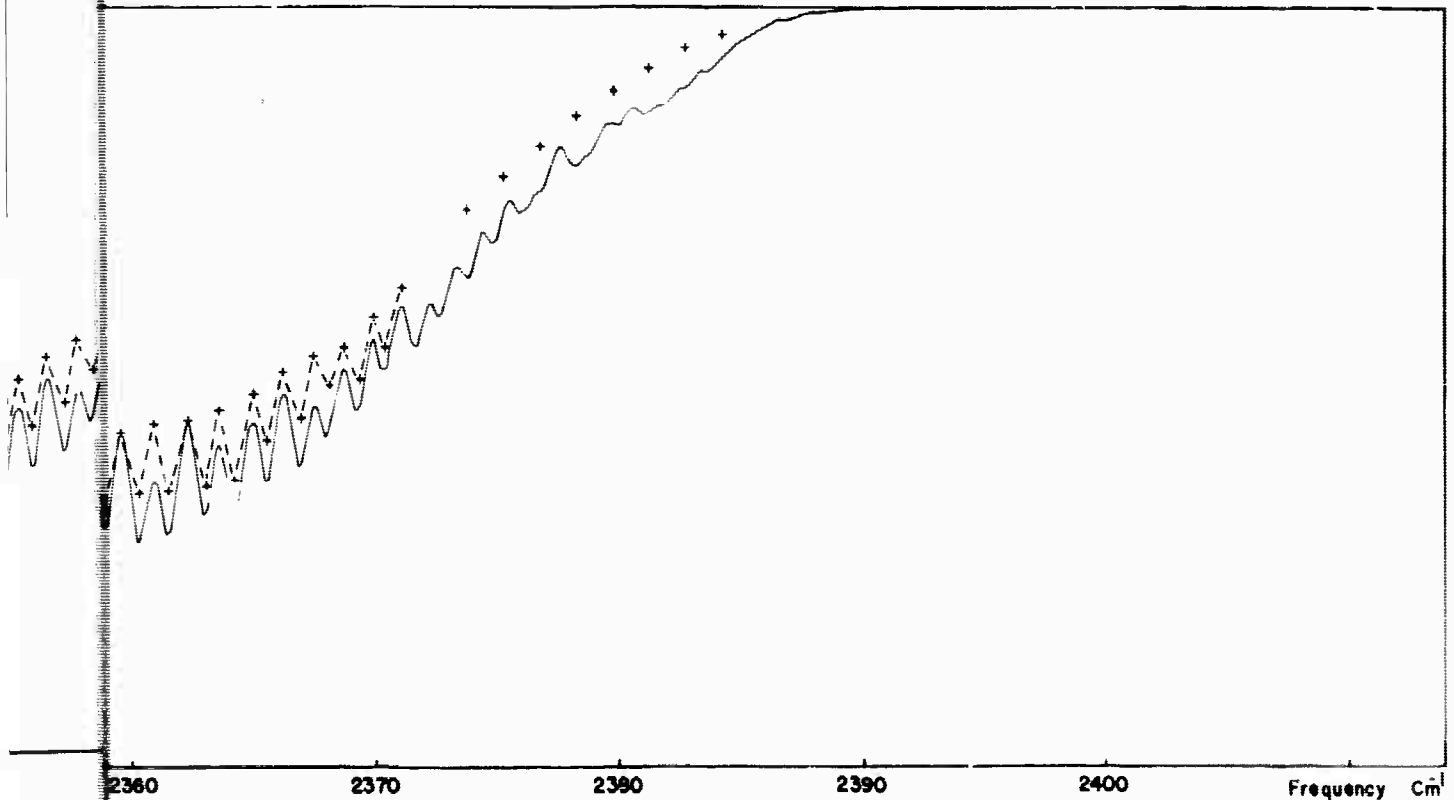
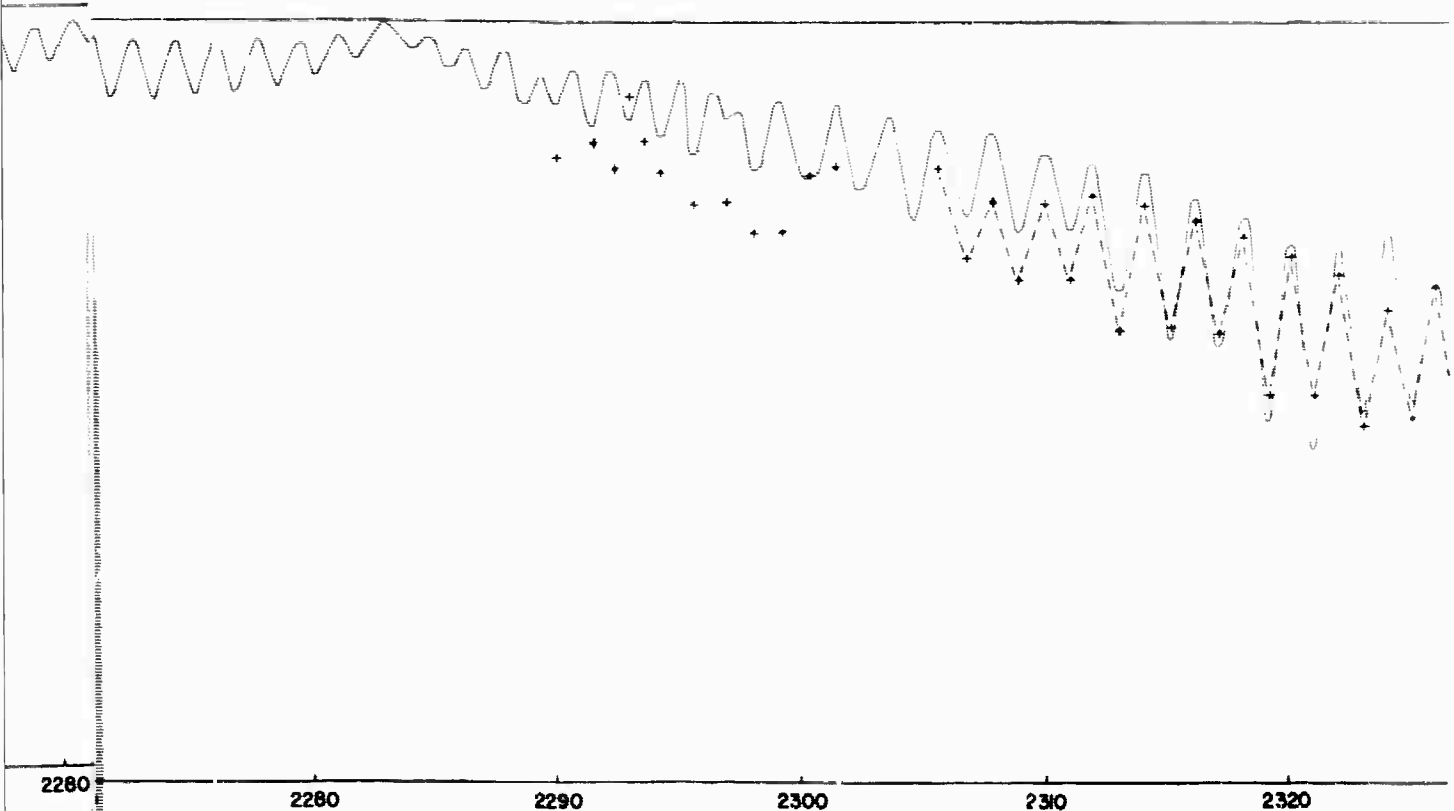


Figure 1. Comparison of Experimental and Theoretical Spectral Transmittance Data for a Path Length of 31.7 km and a Solar Elevation of 42.83 Degrees. (Theoretical Data is shown as a solid line, and experimental data is shown as a dashed line with '+' markers.)

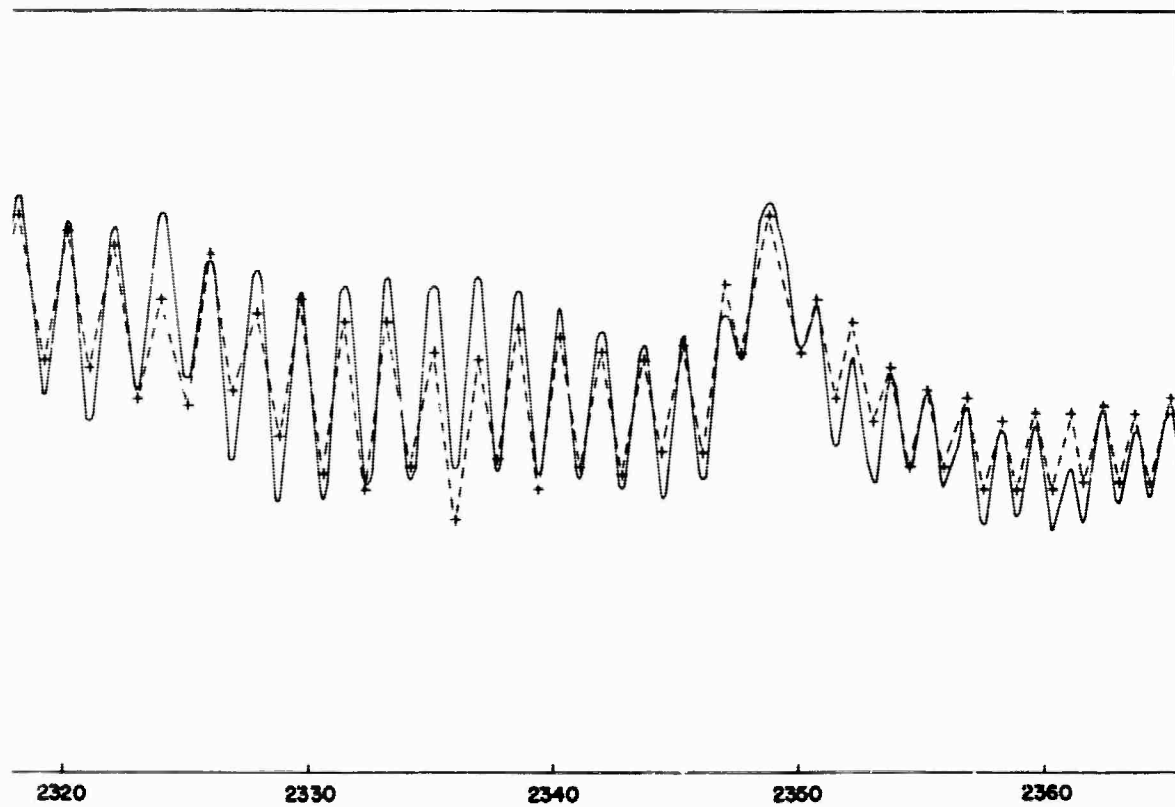
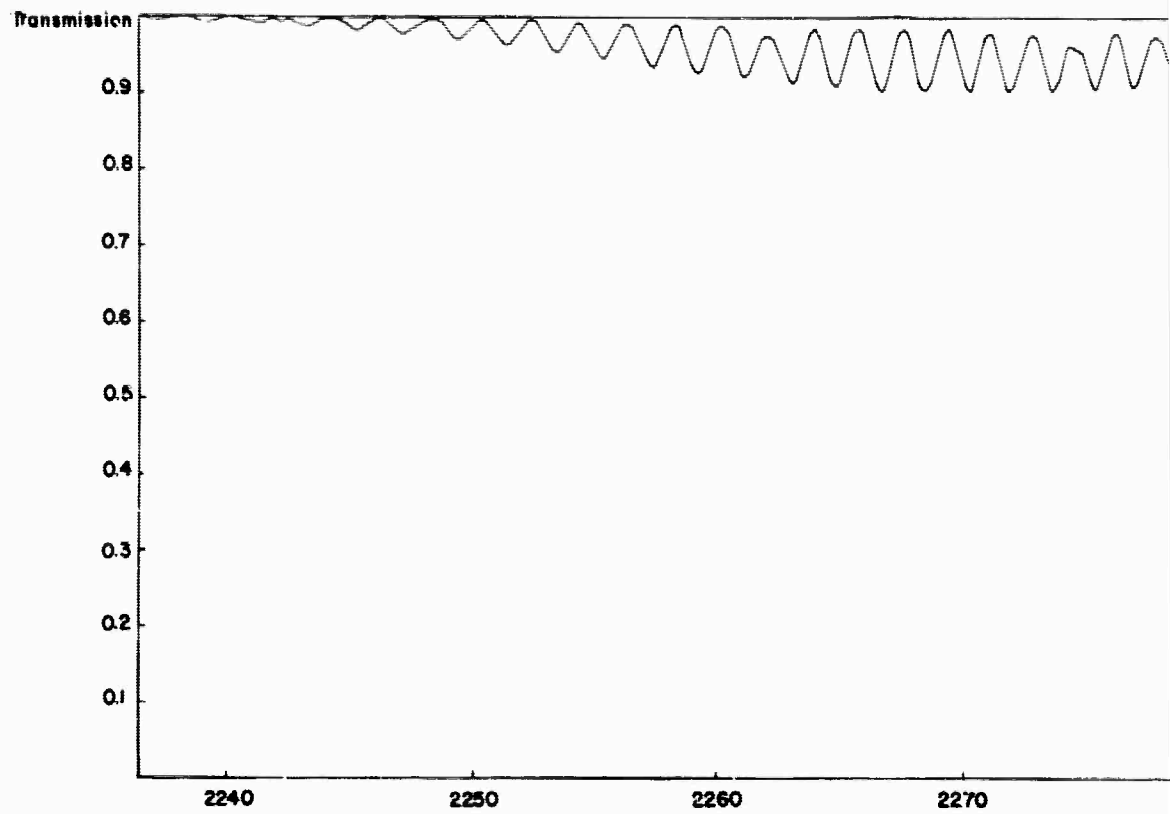
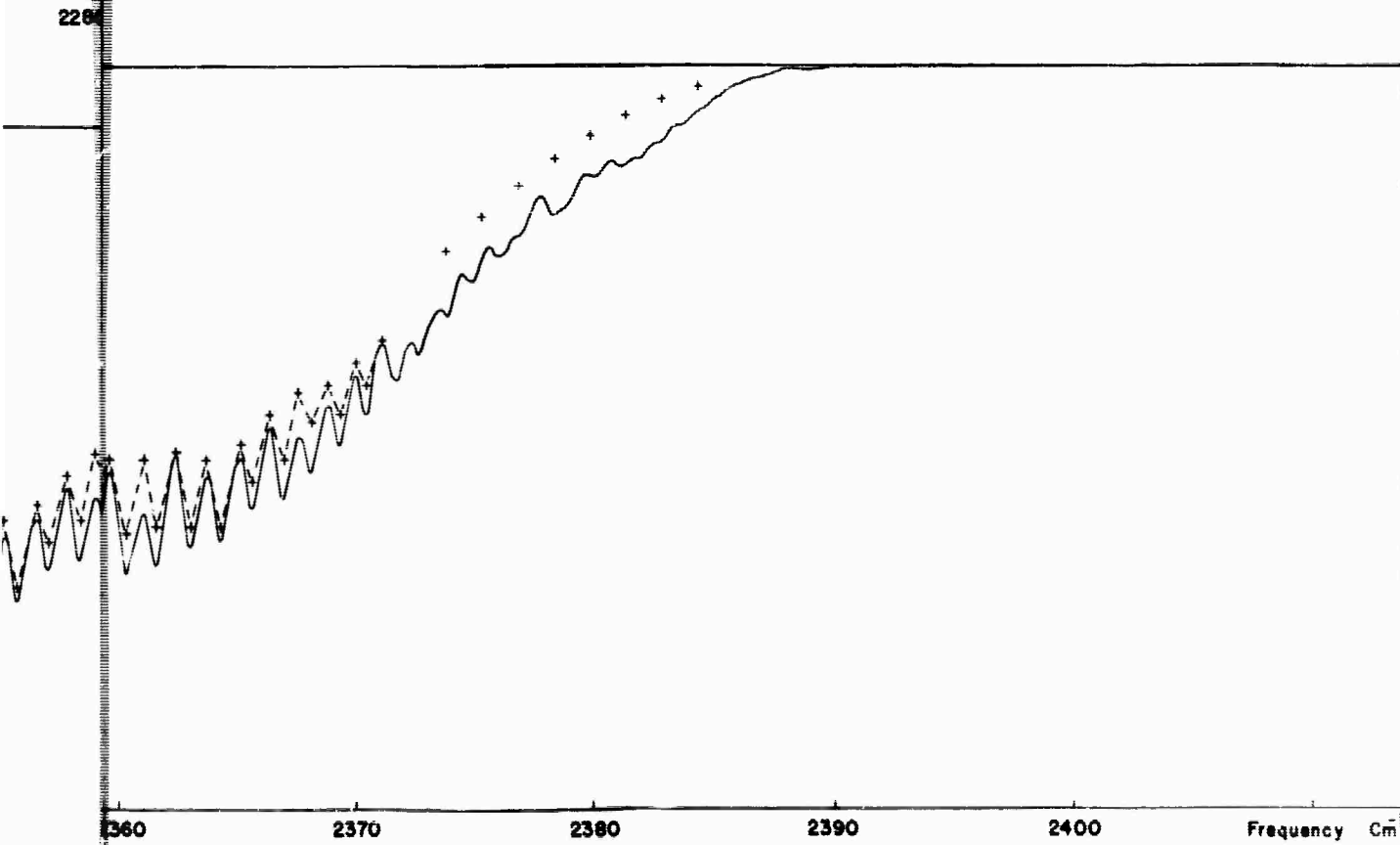
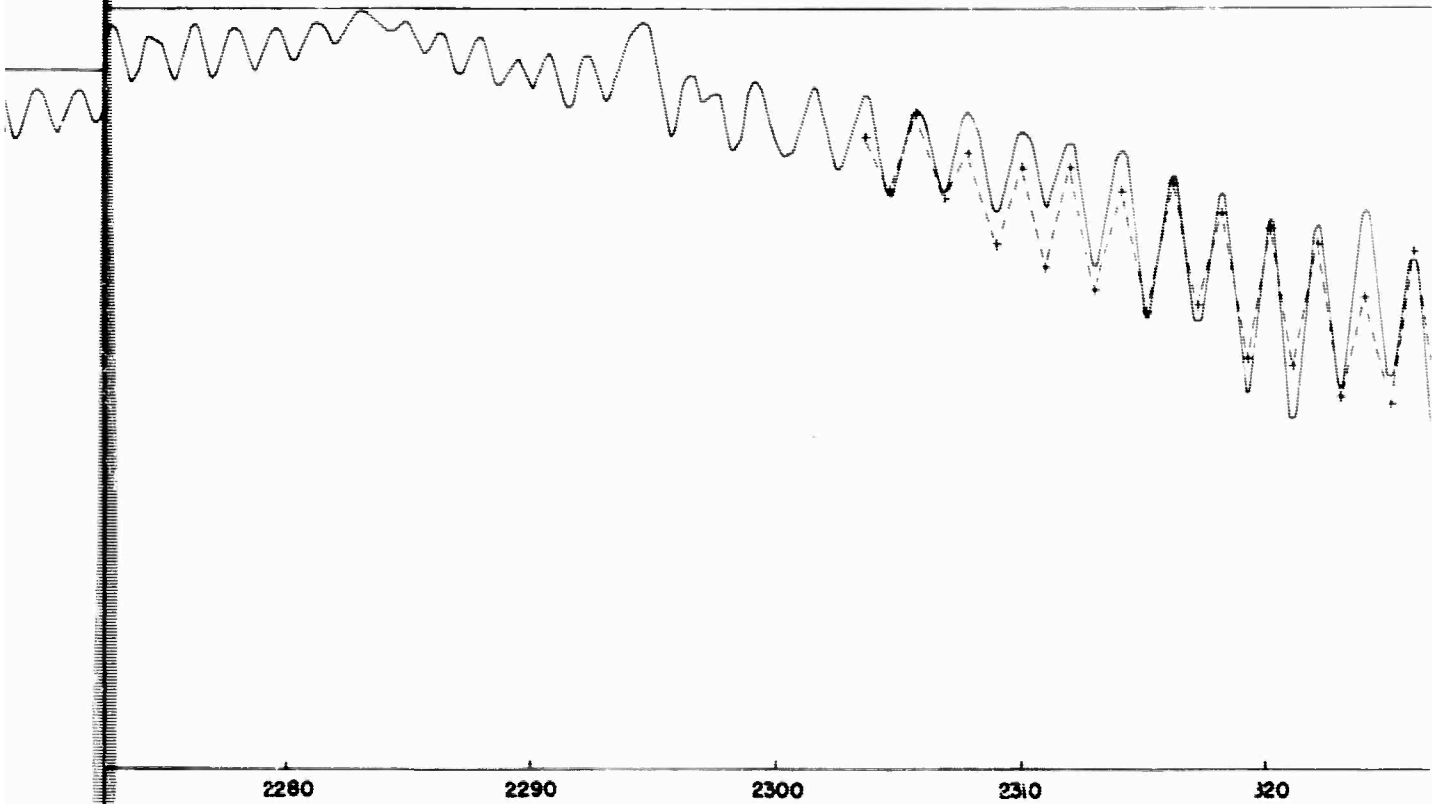


Figure 29. (Record 59) Comparison between Experimental and Calculated Transmission for the 4.3μ CO₂ Band at an Altitude of 3000 ft. (— calculated; +---+ experimental)



Experimental and Theoretical Spectral Transmittance Data
at a Slant Range of 32.0 km and a Solar Elevation of 43.46 Degrees.

Experimental
(Experimental)
)

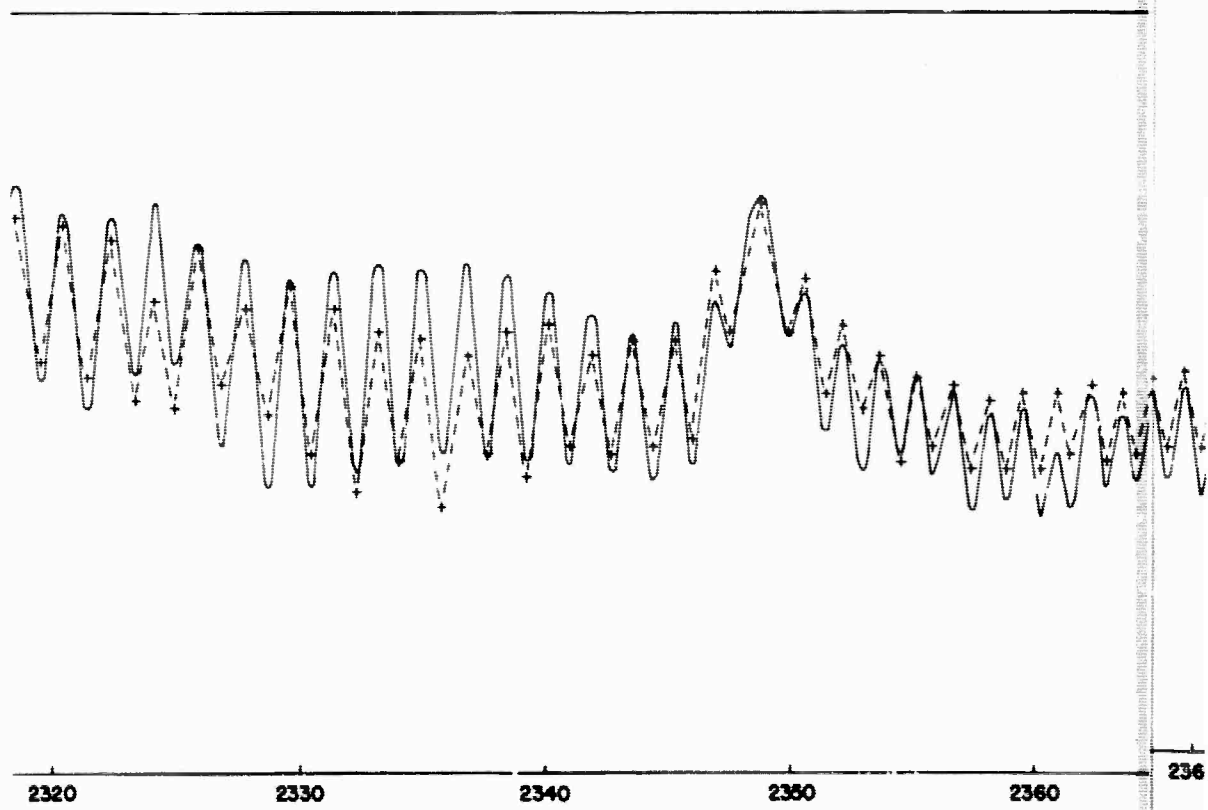
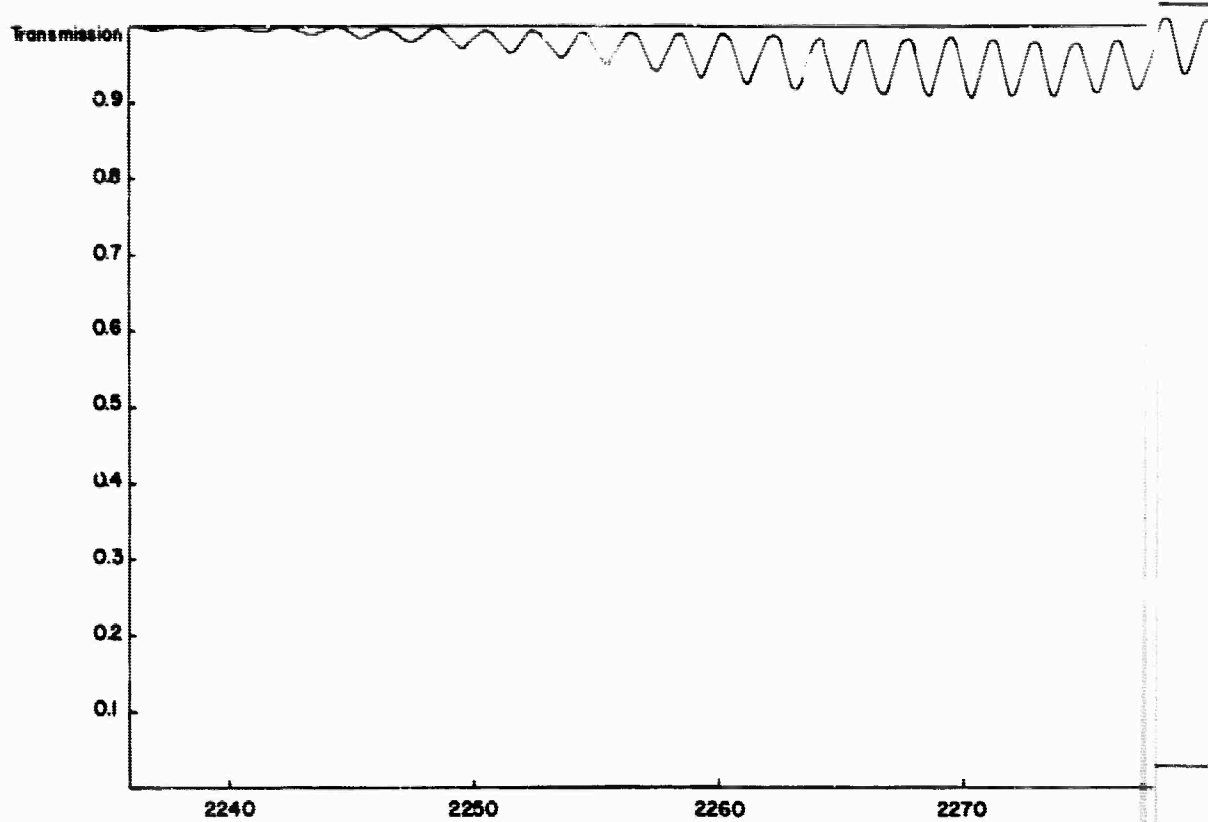
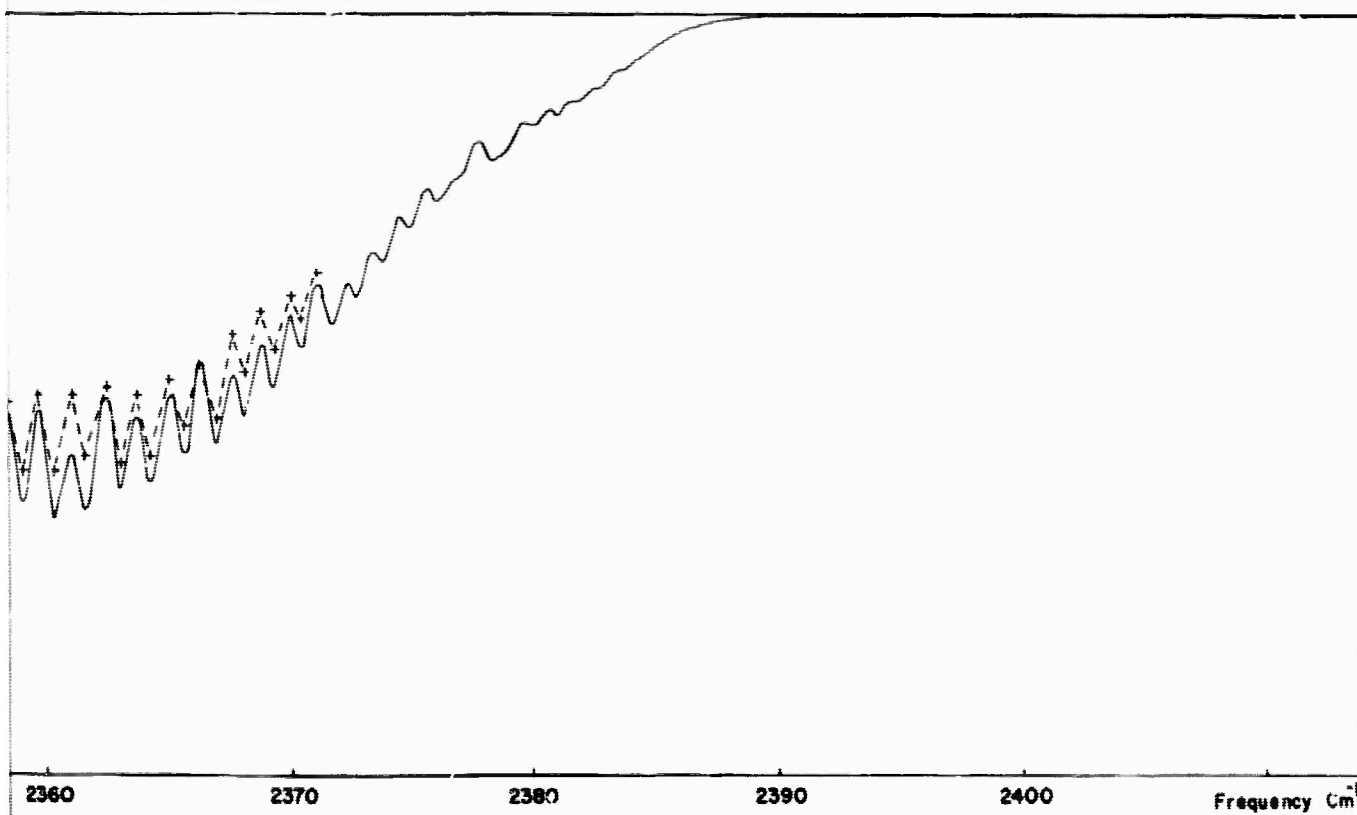
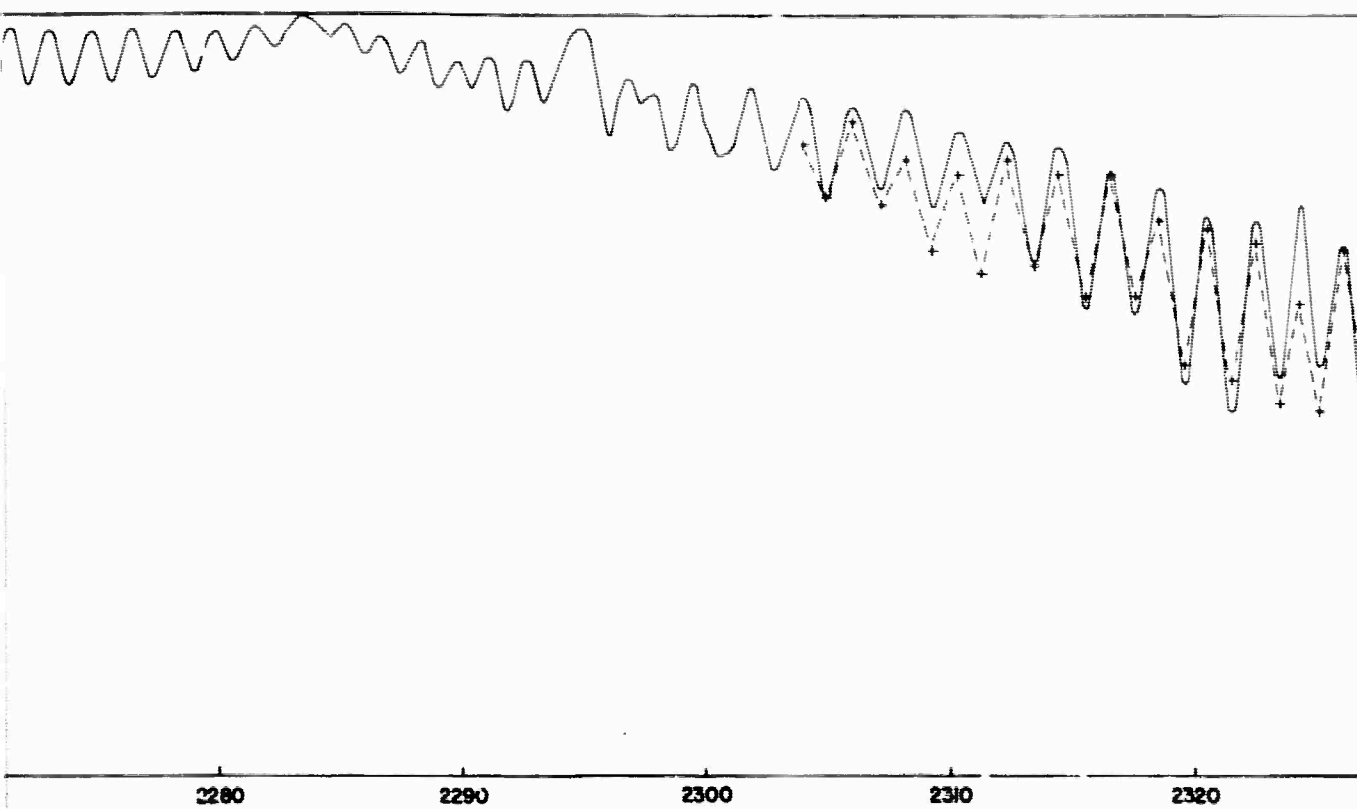


Figure 30. (Record 60) Comparison between Experimental and Calculated Transmission for the 4.3μ CO_2 Band at an Altitude of 10,000 Feet (____ calculated; +---+ experimental)



Comparison of Experimental and Theoretical Spectral Transmittance Data
at an Altitude of 32.3 km and a Solar Elevation of 44.09 Degrees.
(Theoretical Data is shown as a dashed line with '+' markers, and Experimental Data is shown as a solid line.)

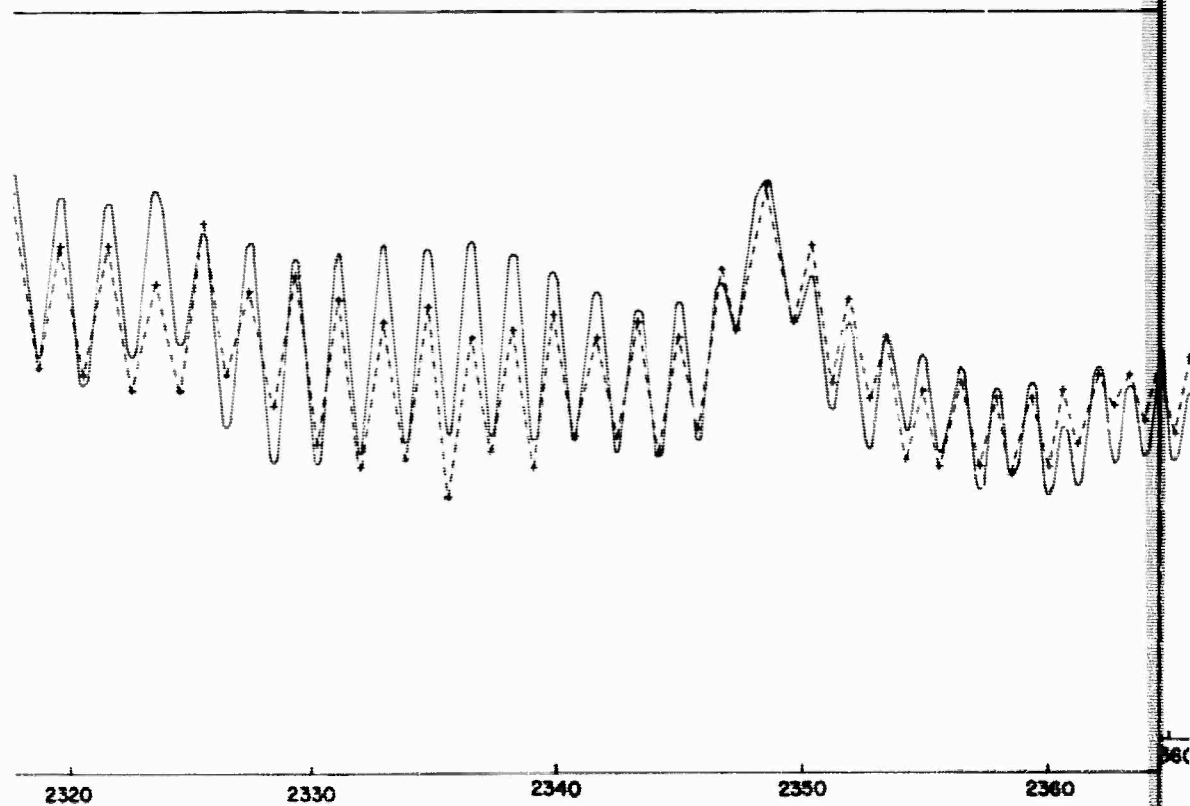
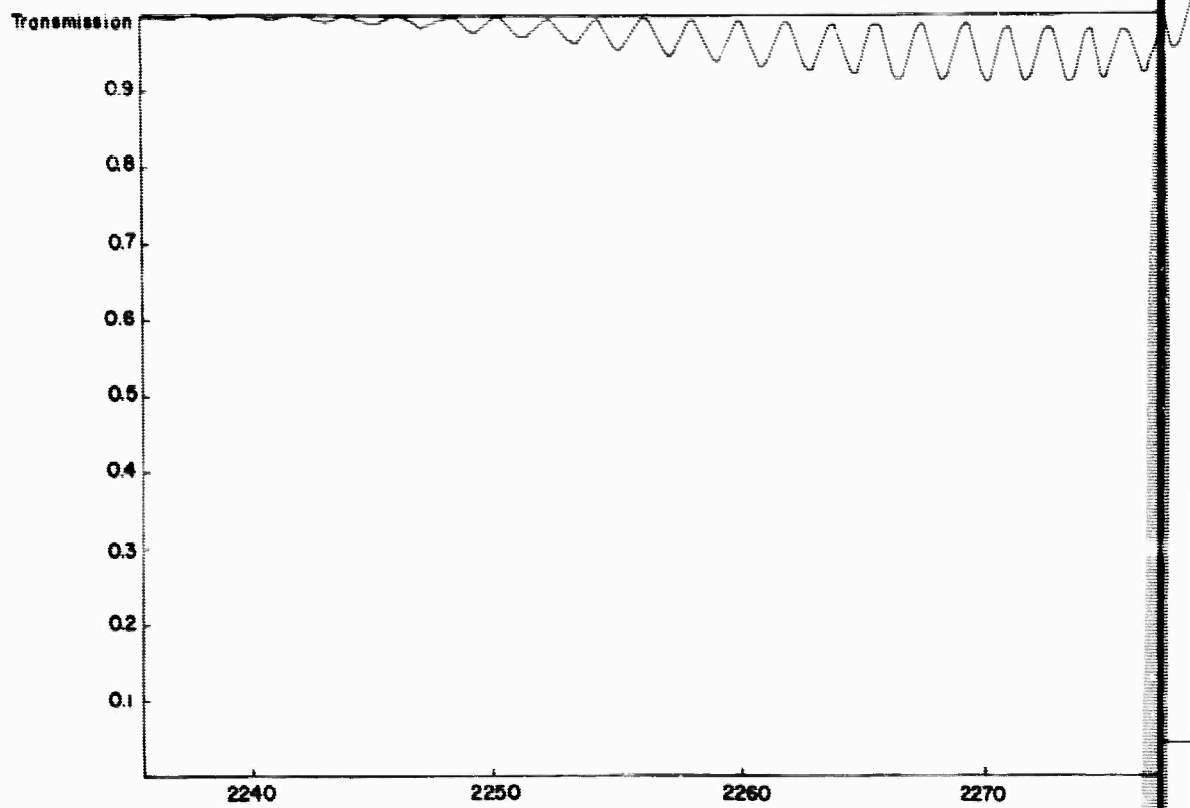
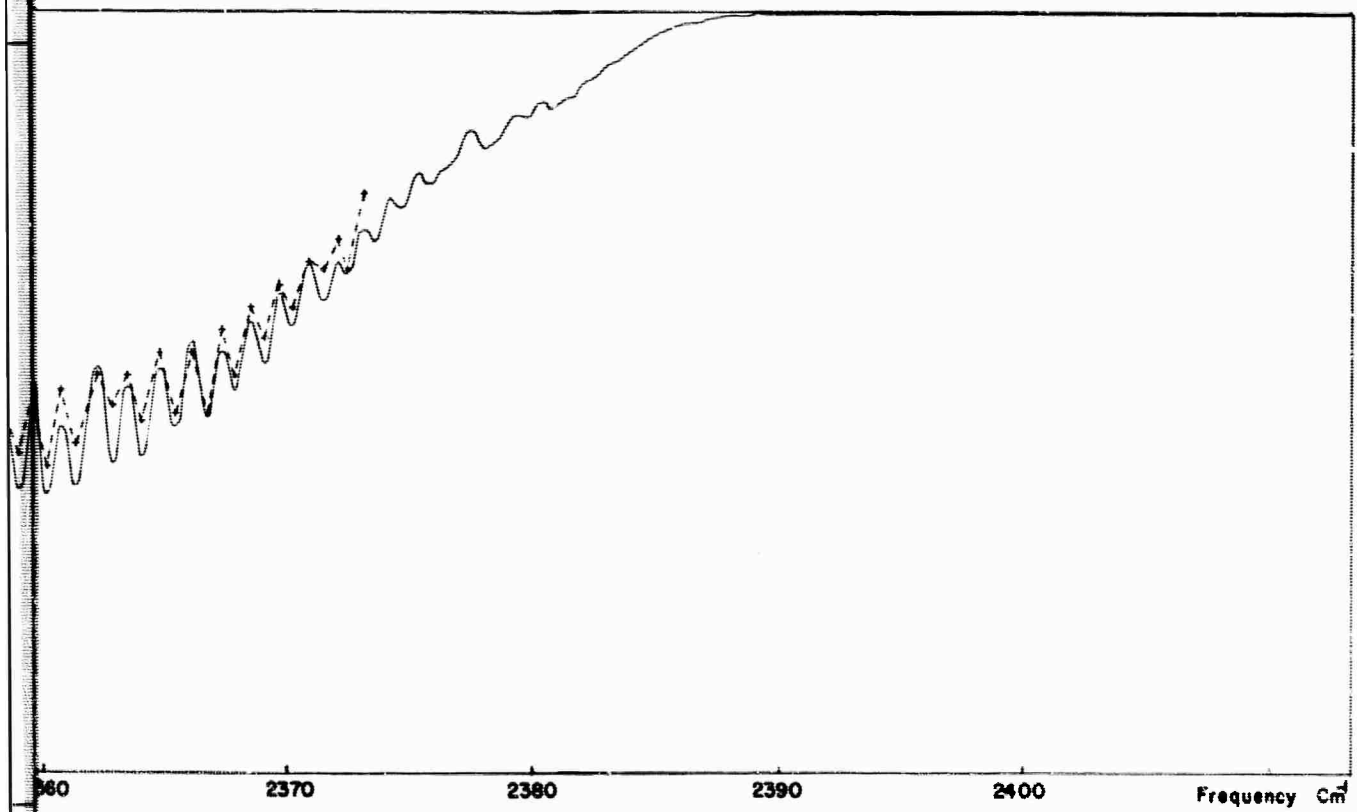
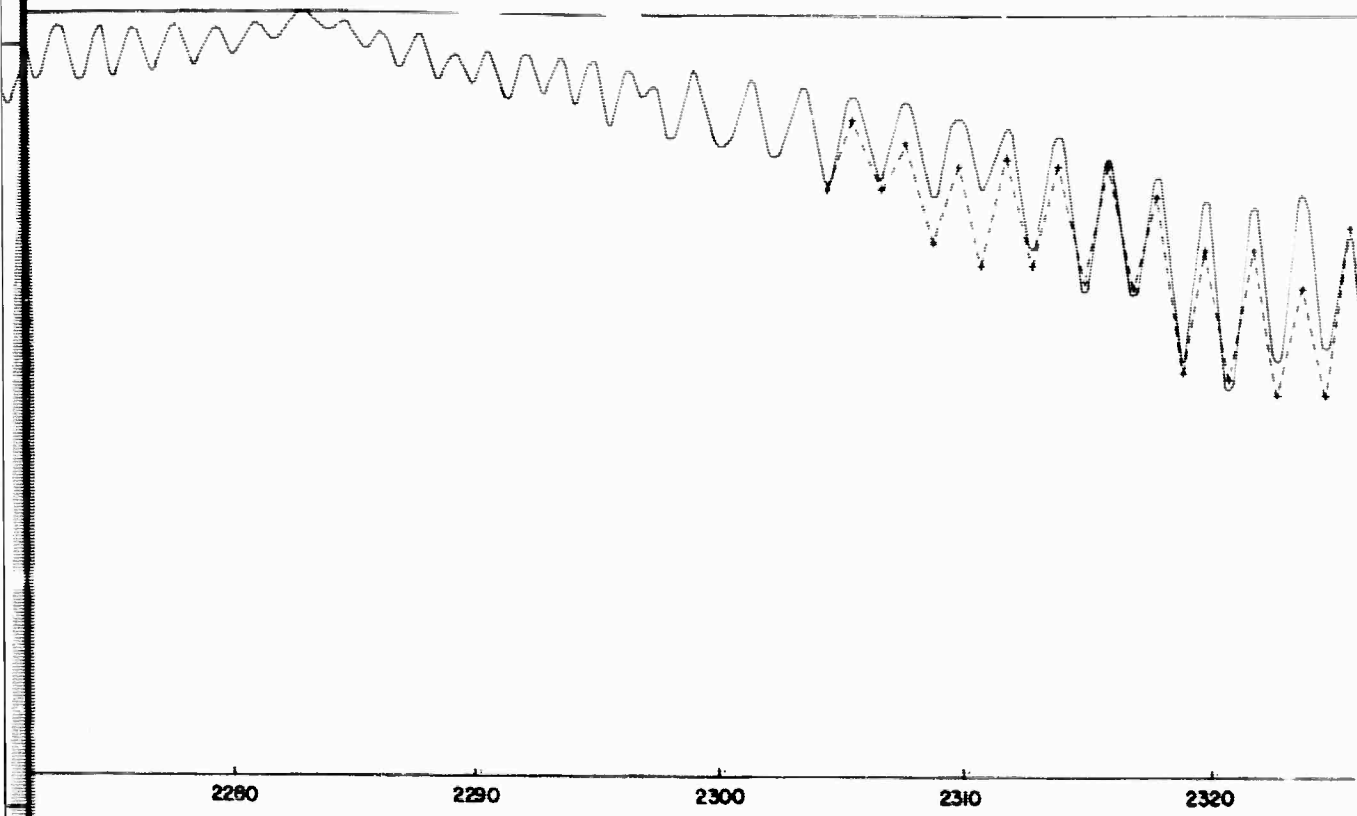


Figure 31. (Record 61) Comparison between Experimental and Calculated Transmission for the 4.3μ CO_2 Band at an Altitude of 10,000 Feet (— calculated; +---+ experimental)



Experimental and Theoretical Spectral Transmittance Data
at a Path Length of 32.5 km and a Solar Elevation of 44.72 Degrees.
(Experimental)